

3rd Generation Partnership Project; Technical Specification Group Radio Access Network; Study on New Radio (NR) to support non-terrestrial networks (Release 15)



Keywords

Satellite, Aerial, 5G

3GPP

Postal address

3GPP support office address

650 Route des Lucioles - Sophia Antipolis
Valbonne - FRANCE
Tel.: +33 4 92 94 42 00 Fax: +33 4 93 65 47 16

Internet

<http://www.3gpp.org>

Copyright Notification

No part may be reproduced except as authorized by written permission.
The copyright and the foregoing restriction extend to reproduction in all media.

© 2020, 3GPP Organizational Partners (ARIB, ATIS, CCSA, ETSI, TSDSI, TTA, TTC).
All rights reserved.

UMTS™ is a Trade Mark of ETSI registered for the benefit of its members

3GPP™ is a Trade Mark of ETSI registered for the benefit of its Members and of the 3GPP Organizational Partners

LTE™ is a Trade Mark of ETSI registered for the benefit of its Members and of the 3GPP Organizational Partners

GSM® and the GSM logo are registered and owned by the GSM Association

Contents

Foreword.....	6
1 Scope	7
2 References	7
3 Definitions, symbols and abbreviations	10
3.1 Definitions	10
3.2 Symbols	11
3.3 Abbreviations.....	11
4 Non-Terrestrial Networks Overview – background information	13
4.1 Roles for Non-Terrestrial Networks in 5G system	13
4.2 5G Use Cases wherein Non-Terrestrial Network components have a role	13
4.2.1 5G use cases introduction.....	13
4.3 Satellite and aerial access network architecture principles	17
4.4 Characteristics of NTN Terminals for satellite / aerial access network	20
4.5 Air/Space borne vehicle characteristics	21
4.6 Coverage pattern of NTN	21
4.7 Non-Terrestrial Network architecture options	22
4.8 Spectrum.....	23
5 Non-Terrestrial Networks deployment scenarios.....	24
5.1 Scenarios overview	24
5.2 Attributes	25
5.3 Doppler and Propagation delay characterisation.....	26
5.3.1 Methodology	26
5.3.1.1 Propagation delay	26
5.3.1.2 Differential delay.....	26
5.3.1.3 Doppler shift/variation.....	26
5.3.2 Geo-stationary platforms.....	27
5.3.2.1 Propagation delay	28
5.3.2.2 Differential delay.....	28
5.3.2.3 Doppler shift.....	29
5.3.3 Aerial vehicle	32
5.3.4 Non geostationary satellites	33
5.3.4.1 Propagation delay	33
5.3.4.2 Differential delay.....	34
5.3.4.3 Doppler Shift and variation rate	34
5.3.4.3.1 Case at 2 GHz	36
5.3.4.3.2 Case in Ka band	37
5.3.4.4 Doppler Shift and variation rate	41
5.3.5 Synthesis for each scenarios.....	42
6 Non-Terrestrial Networks channel models.....	43
6.1 Status/expectation of existing information for satellite/HAPS channels	43
6.1.1 Channel modeling works outside of 3GPP.....	43
6.1.2 Targeted user environment	43
6.1.3 Modeling objectives	43
6.2 Differences between satellite/HAPS and cellular channel modelling.....	43
6.3 Coordinate system	45
6.4 Antenna modelling.....	45
6.4.1 HAPS/Satellite antenna	45
6.4.2 UE antenna pattern	46
6.5 Methodology to define channel models	46
6.5.1 System-level methodology	46
6.5.2 Link-level methodology	47
6.6 Large scale model	48
6.6.1 LOS probability.....	48

6.6.2	Path loss and Shadow fading	48
6.6.3	O2I penetration loss	50
6.6.4	Atmospheric absorption	51
6.6.5	Rain and cloud attenuation	52
6.6.6	Scintillation	52
6.6.6.1	Ionospheric scintillation	52
6.6.6.1.1	Ionospheric scintillation indices.....	53
6.6.6.1.2	Ionospheric scintillation location dependence	53
6.6.6.1.3	Frequency scaling	54
6.6.6.1.4	Model for Ionospheric scintillation loss.....	54
6.6.6.2	Tropospheric scintillation	57
6.6.6.2.1	Model for Tropospheric scintillation loss	57
6.7	Fast fading model	58
6.7.1	Flat fading	58
6.7.2	Frequency selective fading	61
6.8.	Additional modelling components	86
6.8.1	Time-varying Doppler shift.....	86
6.8.2	Faraday rotation	86
6.9	Channel models for link level simulations.....	88
6.9.1	CDL models	88
6.9.2	TDL models	91
6.10	Channel model calibration	94
6.10.1	NTN channel model features per deployment scenarios	94
7	Potential key impact areas on NR to support NTN	96
7.1	Specific constraints associated to NTN	96
7.2	NR features/protocols potentially affected	98
7.3	NR modifications to support the Non-Terrestrial Network deployment scenarios	101
7.3.1	Methodology	101
7.3.2	Motion of the space/aerial vehicles	101
7.3.2.1	Hand-Over and paging	101
7.3.2.1.1	Problem statement.....	101
7.3.2.1.2	Assessment of conditions for NR operation in Non-Terrestrial networks	102
7.3.2.1.3	NR impact considerations	102
7.3.2.2	TA adjustment	102
7.3.2.2.1	Problem statement.....	102
7.3.2.2.2	Assessment of conditions for NR operation in Non-Terrestrial networks	103
7.3.2.2.3	NR impact considerations	104
7.3.2.3	Initial synchronization in downlink	104
7.3.2.3.1	Problem statement.....	104
7.3.2.3.2	Assessment of conditions for NR operation in Non-Terrestrial networks	104
7.3.2.3.3	NR impact considerations	104
7.3.2.4	DMRS time density	105
7.3.2.4.1	Problem statement.....	105
7.3.2.4.2	Assessment of conditions for NR operation in Non-Terrestrial networks	106
7.3.2.4.3	NR impact considerations	106
7.3.3	Altitude of the space/aerial vehicles	106
7.3.3.1	HARQ	106
7.3.3.1.1	Problem statement.....	107
7.3.3.1.2	Assessment of conditions for NR operation in non-terrestrial networks	108
7.3.3.1.3	NR impact considerations	108
7.3.3.2	MAC/RLC procedures	108
7.3.3.2.1	Problem statement.....	108
7.3.3.2.2	Assessment of conditions for NR operation in Non-Terrestrial networks	108
7.3.3.2.3	NR impact considerations	109
7.3.3.3	Physical layer procedures (ACM, power control)	109
7.3.3.3.1	Problem statement.....	109
7.3.3.3.2	Assessment of conditions for NR operation in Non-Terrestrial networks	109
7.3.3.3.3	NR impact considerations	109
7.3.4	Cell size (Beam foot print)	109
7.3.4.1	PRACH and Random access	109
7.3.4.1.1	Problem statement.....	109

7.3.4.1.2	Assessment of conditions for NR operation in Non-Terrestrial networks	110
7.3.4.1.3	NR impact considerations	111
7.3.4.2	TA in Random access response message.....	111
7.3.4.2.1	Problem statement.....	111
7.3.4.2.2	Assessment of conditions for NR operation in Non-Terrestrial networks	112
7.3.4.2.3	NR impact considerations	112
7.3.5	Propagation channel	112
7.3.5.1	DMRS frequency density	112
7.3.5.1.1	Problem statement.....	112
7.3.5.1.2	Assessment of conditions for NR operation in Non-Terrestrial networks	113
7.3.5.1.3	NR impact considerations	113
7.3.5.2	Cyclic prefix	113
7.3.5.2.1	Problem statement.....	113
7.3.5.2.2	Assessment of conditions for NR operation in Non-Terrestrial networks	114
7.3.5.2.3	NR impact considerations	114
7.3.6	Duplex mode	114
7.3.6.1	FDD/TDD Duplexing mode	114
7.3.6.1.1	Problem statement.....	114
7.3.6.1.2	Assessment of conditions for NR operation in Non-Terrestrial networks	115
7.3.6.1.3	NR impact considerations	115
7.3.7	Satellite or aerial Payload performance.....	115
7.3.7.1	PT-RS	115
7.3.7.1.1	Problem statement.....	115
7.3.7.1.2	Assessment of conditions for NR operation in Non-Terrestrial networks	115
7.3.7.1.3	NR impact considerations	116
7.3.7.2	PAPR	116
7.3.7.2.1	Problem statement.....	116
7.3.7.2.2	Assessment of conditions for NR operation in Non-Terrestrial networks	117
7.3.7.2.3	NR impact considerations	117
7.3.8	Network architecture	117
7.3.8.1	Protocols	117
7.3.8.1.1	Problem statement.....	117
7.3.8.1.2	Assessment of conditions for NR operation in Non-Terrestrial Networks	118
7.3.8.1.3	NR impact considerations	120
8	Recommendations on the way forward	122
8.1	General outcomes	122
8.2	Reference deployment scenarios.....	122
8.3	Non-Terrestrial network channel modelling	122
8.4	NR impacts to support Non-Terrestrial networks	122
8.4.1	Type of potential NR impacts	122
8.4.2	Assessment of potential NR impacts to support Non-Terrestrial networks.....	122
Annex A:	Example of reference scenario for calibration of large scale parameters.....	125
Annex B:	Non Terrestrial network characteristics.....	126
B.1	NTN Phase noise masks	126
Annex C:	Change History	127

Foreword

This Technical Report has been produced by the 3rd Generation Partnership Project (3GPP).

The contents of the present document are subject to continuing work within the TSG and may change following formal TSG approval. Should the TSG modify the contents of the present document, it will be re-released by the TSG with an identifying change of release date and an increase in version number as follows:

Version x.y.z

where:

- x the first digit:
 - 1 presented to TSG for information;
 - 2 presented to TSG for approval;
 - 3 or greater indicates TSG approved document under change control.
- y the second digit is incremented for all changes of substance, i.e. technical enhancements, corrections, updates, etc.
- z the third digit is incremented when editorial only changes have been incorporated in the document.

1 Scope

This technical report is related to a study item New Radio to support Non-Terrestrial Networks. The purpose of this TR is to collect the TSG RAN and RAN WG1 findings related to the study.

The objectives for the study are the following

- Definition of the Non-Terrestrial Networks deployment scenarios and related system parameters such as architecture, altitude, orbit etc.
 - Adaptation of the 3GPP channel models for non-terrestrial networks (propagation conditions, mobility, ...).
 - For the described deployment scenarios, identification of any key impact areas on the New Radio interface that may need further evaluations.
-

2 References

The following documents contain provisions which, through reference in this text, constitute provisions of the present document.

- References are either specific (identified by date of publication, edition number, version number, etc.) or non-specific.
- For a specific reference, subsequent revisions do not apply.
- For a non-specific reference, the latest version applies. In the case of a reference to a 3GPP document (including a GSM document), a non-specific reference implicitly refers to the latest version of that document *in the same Release as the present document*.

- [1] 3GPP TR 21.905: "Vocabulary for 3GPP Specifications".
- [2] 3GPP TS 36.101: "Technical Specification Group Radio Access Network; Evolved Universal Terrestrial Radio Access (E-UTRA); User Equipment (UE) radio transmission and reception (Release 14)".
- [3] 3GPP TR 38.801: "Technical Specification Group Radio Access Network; Study on new radio access technology: Radio access architecture and interfaces (Release 14)".
- [4] 3GPP TR 38.804: "Technical Specification Group Radio Access Network; Study on New Radio Access Technology; Radio Interface Protocol Aspects (Release 14)".
- [5] 3GPP TR 38.913: "Study on Scenarios and Requirements for Next Generation Access Technologies (Release 14)".
- [6] 3GPP TS 22.261: "Service requirements for next generation new services and markets".
- [7] A. Guidotti *et. al*, "Satellite-enabled LTE systems in LEO Constellations", 2017 IEEE International Conference on Communications (ICC), Paris, May 2017, pp. 876-881, doi: 10.1109/ICC.2017.7962769
- [8] 3GPP TR 38.802 v14.1.0, "Study on New Radio Access Technology Physical Layer Aspects (Release 14)".
- [9] Void
- [10] Recommendation ITU-R P.681-10, "Propagation data required for the design of earth-space land mobile telecommunication systems", Dec. 2017.
- [11] Recommendation ITU-R P.618-13, "Propagation data and prediction methods required for the design of Earth-space telecommunication systems", Dec. 2017.

- [12] 3GPP TR 38.901: "Study on channel model for frequencies from 0.5 to 100 GHz (Release 14)".
- [13] Recommendation ITU-R P.531-13, "Ionospheric propagation data and prediction methods required for the design of satellite services and systems", September 2016.
- [14] Wheelon, A.D., Electromagnetic Scintillation II. Weak Scattering, Cambridge Univ. Press, pp. 110-111, Cambridge, U.K., 2005.
- [15] F. P. Fontan, M. Vazquez-Castro, C. E. Cabado, J. P. Garcia and E. Kubista, "Statistical modeling of the LMS channel," in IEEE Transactions on Vehicular Technology, vol. 50, no. 6, pp. 1549-1567, Nov 2001
- [16] A. Jahn and E. Lutz, "Propagation Data and channel model for LMS systems", Final Rep. ESA PO 141 742. DLR, 1995.
- [17] Prieto-Cerdeira, R., Perez-Fontan, F., Burzigotti, P., Bolea-Alamañac, A. and Sanchez-Lago, I., "Versatile two-state land mobile satellite channel model with first application to DVB-SH analysis", Int. J. Satell. Commun. Network., 28: 291–315., June 2010.
- [18] Void
- [19] Void
- [20] 3GPP TS 38.321 "Technical Specification Group Radio Access Network; NR; Medium Access Control (MAC) protocol specification (Release 15)".
- [21] 3GPP TS 38.211, "Technical Specification Group Radio Access Network; NR; Physical channels and modulation (Release 15)".
- [22] 3GPP TS 38.133 "Technical Specification Group Radio Access Network; NR; Requirements for support of radio resource management (Release 15)".
- [23] 3GPP TS 38.214, "Technical Specification Group Radio Access Network; NR; Physical layer procedures for data (Release 15)".
- [24] 3GPP TR 38.802 v14.1.0, "Study on New Radio Access Technology Physical Layer Aspects (Release 14)", June 2016.
- [25] 3GPP TS 36.101: "Technical Specification Group Radio Access Network; Evolved Universal Terrestrial Radio Access (E-UTRA); User Equipment (UE) radio transmission and reception (Release 14)".
- [26] 3GPP TS 38.101, "Technical Specification Group Radio Access Network; NR; User Equipment (UE) radio transmission and reception".
- [27] 3GPP TS 36.104, "Technical Specification Group Radio Access Network; Evolved Universal Terrestrial Radio Access (E-UTRA); Base Station (BS) radio transmission and reception".
- [28] O. Kodheli, A. Guidotti, and A. Vanelli-Coralli. "Integration of Satellites in 5G through LEO Constellations", CoRR abs/1706.06013 (2017): pp. 1-6
- [29] 3GPP TS 36.321, "Evolved Universal Terrestrial Radio Access (E-UTRA); Medium Access Control (MAC) protocol specification (Release 15)", v1.0.0 (2017-12).
- [30] R1-1802632, "Considerations on random access for non-terrestrial networks", Interdigital Inc., 3GPP TSG RAN WG1 Meeting #93, Busan, Korea, May 21st – 25th, 2018.
- [31] R1-1804236, "Discussion on the NR impacts on random access for NTN", ZTE, 3GPP TSG RAN WG1 Meeting #93, Busan, Korea, May 21st – 25th, 2018.
- [32] RP-180664, "NR-NTN: solution principles for NR to support non-terrestrial networks", Thales et al, 3GPP TSG RAN Meeting #80, La Jolla, USA, June 11th – 14th, 2018.
- [33] R1-1806768 "Considerations on timing advance and random access for NTN", Nokia, Nokia Shanghai Bell, 3GPP TSG RAN WG1 Meeting #93, Busan, Korea, May 21st – 25th, 2018.

- [34] ITU-R M.1225, "Guidelines for evaluation of radio transmission technologies for IMT-2000", 1997
- [35] E. Lutz, M. Werner, and A. Jahn, "Satellite Systems for Personal and Broadband Communications", Berlin, Germany, Springer-Verlag, 2000.
- [36] T. Rappaport, "Wireless Communications", New Jersey: Prentice Hall, 1996
- [37] DVB Document A171-2, Digital Video Broadcasting (DVB) Implementation guidelines for the second generation system for Broadcasting, Interactive Services, News Gathering and other broadband satellite applications; Part 2 - S2 Extensions (DVB-S2X), March 2015.
- [38] 3GPP TR 38.803 v14.2.0, "Study on new radio access technology: Radio Frequency (RF) and co-existence aspects".
- [39] R1-1806750, "Considerations on random access for NTN", Samsung, 3GPP TSG RAN WG1 Meeting #93, Busan, Korea, May 21st – 25th, 2018.
- [40] 3GPP TS 38.104, "Technical Specification Group Radio Access Network; NR; Base Station (BS) radio transmission and reception".
- [41] R. Ali Ahmad, J. Lacan, F. Arnal, M. Gineste and L. Clarac, "Enhancing satellite system throughput using adaptive HARQ for delay tolerant services in mobile communications", 2015 Wireless Telecommunications Symposium (WTS), New York, NY, 2015, pp. 1-7.
- [42] Tae Chul Hong, Kunseok Kang, Bon-Jun Ku, Dae-Ig Chang, "Receiver memory management method for HARQ in LTE-based satellite communication system", International Journal of Satellite Communications and Networking, 2017, 35, 1, 3.
- [43] R1-1802613, "NTN NR impacts on the HARQ Operation", Fraunhofer, 3GPP TSG RAN1 meeting #92, Athens, Greece, Feb. 26 - Mar. 2, 2018.
- [44] R1-1804857, "Deactivating HARQ for Non-Terrestrial Networks", InterDigital Inc, 3GPP TSG RAN WG1 Meeting #93, Busan, Korea, May 21st – 25th, 2018.
- [45] R1-1805848, "Consideration on HARQ Impact for NTN", Nokia, Nokia Shanghai Bell, 3GPP TSG RAN WG1 Meeting #93, Busan, Korea, May 21st – 25th, 2018.
- [46] O. Kodheli, A. Guidotti, and A. Vanelli-Coralli. "Integration of Satellites in 5G through LEO Constellations", CoRR abs/1706.06013 (2017): pp. 1-6.
- [47] R1-1807164, "NR-NTN Channel Modeling – Flat fading criteria", THALES, 3GPP TSG RAN WG1 Meeting #93, Busan, Korea, May 21st – 25th, 2018.
- [48] R1-1802551, "UE antenna assumption and beam modelling for NTN", Nokia, 3GPP TSG RAN WG1 Meeting #92, Athens, Greece, February 20th – March 2nd, 2018.

3 Definitions, symbols and abbreviations

3.1 Definitions

For the purposes of the present document, the terms and definitions given in 3GPP TR 21.905 [1] and the following apply. A term defined in the present document takes precedence over the definition of the same term, if any, in 3GPP TR 21.905 [1].

Aerial: an airborne vehicle embarking a bent pipe payload or a regenerative payload telecommunication transmitter, typically at an altitude between 8 to 50 km.

Airborne vehicles: Unmanned Aircraft Systems (UAS) encompassing tethered UAS (TUA), Lighter than Air UAS (LTA), Heavier than Air UAS (HTA), all operating in altitudes typically between 8 and 50 km including High Altitude Platforms (HAPs)

Availability: % of time during which the RAN is available for the targeted communication. Unavailable communication for shorter period than [Y] ms shall not be counted. The RAN may contain several access network components among which an NTN to achieve multi-connectivity or link aggregation.

Beam throughput: data rate provided in a beam

Bentpipe payload: payload that changes the frequency carrier of the uplink RF signal, filters and amplifies it before transmitting it on the downlink

Connectivity: capability to establish and maintain data / voice / video transfer between networks and parts thereof

Geostationary Earth orbit: Circular orbit at 35,786 kilometres above the Earth's equator and following the direction of the Earth's rotation. An object in such an orbit has an orbital period equal to the Earth's rotational period and thus appears motionless, at a fixed position in the sky, to ground observers.

Low Earth Orbit: Orbit around the around Earth with an altitude between 500 kilometres (orbital period of about 88 minutes), and 2,000 kilometres (orbital period of about 127 minutes).

Medium Earth Orbit: region of space around the Earth above low Earth orbit and below geostationary Earth Orbit.

Mobile Services: a radiocommunication service between mobile and land stations, or between mobile stations

Mobile Satellite Services: A radiocommunication service between mobile earth stations and one or more space stations, or between space stations used by this service; or between mobile earth stations by means of one or more space stations

Non Geostationary Satellites: Satellites (LEO and MEO) orbiting around the Earth with a period that varies approximately between 1.5 hour and 10 hours. It is necessary to have a constellation of several Non Geostationary satellites associated with handover mechanisms to ensure a service continuity.

Non-terrestrial networks: Networks, or segments of networks, using an airborne or space-borne vehicle to embark a transmission equipment relay node or base station.

On Board processing: digital processing carried out on uplink RF signals aboard a satellite or an aerial.

One way latency: time required to propagate through the RAN from a terminal to the gateway or from the gateway to the terminal. This is especially used for voice and video conference applications.

Regenerative payload: payload that transforms and amplifies an uplink RF signal before transmitting it on the downlink. The transformation of the signal refers to digital processing that may include demodulation, decoding, re-encoding, re-modulation and/or filtering.

Relay node: Relay of Uu radio interface. The relay function can take place at Layer 1, 2 or 3.

Reliability: probability that the RAN performs in a satisfactory manner for a given period of time when used under specific operating conditions. The RAN may contain several access network components including an NTN to achieve multi-connectivity or link aggregation.

Round Trip Delay: time required for a network communication to travel from a terminal to the gateway or from the gateway to the terminal and back. This is especially used for web based applications.

Satellite: a space-borne vehicle embarking a bent pipe payload or a regenerative payload telecommunication transmitter, placed into Low-Earth Orbit (LEO) typically at an altitude between 500 km to 2000 km, Medium-Earth Orbit (MEO) typically at an altitude between 8000 to 20000 km, or Geostationary-satellite Earth Orbit (GEO) at 35 786 km altitude.

Space-borne vehicles: Satellites including Low Earth Orbiting (LEO) satellites, Medium Earth Orbiting (MEO) satellites, Geostationary Earth Orbiting (GEO) satellites as well as Highly Elliptical Orbiting (HEO) satellites

User Connectivity: capability to establish and maintain data / voice / video transfer between networks and Terminals

User Throughput: data rate provided to a terminal

3.2 Symbols

For the purposes of the present document, the following symbols apply:

<symbol> <Explanation>

3.3 Abbreviations

For the purposes of the present document, the abbreviations given in 3GPP TR 21.905 [1] and the following apply. An abbreviation defined in the present document takes precedence over the definition of the same abbreviation, if any, in 3GPP TR 21.905 [1].

2D	two-dimensional
3D	three-dimensional
ACM	Adaptive Modulation and Coding
AMF	Access and Mobility Management Function
AOA	Azimuth angle Of Arrival
AOD	Azimuth angle Of Departure
ARQ	Automatic Repeat Request
AS	Angular Spread
ASA	Azimuth angle Spread of Arrival
ASD	Azimuth angle Spread of Departure
AWGN	Additive White Gaussian Noise
BLOS	Beyond Line of Sight
BS	Base Station
BW	Bandwidth
C2	Control and Command
CDF	Cumulative Distribution Function
CDL	Cluster Delay Line
CFO	Carrier Frequency Offset
CP	Cyclic Prefix
CPE	Common Phase Error
DS	Delay Spread
EIRP	Equivalent Isotropically Radiated Power
eMBB	enhanced Mobile Broadband
FDM	Frequency-Division Multiplexed
FOTA	Firmware Over The Air services
FSS	Fixed Satellite Services
GEO	Geostationary Earth Orbiting
gNB	next Generation Node B
GNSS	Global Navigation Satellite System
GSO	Geo Synchronous Orbit
GW	Gateway
HAPS	High Altitude Platform Station
HARQ	Hybrid Automatic Repeat Request
HD	High Definition

HEO	Highly Elliptical Orbiting
ICI	Inter-Carrier Interference
IoT	Internet of Things
K	Ricean K factor
KPI	Key Performance Indicator
IMUX	Input MULTipleXer
ISL	Inter-Satellite Links
LEO	Low Earth Orbiting
LMS	Land Mobile Satellite
LOS	Line of Sight
Mbps	Mega bit per second
MEO	Medium Earth Orbiting
mMTC	massive Machine Type Communications
MS	Mobile Services
MSS	Mobile Satellite Services
NGSO	Non Geostationary Satellite Orbit
NLOS	Non-LOS
NT	Non Terrestrial
NTN	Non Terrestrial Network
O2I	Outdoor-to-Indoor
OBO	Output Backoff
OMUX	Output MULTipleXer
PA	Power Amplifier
PAPR	Peak-to-Average Power Ratio
PL	Path Loss
POI	Point of Interest
PRACH	Physical Random Access Channel
PSS	Primary Synchronization Signal
RACH	Random Access Channel
RAN	Radio Access Network
RAR	Random Access Response
RAT	Radio Access Technology
RTT	Round Trip Time
RRH	Remote Radio Head
SCS	Subcarrier Spacing
SIB	System Information Block
SNR	Signal-to-Noise Ratio
RMa	Rural Macro
RMS	Root Mean Square
Rx	Receiver
SF	Shadow Fading
SOTA	Software Over The Air services
SSPA	Solid-State Power Amplifier
SSS	Secondary Synchronization Signal
TA	Timing Advance
TAG	Timing Advance Group
TDL	Tapped Delay Line
TOA	Time Of Arrival
Tx	Transmitter
TV	Television
UAS	Unmanned Aerial System
UE	User Equipment
UMa	Urban Macro
UMi	Urban Micro
URLLC	Ultra-Reliable Low Latency Communications
VSAT	Very Small Aperture Terminal
XPR	Cross-Polarization Ratio
ZOA	Zenith angle Of Arrival
ZOD	Zenith angle Of Departure
ZSA	Zenith angle Spread of Arrival
ZSD	Zenith angle Spread of Departure

4 Non-Terrestrial Networks Overview – background information

4.1 Roles for Non-Terrestrial Networks in 5G system

Thanks to the wide service coverage capabilities and reduced vulnerability of space/airborne vehicles to physical attacks and natural disasters, Non-Terrestrial Networks are expected to

- foster the roll out of 5G service in un-served areas that cannot be covered by terrestrial 5G network (isolated/remote areas, on board aircrafts or vessels) and underserved areas (e.g. sub-urban/rural areas) to upgrade the performance of limited terrestrial networks in cost effective manner,
- reinforce the 5G service reliability by providing service continuity for M2M/IoT devices or for passengers on board moving platforms (e.g. passenger vehicles-aircraft, ships, high speed trains, bus) or ensuring service availability anywhere especially for critical communications, future railway/maritime/aeronautical communications, and to
- enable 5G network scalability by providing efficient multicast/broadcast resources for data delivery towards the network edges or even user terminal.

The benefits relate to either Non-Terrestrial networks operating alone or to integrated terrestrial and Non-Terrestrial networks. They will impact coverage, user bandwidth, system capacity, service reliability or service availability, energy consumption, connection density (See [5]).

A role for Non-Terrestrial Network components in the 5G system is expected for the following verticals: transport, Public Safety, Media and Entertainment, eHealth, Energy, Agriculture, Finance, Automotive.

4.2 5G Use Cases wherein Non-Terrestrial Network components have a role

4.2.1 5G use cases introduction

A use case, typically refers to the interactions between a role and a system, to achieve a specific goal. Hence, it is necessary to identify the goal of the service enabled by a Non-Terrestrial network component integrated in the 5G system.

The tables in the clauses after respectively identify for each of the 5G service enablers, the use cases wherein Non-Terrestrial Network components have a role to play.

- 5G service enablers refer to eMBB (enhanced Mobile Broadband), URLLC (Ultra-Reliable Low Latency Communications) and mMTC (massive Machine Type Communications).
- 5G use cases correspond to the interactions between a stakeholder (user, operator, service provider) and the 5G system, to achieve a specific goal.
- The role of the Non-Terrestrial Network refers to services enabled by the Non-Terrestrial Network component in the 5G system to support the use case.
- 3GPP reference documents are provided in which the use cases are mentioned.

NOTE: While the propagation delay of satellite systems may be an issue for certain applications requiring ultra low latency, the importance of satellite for Critical Communications including public safety communications due to their dependability and large coverage area is well known.

Table 4.2.1-1: 5G use cases for Satellite access networks

5G Service enabler	5G Use case	5G Use case description	Satellite service	3GPP References
eMBB	Multi connectivity	Users in underserved areas (home or in Small Offices, big events in ad-hoc built-up facilities) are connected to the 5G network via multiple network technologies and benefit from 50 Mbps+. Delay sensitive traffic may be routed over short latency links while less delay sensitive traffic can be routed over the long latency links.	Broadband connectivity to cells or relay node in underserved areas in combination with terrestrial wireless/cellular or wire line access featuring limited user throughput.	TR 22.864, §5.5: Backhauling TR 22.863, §5.6: Fixed Mobile Convergence TR 22.863, §5.7: Femto cell TR 22.863, §5.4: Higher user mobility TS 22.261 (related to §6.3)
eMBB	Fixed cell connectivity	Users in isolated villages or industry premises (Mining, off shore platform) access 5G services and benefit from 50 Mbps+.	Broadband connectivity between the core network and the cells in un-served areas (isolated areas).	TR 22.863, §5.3: Deployment and coverage
eMBB	Mobile cell connectivity	Passengers on board vessels or aircrafts access 5G services and benefit from 50 Mbps+.	Broadband connectivity between the core network and the cells on board a moving platform (e.g. aircraft or vessels).	TR 22.863, §5.3: Deployment and coverage TS 22.261 (related to §7.1)
eMBB	Network resilience	Some critical network links requires high availability which can be achieved through the aggregation of two or several network connections in parallel. The intent is to prevent complete network connection outage.	Secondary/backup connection (although potentially limited in capability compared to the primary network connection).	TR 22.862, §5.5: Higher availability TS 22.261 (related to §6.3)
eMBB	Trunking	A network operator may want to deploy or restore (disaster relief) 5G service in an isolated area (not connected to public data network). A network operator may want to interconnect various 5G local access network islands not otherwise connected	Broadband connectivity between the public data network and a mobile network anchor point or between the anchor points of two mobile networks.	TR 22.863, §5.3: Deployment and coverage
eMBB	Edge network Delivery	Media and entertainment content such as live broadcasts, ad-hoc broadcast/multicast streams, group communications, Mobile Edge Computing's Virtual Network Function updates are transmitted in multicast mode to a RAN equipment at the network edge where it may be stored in a local cache or further distributed to the User Equipment. The intent is to off load popular content from the mobile network infrastructure (especially at backhaul level).	Broadcast channel to support Multicast delivery to 5G network edges.	TR 22.864, §5.4: Efficient content delivery TS 22.261 (related to §6.6)

5G Service enabler	5G Use case	5G Use case description	Satellite service	3GPP References
eMBB	Mobile cell hybrid connectivity	Passengers on board public transport vehicles (e.g. high speed/regular trains, buses, river boats) access reliable 5G services. They are served by a base station which is connected by a hybrid cellular/satellite connection. The cellular connectivity may be intermittent and/or support limited user throughput.	Broadband connectivity combined with terrestrial cellular access to connect a cell/group of cells or relay node(s) on board moving platforms.	TR 22.863, §5.3: Deployment and coverage TR 22.862, §5.5: Higher availability TS 22.261 (related to §7.1)
eMBB	Direct To Node broadcast	TV or multimedia service delivery to home premises or on board a moving platform	Broadcast/Multicast service to access points in homes or on board moving platforms.	TR 22.864, §5.4: Efficient content delivery TS 22.261 (related to §6.6)
mMTC	Wide area IoT service	Global continuity of service for telematic applications based on a group of sensors/actuators (IoT devices, battery activated or not) scattered over or moving around a wide area and reporting information to or controlled by a central server. These sensors and/or actuators may be used for example the following telematics applications: <ul style="list-style-type: none">- Automotive and road transport: high density platooning, HD map updates, Traffic flow optimisation, Vehicle software updates, automotive diagnostic reporting, user base insurance information (e.g. speed limit, driving behaviour), safety status reporting (e.g. air-bag deployment reporting), advertising based revenue, Context awareness information (e.g. neighbouring bargain opportunities based on revenue), remote access functions (e.g. remote door unlocking).- Energy: Critical surveillance of oil/gas infrastructures (e.g. pipeline status)- Transport: Fleet management, asset tracking, digital signage, remote road alerts- Agriculture: Livestock management, farming	Connectivity between IoT devices (battery activated sensors/actuators or not) and spaceborne platform. Continuity of service across spaceborne platforms and terrestrial base stations is needed.	TR 22.861, §5.2: connectivity aspects TR 22.864, §5.6: Access TR 22.862, §5.1: Higher reliability and lower latency TS 22.261 (related to §6.2.3 Service continuity across different access technologies)
mMTC	Local area IoT service	Group of sensors that collect local information, connect to each other and report to a central point. The central point may also command a set of actuators to take local actions such as on-off activities or far more complex actions. The sensors/actuators served by a local area network may be located in a smart grid subsystem (Advanced Metering) or on board a moving platform (e.g. container on board a vessel, a truck or a train).	Connectivity between mobile core network and base station serving IoT devices in a cell or a group of cells.	TR 22.863, §5.3: Deployment and coverage TS 22.261 (related to §7.1)

5G Service enabler	5G Use case	5G Use case description	Satellite service	3GPP References
eMBB	Direct to mobile broadcast	<p>Public safety authorities want to be able to instantaneously alert/warn the public (or specific subsets thereof) of catastrophic events and provide guidance to them during the disaster relief while the terrestrial network might be down.</p> <p>Automotive industry players, are interested to provide instantaneously Firmware/Software Over The Air services (FOTA/SOTA) to their customers wherever they are. This will include information updates such as map information including points of interest (POI), real-time traffic, weather, and early warning broadcasts (e.g. floods, earthquakes and other extreme weather situations, as well as terror attacks), parking availability, infotainment, etc.</p> <p>Media and entertainment industry can provide entertainment services in vehicles (cars, buses, trucks).</p>	Broadcast/Multicast service directly to User Equipment whether handheld or vehicle mounted.	TR 22.864, §5.4: Efficient content delivery TR 22.862, §5.6: Mission critical services TS 22.261 (related to)
eMBB	Wide area public safety	Emergency responders, such as police, fire brigade and medical personnel can exchange messaging and voice services in outdoor conditions anywhere they are and achieve continuity of service whatever mobility scenarios.	Access to User Equipment (handset or vehicle mounted).	TR 22.862, §5.6: Mission critical services TS 22.261 (related to)
eMBB	Local area public safety	Emergency responders, such as police, fire brigade, and medical personnel can set up a tactical cell wherever they need to operate. This cell can be connected to the 5G system via satellite to exchange data, voice and video based services between the public safety users within a tactical cell or with the remote coordination centre.	Broadband connectivity between the core network and the tactical cells.	TR 22.862, §5.6: Mission critical services TS 22.261 (related to)

Table 4.2.1-2: 5G use cases for Aerial access networks

5G Service enabler	5G Use case	5G Use case description	Aerial access service	3GPP References
eMBB	Hot spot on demand	Users in un/underserved areas (big events) are connected to the 5G network and benefit from 50 Mbps+.	Broadband connectivity to cells or relay node in un/underserved areas.	TR 22.863, §5.3: Deployment and coverage TS 22.261 (related to)
eMBB	Regional area public safety	Emergency responders, such as police, fire brigades, and medical personnel can exchange messaging, voice and video services in indoor/outdoor conditions anywhere they are and whatever mobility scenarios.	Access to User Equipment (handset or vehicle mounted). Adhoc connectivity between two cells	TR 22.862, §5.6: Mission critical services TS 22.261 (related to)
eMBB	Fixed cell connectivity	Users in isolated villages or industry premises (Mining, off shore platform) access 5G services and benefit from 50 Mbps+.	Broadband connectivity between the core network and the cells in un-served areas (isolated areas).	TS 22.261 (related to §7.1) TR 22.863, §5.3: Deployment and coverage

4.3 Satellite and aerial access network architecture principles

Non-Terrestrial Network access typically features the following system elements:

- NTN Terminal: It may refer to directly the 3GPP UE or a terminal specific to the satellite system in case the satellite doesn't serve directly 3GPP UEs.
- A service link which refer to the radio link between the user equipment and the space/airborne platform. In addition the UE may also support a radio link with terrestrial based RAN.
- A space or an airborne platform embarking a payload which may implement either a bent-pipe or a regenerative payload configuration:
 - A bent pipe payload: Radio Frequency filtering, Frequency conversion and amplification;
 - A regenerative payload: Radio Frequency filtering, Frequency conversion and amplification as well as demodulation/decoding, switch and/or routing, coding/modulation. This is effectively equivalent to having base station functions (e.g. gNB) on board the space/airborne vehicle
- Inter satellite/aerial links in case of regenerative payload and a constellation of satellites. ISL may operate in RF frequency or optical bands
- Gateways that connect the satellite or aerial access network to the core network
- Feeder links which refer to the radio links between the Gateways and the space/airborne platform

We shall distinguish between two types of Satellite and Aerial access network

- Broadband access network serving Very Small Aperture Terminals that can be fixed or mounted on a moving platform (e.g. bus, train, vessel, aircraft, etc.). In this context, Broadband refers to at least 50 Mbps data rate and even up to several hundred Mbps (satellite) or even up to several Gbps (aerial) on the downlink. The service links operate in frequency bands allocated to satellite and aerial services (Fixed, Mobile) above 6 GHz.
- Narrow or wide band access network serving terminals equipped with Omni or semi directional antenna (e.g. handheld terminal). In this context, Narrowband refers to less than 1 or 2 Mbps data rate on the downlink. The service links operate typically in frequency bands allocated to mobile satellite or aerial services below 6 GHz.

It is also helpful to distinguish between satellite and aerial systems with inter-satellite links (ISL) or inter-aerial links (IAL) and those without ISL/IAL.

For Aerial networks, we consider a configuration where base station functions are on board the airborne vehicle. The purpose of this network component is to provide the 5G service enablers to handheld devices.

Based on these principles, the figures below illustrate possible satellite and aerial access network architectures.

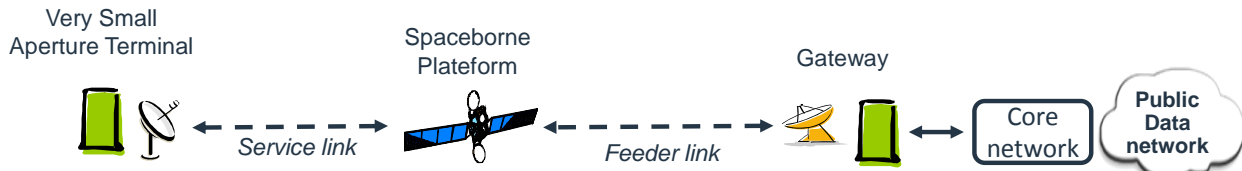


Figure 4.3-1: Satellite access network (without ISL) with a service link operating in frequency bands above 6 GHz allocated to Fixed and Mobile Satellite Services (FSS and MSS)

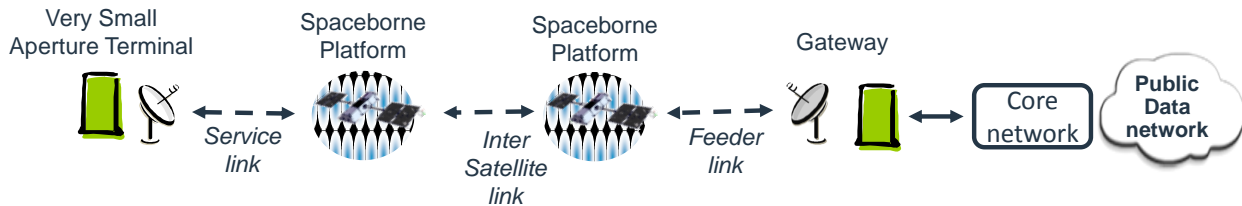


Figure 4.3-2: Satellite access network (with ISL) with a service link operating in frequency bands above the 6 GHz allocated to Fixed and Mobile Satellite Services (FSS and MSS)

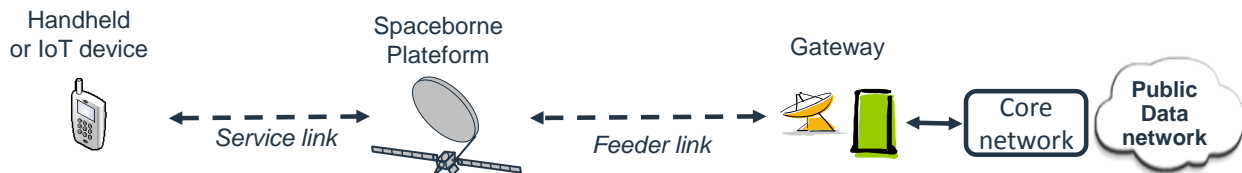


Figure 4.3-3A: Satellite access network with a service link operating in frequency bands below 6 GHz allocated to Mobile Satellite Services (MSS)

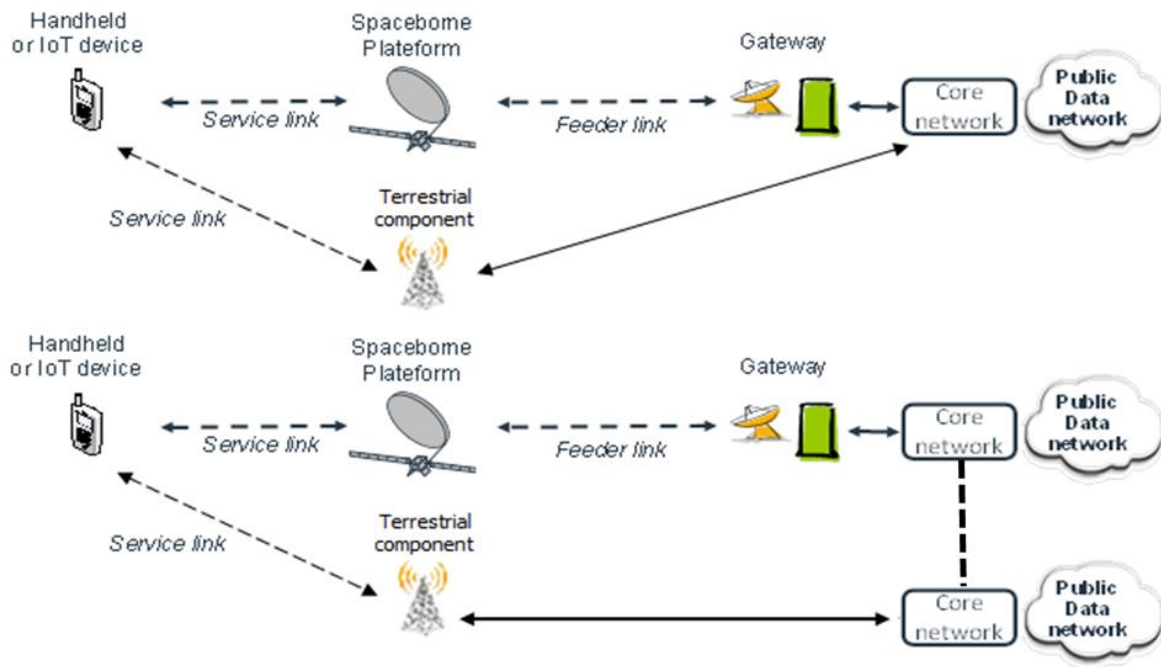


Figure 4.3-3B: Satellite access network which service link operates below 6 GHz frequency bands allocated to Mobile Satellite Services (MSS) and complemented with the terrestrial access network served by the same or independent core networks.



Figure 4.3-4: Aerial access network (without IAL) with a service link operating in frequency bands below or above 6 GHz

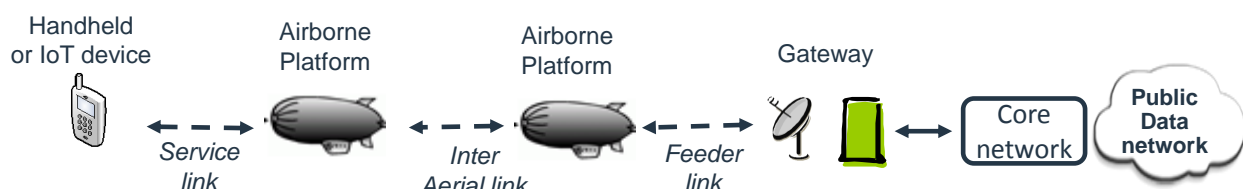


Figure 4.3-4B: Aerial access network (with IAL) with a service link operating in frequency bands below or above 6 GHz

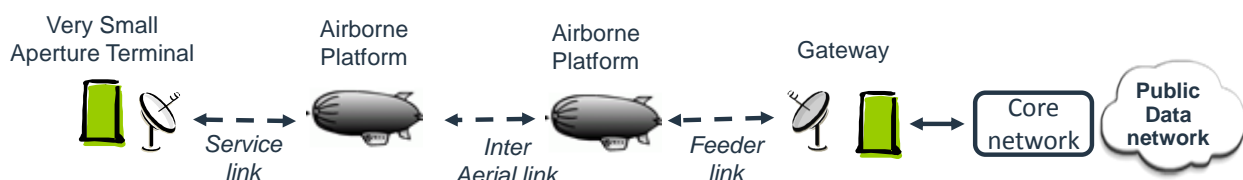


Figure 4.3-4C: Aerial access network (with IAL) with a service link operating in frequency bands above 6 GHz

It is recommended to select a range of deployment scenarios with either bent pipe or regenerative payloads. Note that the technical details of implementing the ISL interface is beyond the scope of this study.

4.4 Characteristics of NTN Terminals for satellite / aerial access network

Table 4.4-1 gives the minimum RF characteristics of the terminals operating respectively in Ka band (e.g. very small aperture terminals) and in S band (e.g. handheld terminals).

Table 4.4-1: Typical minimum RF characteristics of UE in satellite and aerial access networks

	Very Small Aperture Terminal (fixed or mounted on moving platforms)	Handheld or IoT devices (3GPP class 3, see [2])
Transmit Power	2 W (33 dBm)	200 mW (23 dBm)
Antenna type	60 cm equivalent aperture diameter (circular polarisation)	Omnidirectional antenna (linear polarisation)
Antenna gain	Tx: 43.2 dBi Rx: 39.7 dB	Tx and Rx: 0 dBi
Noise figure	1.2 dB	9 dB
EIRP	45.75 dBW	-7 dBW
G/T (NOTE 1)	18.5 dB/K	-33.6 dB/K
Polarisation (NOTE 2)	Circular	Linear

NOTE 1: For the computation of G/T or figure of merit, following formula applies in dB:

$$G/T = Ga - NF - 10 * \text{LOG} (To + (Ta - To) / (10^{0.1 * NF}))$$

Where:

- Antenna Gain : Ga in dBi
- Ambient Temperature : T0 (usually 290 K)
- Antenna temperature : Ta (typically 290 K with 0 dBi gain and 150 K with >30 dBi gain)
- Noise Figure: NF in dB

NOTE 2: For S band, we assume that the User Equipment has an omni-directional antenna of linear polarization, while the antenna on board space-borne or airborne platforms features typically employs circular polarization. Hence a polarization mismatch of 3 dB has to be taken into account for the radio link budget computation. This will impact the UE RF characteristics as below:

- Equivalent EIRP of 20 dBm (-10 dBW) under satellite coverage.
- Equivalent G/T of -36,6 dB/K under satellite coverage.

Note that other performance may be considered.

4.5 Air/Space borne vehicle characteristics

Table 4.5-1 provides characteristics of aerial and satellite vehicles that are relevant for the purpose of the study item:

Table 4.5-1: Typical characteristics of Airborne or Space-borne vehicles

Characteristics	Geostationary satellites	Non-Geostationary satellites	Airborne platforms
Altitude	35 786 km	Low Earth Orbiting satellites: From 600 km up to 1500 km Medium Earth Orbiting satellites: From 7000 up to 20000 km	Typically from 8 to 50 km
Motion	Typically within a cube of 50-100 km side around the theoretical orbital position fixed in terms of elevation/azimuth with respect to a given earth point	We shall assume here only circular orbits around the earth	Typically in motion within TBD km from the notional station keeping position fixed in terms of elevation/azimuth with respect to a given earth point
Elevation angle (NOTE 1)	Typically more than 10° for user terminal and more than 5° for gateways		
NOTE 1: The minimum Elevation angle refers to the minimum angle under which the airborne/spaceborne platform can be seen by a terminal. Below is a summary table of minimum elevation angles for different types of satellite and aerial based systems applications.			

The characteristics of the air/space-borne vehicles create specific Doppler and propagation delay conditions that NR has to cope with.

Table 4.5-2: Typical elevation angles in aerial and satellite based systems

Satellite & aerial Systems	Typical minimum Elevation Angle for terminals	Rationale/remarks
International GEO (Trunking)	5 degrees	Serving earth stations equipped with very large antennas
Regional GEO	10 degrees	Addressing regions in lower and medium latitude
International (GEO) Maritime	5 degrees	Addressing large ships
Aeronautical	20 degrees	Taking into account aero-dynamic constraints prevents operation at lower angles
Vehicles	15 degrees	Taking into account road conditions, terrain, and vehicle mechanics
Non GSO	10 to 30 degrees	Ensuring service continuity optimising the number of satellites
Aerial	In the range of 10 degrees	Maximising the service area

4.6 Coverage pattern of NTN

Satellite or aerial vehicles typically generate several beams over a given area. The foot print of the beams are typically elliptic shape.

The beam footprint may be moving over the earth with the satellite or the aerial vehicle motion on its orbit. Alternatively, the beam foot print may be earth fixed, in such case some beam pointing mechanisms (mechanical or electronic steering feature) will compensate for the satellite or the aerial vehicle motion.

Table 4.6-1: Typical beam foot print size

Attributes	GEO	Non-GEO	Aerial
Beam foot print size in diameter	200 – 1000 km	100 – 500 km	5 - 200 km

Typical beam patterns of various NTN access networks are depicted below:

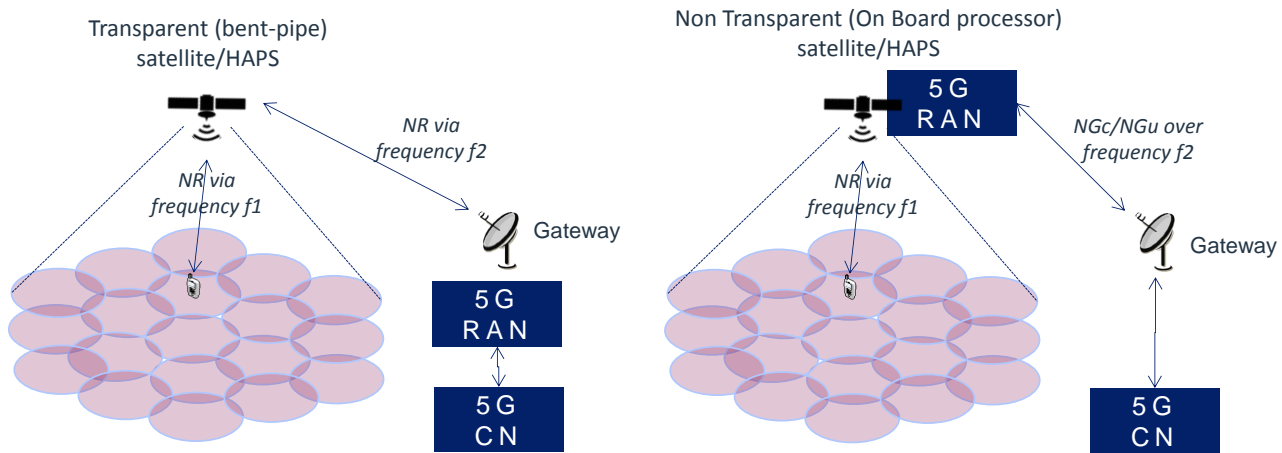


Figure 4.6-1: NTN Beam patterns

4.7 Non-Terrestrial Network architecture options

The possible options of NTN architecture in 5G context based on the RAN architecture principles described in [3] are shown below:



Figure 4.7-1: NTN featuring an access network serving UEs and based on a satellite/aerial with bent pipe payload and gNB on the ground (Satellite hub or gateway level)

In figure 4.7-1, the satellite or the aerial will relay a "Satellite friendly" NR signal between the gNB and the UEs in a transparent manner.



Figure 4.7-2: NTN featuring an access network serving UEs and based on a satellite/aerial with gNB on board

In figure 4.7-2, the satellite or the aerial includes full or part of a gNB to generate/receive a "Satellite friendly" NR signal to/from the UEs. This requires sufficient on board processing capabilities to be able to deploy gNB or Relay Node functions.



Figure 4.7-3: NTN featuring an access network serving Relay Nodes and based on a satellite/aerial with bent pipe payload

In figure 4.7-3, the satellite or the aerial will relay a "Satellite friendly" NR signal between the gNB and the Relay Nodes in a transparent manner.



Figure 4.7-4: NTN featuring an access network serving Relay Nodes and based on a satellite/aerial with gNB

In figure 4.7-4, the satellite or the aerial includes full or part of a gNB to generate/receive a "Satellite friendly" NR signal to/from the Relay Nodes. This requires sufficient on board processing capabilities to be able to deploy gNB or a Relay Node functionality.

NOTE: In the figures above a satellite represents both satellite and aerial platforms.

Table 4.7-1: 5G system elements mapping in NTN architecture

5G elements - NTN elements mapping			
NTN architecture options	NTN Terminal	Space or HAPS	NTN Gateway
A1: access network serving UEs via bentpipe satellite/aerial	UE	Remote Radio Head (Bent pipe relay of Uu radio interface signals)	gNB
A2: access network serving UEs with gNB on board satellite/aerial	UE	gNB or Relay Node functions	Router interfacing to Core network
A3: access network serving Relay Nodes via bent pipe satellite/aerial	Relay Node	Remote Radio Head (Bent pipe relay of Uu radio interface signals)	gNB
A4: access network serving Relay Nodes with gNB on board satellite/aerial	Relay Node	gNB or Relay Node functions	Router interfacing to Core network

4.8 Spectrum

Satellite and Aerial systems operate in allocated frequency bands as per ITU-R/national allocation regime.

5 Non-Terrestrial Networks deployment scenarios

5.1 Scenarios overview

Based on the NTN overview background information presented in clause 4 and in examples of deployment scenarios, defined in the TR 38.913 [5] under clause 6.1.12 "Satellite extension to Terrestrial", the following Non-Terrestrial Network (NTN) reference deployment scenarios are down selected and will be further detailed in the study and used for the evaluations:

Table 5.1-1: Reference Non-Terrestrial Network Deployment scenarios to be considered in the NR-NTN study

Main attributes	Deployment-D1	Deployment-D2	Deployment-D3	Deployment-D4	Deployment-D5
Platform orbit and altitude	GEO at 35 786 km	GEO at 35 786 km	Non-GEO down to 600 km	Non-GEO down to 600 km	UAS between 8 km and 50 km including HAPS
Carrier Frequency on the link between Air / space-borne platform and UE	Around 20 GHz for DL Around 30 GHz for UL (Ka band)	Around 2 GHz for both DL and UL (S band)	Around 2 GHz for both DL and UL (S band)	Around 20 GHz for DL Around 30 GHz for UL (Ka band)	Below and above 6 GHz
Beam pattern	Earth fixed beams	Earth fixed beams	Moving beams	Earth fixed beams	Earth fixed beams
Duplexing	FDD	FDD	FDD	FDD	FDD
Channel Bandwidth (DL + UL)	Up to 2 * 800 MHz	Up to 2 * 20 MHz	Up to 2 * 20MHz	Up to 2 * 800 MHz	Up to 2 * 80 MHz in mobile use and 2 * 1800 MHz in fixed use
NTN architecture options (See clause 4)	A3	A1	A2	A4	A2
NTN Terminal type	Very Small Aperture Terminal (fixed or mounted on Moving Platforms) implementing a relay node	Up to 3GPP class 3 UE [2]	Up to 3GPP class 3 UE [2]	Very Small Aperture Terminal (fixed or mounted on Moving Platforms) implementing a Relay node	Up to 3GPP class 3 UE [2] Also Very Small Aperture Terminal
NTN terminal Distribution	100% Outdoors	100% Outdoors	100% Outdoors	100% Outdoors	Indoor and Outdoor
NTN terminal Speed	up to 1000 km/h (e.g. aircraft)	up to 1000 km/h (e.g. aircraft)	up to 1000 km/h (e.g. aircraft)	up to 1000 km/h (e.g. aircraft)	up to 500 km/h (e.g. high speed trains)
Main rationales	GEO based indirect access via relay node	GEO based direct access	Non-GEO based direct access	Non-GEO based indirect access via relay node	Support of low latency services for 3GPP mobile UEs, both indoors and outdoors
Supported Uses cases, see clause 4	1/ eMBB: multi-connectivity, fixed cell connectivity, mobile cell connectivity, network resilience, Trunking, edge network delivery, Mobile cell hybrid connectivity, Direct To Node multicast/ broadcast	1/eMBB: Regional area public safety, Wide area public safety, Direct to mobile broadcast, Wide area IoT service	1/eMBB: Regional area public safety, Wide area public safety, Wide area IoT service	1/ eMBB: multi-homing, fixed cell connectivity, mobile cell connectivity, network resilience, Trunking, Mobile cell hybrid connectivity	1/ eMBB: Hot spot on demand

The scenarios attributes used in the Table 5.1-1 are described below.

Only the main attributes are discussed in this clause, for simplification purposes. Complementary attributes that should be set up for each scenario are described in the clause 7.

The use cases mentioned in the Table 5.1-1, are described in clause 4.2.1.

5.2 Attributes

Platform orbit and altitude

This attribute stands for the Platform orbit type (GEO, Non-GEO) and its altitude. A platform is either a satellite (alias space-borne vehicle), or a HAPS (airborne vehicle). See clause 4.5 for further characteristics of Air / space borne vehicles.

Carrier frequency between air / space-borne platform and UE

The study addresses the whole frequency range between 0.5 – 100 GHz. For channel modelling and for the identification of areas of impact on the NR, the following frequency bands will be in particular considered:

- For VSAT, Ka band: Downlink: 19.7 - 21.2 GHz, Uplink: 29.5 – 30.0 GHz
- For UE, S band: Downlink: 2170 - 2200 MHz, Uplink: 1980 - 2010 MHz

The UE characteristics are described in clause 4.4.

Beam pattern

Beam pattern stands for "beam coverage pattern". It is described in clause 4.6.

Access scheme

For these scenarios, the FDD (Frequency Division Duplexing) is selected, versus TDD (Time Division Duplexing).

FDD means that the transmitter and the receiver operate at different carrier frequencies. Uplink and downlink sub-bands are separated by the named frequency offset.

Channel Bandwidth (DL + UL)

This scenario attribute stands for the available bandwidth for channels, for DL and for UL. It depends on the used carrier frequencies. For evaluation purposes, we will consider:

- For Satellite and aerial networks operating in frequency bands above 6 GHz, the bandwidth is up to 800MHz on both Downlink and Uplink
- For Satellite and aerial networks operating in frequency bands below 6 GHz, the bandwidth is up to 80MHz on both Downlink and Uplink

NTN architecture options

See clause 4.7.

NTN terminal type

For evaluation purposes:

- The VSAT transmit power will be set to 33dBm (2W), with a 60 cm equivalent aperture diameter (circular polarisation).
- For each 3GPP FDD power class (PC), the maximum output Power is: 33dBm (2W) for PC 1, 27dBm (0.5W) for PC 2 and 23dBm (0.20W) for the PC 3, with an omnidirectional antenna. In a 1st approach and for evaluation purposes, the PC 3 UE will have a Transmit Power set to 23dBm (0.20W).

Relay node is defined in clause 3.1.

See clause 4.4 for further characteristics of UE of satellite / aerial access network.

NTN terminal distribution

This attribute is set to either:

- 100% outdoors UEs,
- 100% indoors UEs,
- Or mixed indoors & outdoors UE distribution

NTN terminal Speed

This attribute is a generic term relative to the transmitter/receiver which is on board the satellite or aerial platform. It stands for:

- High speed / low speed UE
- High speed / low speed platform (such as Trains, Boats embedding base stations)

For evaluation purposes, the selected maximum values are:

- 1000 km/h (e.g. aircraft)
- 500 km/h (e.g. high speed trains)

The effect of the maximum NTN terminal speed as well as satellite or aerial motion are considered in each deployment scenario.

See clause 4.5 for further characteristics on air / space borne platform.

5.3 Doppler and Propagation delay characterisation

5.3.1 Methodology

We shall distinguish between geostationary satellite, non geo stationary satellite and HAPS platforms.

5.3.1.1 Propagation delay

We consider the one way propagation delay as the delay:

- from the Gateway to the UE via the space/airborne platform (bent pipe payload)
- from the space/airborne platform to the UE (regenerative payload)

The Round Trip Time corresponds to the two way propagation delay:

- from the Gateway to the UE via the space/airborne platform and return (bent pipe payload)
- from the space/airborne platform to the UE and return (regenerative payload)

For the propagation delay analysis, we consider a minimum gateway elevation angle of 5° (the elevation angle of the space/air borne platform from the Gateway). While the minimum terminal elevation angle is typically 10°.

The actual propagation delay depends on the space/airborne platform altitude and respective position of the gateway and terminal.

5.3.1.2 Differential delay

The differential delay corresponds to the difference of propagation delays between two chosen points that are at some specific positions within the beam foot print: for example the points can be selected at nadir and Edge of Coverage.

The path to gateway is likely to be the same for all terminals, but this just to simplify the computation.

5.3.1.3 Doppler shift/variation

Doppler shift: Shift of the signal frequency due to the motion of the receiver, the transmitter or both.

Doppler variation rate: During time, the Doppler shift is evolving. This is called the Doppler variation rate or simply Doppler rate.

The Doppler shift and Doppler variation depend on the relative speed of the space/airborne platforms, the speed of the UE, and the carrier frequency.

The figure below recalls the basic geometry of the system. The carrier frequency of the signal received at satellite is affected by the motion of the transmitter. The Doppler on the signal received by the UE from the satellite is also

impacted by the motion of the UE in addition to the motion of the satellite or HAPS. Since both the air/spaceborne vehicle and the UE are moving relatively to the Earth, their respective effects can be added algebraically.

In the present document, we can follow a non-relativistic approach to compute the Doppler shift and variation rate given that the ratio between the relative speed of the transmitter or receiver and the light velocity is negligible.

- For a terminal at a speed of 1000 km/h (or 0.277 km/s): this ratio is $0.277/300000 = 0.000009$
- For a relative speed of Non-Geo satellite of 7.5 km/s (orbital speed): the ratio is 0.000025

The signal received by the satellite at a nominal carrier frequency F_0 is affected by a Doppler shift.

The Doppler shift is computed with the formula:

$$\text{Doppler shift formula: } \Delta F = F_0 * V * \cos(\theta) / c$$

Where

- F_0 : nominal carrier frequency
- V = UE velocity
- θ is the angle between the velocity vector V of the mobile (Transmitter or receiver) and the direction of propagation of the signal between the UE and the space/airborne platform.

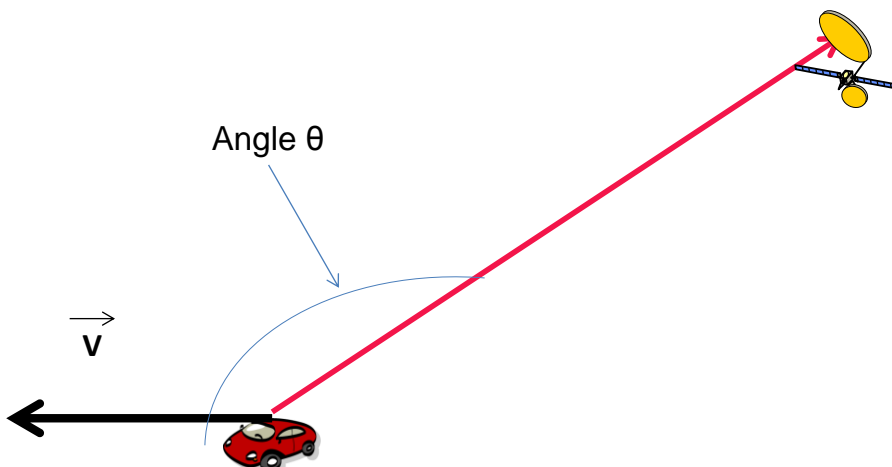


Figure 5.3.1.3-1: Definition of the theta angle between space/airborne platform and the direction of the UE in motion

When a transmitter is moving away from a receiver, ΔF is negative.

When a transmitter is moving towards a receiver, ΔF is positive.

The Doppler shift variation corresponds to the variation of the Doppler shift over time. In other words, it refers to the derivative of the Doppler shift function of time.

5.3.2 Geo-stationary platforms

Geostationary platform are orbiting at 35786 km altitude in the equatorial plan, and is fixed with respect to the earth. Nevertheless, due to some imperfection of the terrestrial potential, the satellite has some motion around its orbital position, as described in a further section.

5.3.2.1 Propagation delay

One should distinguish between

- Bent pipe payloads
 - One way propagation delay is the sum of feeder link propagation delay and user link propagation delay, thus the propagation delay between Gateway and UE via the satellite
 - Round Trip Time is the delay over the path, Gateway-Satellite-UE-Satellite-Gateway. It corresponds to twice the one way propagation delay
- Regenerative payloads (decoding/coding on board)
 - One way propagation delay is the propagation delay between the satellite and the UE
 - Round Trip Time is the delay over path: satellite-UE-satellite

In both cases the transit time and/or processing time are not taken into account.

For the propagation delay computation, the min elevation angle is set at 5° for the Gateway, and is set at 10° for the terminal can be set at various elevation angles, but we consider that the worst case is 10° elevation angle.

The following table summarises the different situation and the different distances in km and the different propagation delays in ms.

Table 5.3.2.1-1: Propagation delays for GEO satellite at 35786 km

GEO at 35786 km			
Elevation angle	Path	D (km)	Time (ms)
UE :10°	satellite - UE	40586	135.286
GW : 5°	satellite - gateway	41126.6	137.088
90°	satellite - UE	35786	119.286
Bent Pipe satellite			
One way delay	Gateway-satellite_UE	81712.6	272.375
Round trip Time	Twice	163425.3	544.751
Regenerative Satellite			
One way delay	Satellite -UE	40586	135.286
Round Trip Time	Satellite-UE-Satellite	81172	270.572

5.3.2.2 Differential delay

In this clause, we compute the differential delays between specific positions: for instance at nadir and Edge of Coverage.

The path to gateway is supposed to be the same for all UEs.

Table 5.3.2.2-1: Differential Delay for GEO satellite

GEO at 35786 km		
	Delta D (km)	Delta Time (ms)
Differential One way delay between nadir and EOC paths	4800	16
Percentage of the difference compared to maximum delay (bent pipe)		5.9 %
Percentage of the difference compared to maximum delay (regenerative satellite)		11.9 %

For Geostationary satellites we have also taken a satellite located at 10 ° E and we have computed different differential delays between some points, provided all points were linked to the same Gateway.

The table is valid for both bent pipe satellite and regenerative satellite.

Table 5.3.2.2-2: Differential delay examples

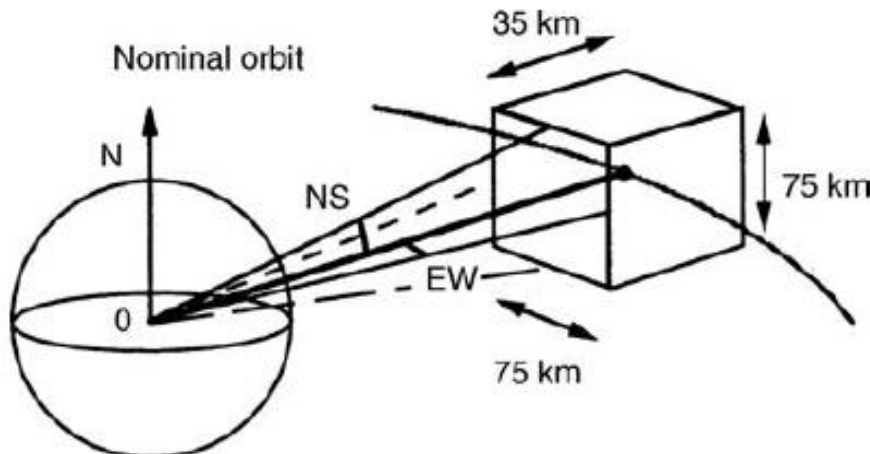
Duo of Cities	Delta Time(ms)
Paris-Marseille	1.722
Lille-Toulouse	2.029
Brest-Strasbourg	0.426
Oslo-Tromsoe	-3.545
Oslo-Svalbard	-6.555
Oslo-Paris	3.487

5.3.2.3 Doppler shift

In principle, the Geostationary satellite is fixed and therefore no Doppler shift is induced except that due to possible UE motion.

In reality the satellite is moving around its nominal orbital position, due to perturbations (e.g. sun, moon) and to non-spherical component earth attraction which impact the earth gravitational force.

The satellite must be kept to inside a box described here below. The satellite is typically maintained inside a box that has the following dimensions, by thrust or plasmic propulsion.

**Figure 5.3.2.3-1: Trajectory box for a Geostationary satellite**

Without maintaining the satellite inside the box, the motion could be a higher value like inclination up to $\pm 6^\circ$.

We take the hypothesis that the satellite is kept in the limited box. The trajectory that the satellite follows is an "8" as shown in next figure. The plane is seen from the centre of the Earth. The blue arrows in the next figure indicate the sense of motion of the satellite around its orbital position So.

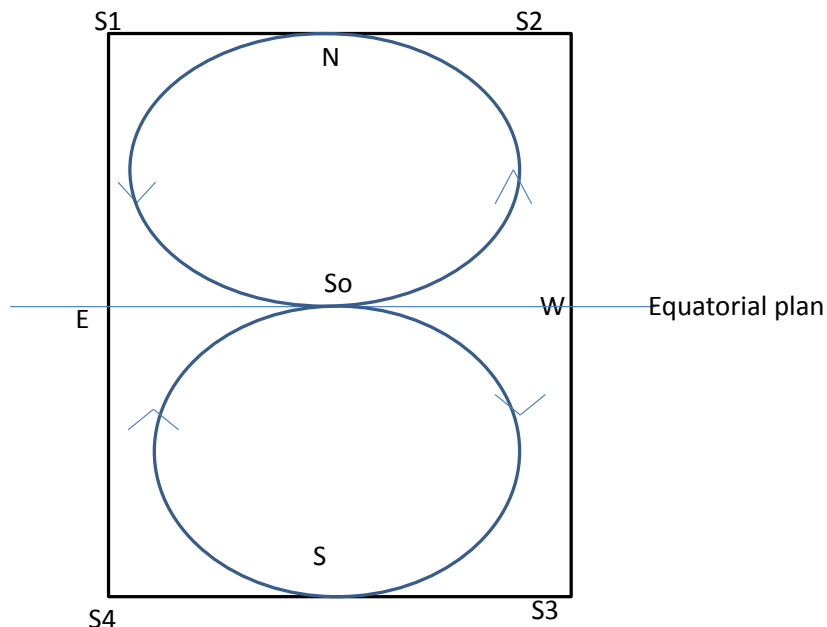


Figure 5.3.2.3-2: Geostationary satellite trajectory

In the figure above, the trajectory of the satellite is represented as seen from a point at the equator having same longitude as the nominal Geostationary satellite orbital position.

A geostationary satellite will cover the whole trajectory in 24 Hours.

The average tangential velocity of a geostationary satellite with respect to an earth point is around 2.74 m/s.

Satellite maintained in a typical trajectory box (see figure 2) characterized by

- +/- 37.5 km in both latitude and longitude directions corresponding to an aperture angle of +/- 0.05 °.
- +/- 17.5 km in the equatorial plane.

To illustrate the Doppler shift computation using the Doppler Shift formula, we shall consider some concrete cases:

- Geostationary Satellite at 10 ° E (over Europe)
- First a High Speed Train (500 km/h) from Paris to Lille (France) and from Paris to Strasbourg (France)
- Secondly an air plane (1000 km/h and 10 km altitude) moving in the same directions.

We first compute the Doppler shift while supposing the satellite has no motion, but on a moving UE, and secondly we evaluate the impact of the satellite motion on a fixed UE.

First case: Satellite is considered fixed with respect to earth point

In the high speed train going north from Paris the obtained Doppler shift is provided here below

Table 5.3.2.3-1: Examples of Doppler shift with GEO and a terminal on board a High Speed Train in opposition direction

Frequency	2GHz	20 GHz	30 GHz
Doppler shift (Hz)	-707	-7074	-10612

Table 5.3.2.3-2: Example of Doppler shift with GEO and a terminal on board an aircraft in opposition direction

Frequency	2GHz	20 GHz	30 GHz
Doppler shift (Hz)	-1414	-14149	-21224

And going from Paris to east.

Table 5.3.2.3-3: Example of Doppler shift with GEO and in High Speed Train

Frequency	2GHz	20 GHz	30 GHz
Doppler shift (Hz) in Paris	147	1478	2217
Doppler shift (Hz) in Lille	138	1383	2075

Table 5.3.2.3-4: Example of Doppler shift with GEO and in a plane

Frequency	2GHz	20 GHz	30 GHz
Doppler shift (Hz)	295	2956	4434

The Doppler shift is highest for a platform moving along longitude compared to a moving platform along latitude.

In the figure below, we consider a train travelling North from the Equator at a constant speed of 500 km/h. The two extreme points in the figure are 3600 seconds apart. The Doppler shift plotted as a function of the latitude. The maximum rate of change of Doppler shift is approximately -23 mHz/s

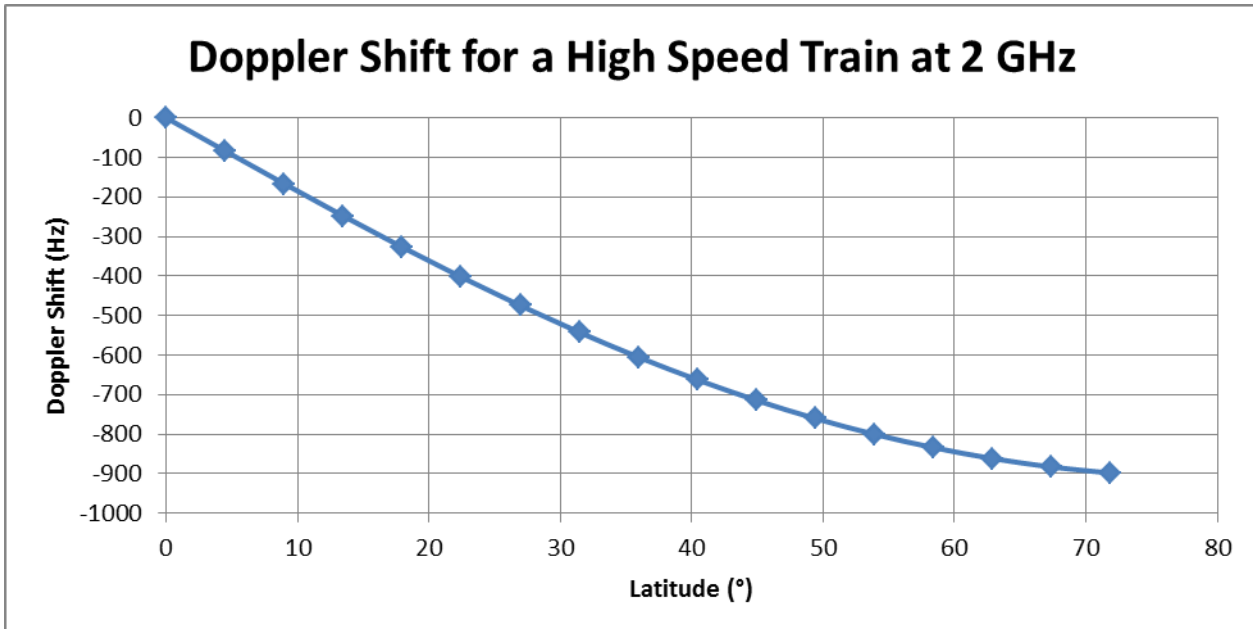


Figure 5.3.2.3-3: Doppler Shift at 2 GHz for a High Speed Train travelling along a longitude (North direction)

In the figure below, we consider an aircraft travelling North from the Equator at a constant speed of 1000 km/h. Similarly to the previous plot, the two extreme points are 1800 seconds apart. The Doppler shift plotted as a function of the latitude. The maximum rate of change of Doppler shift is approximately -90 mHz/s.

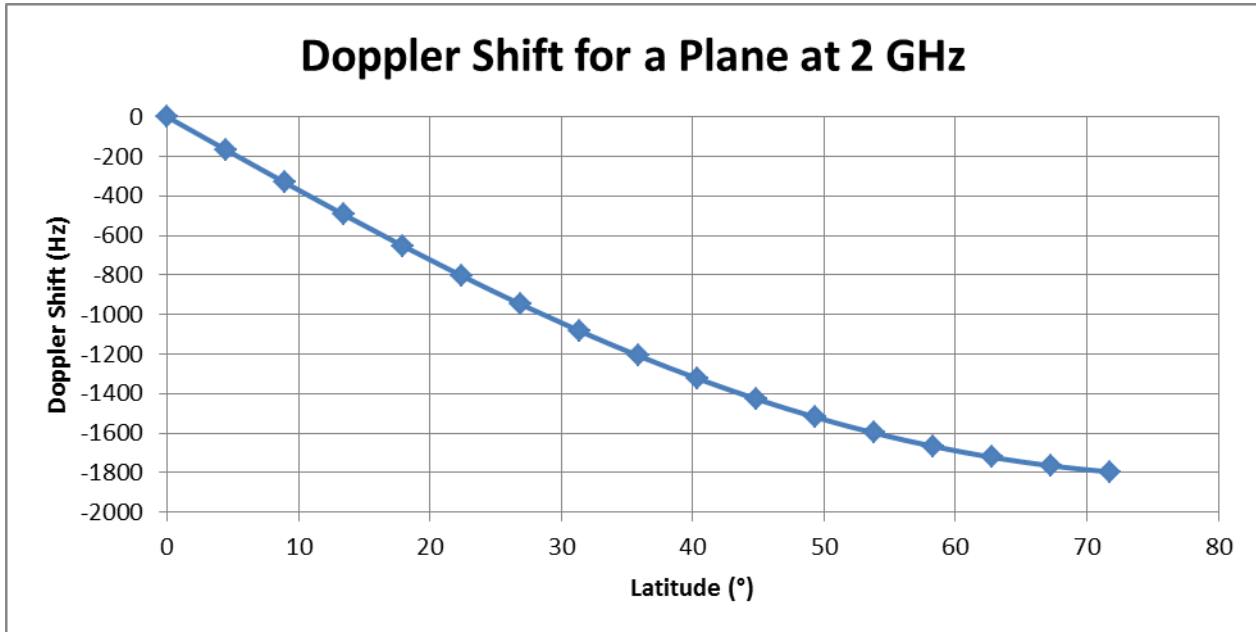


Figure 5.3.2.3-4: Doppler Shift at 2 GHz for an aircraft travelling north

However these values are reached only when $\cos(\theta)$ is equal to 1 or -1. Where θ is the angle between the vector speed and the direction of wave propagation (the axis UE-Satellite).

Second case: Satellite is moving on its "8"

When satellite is moving from S2 to S1, the Doppler shift in Paris is the following

Table 5.3.2.3-4: Example of Doppler shift when satellite is moving

Frequency	2GHz	20 GHz	30 GHz
Doppler shift (Hz)	-0.25	-2.4	-4.0

When satellite is moving from S1 to S4, the Doppler shift in Paris is the following

Table 5.3.2.3-5: Example of Doppler shift when satellite is moving

Frequency	2GHz	20 GHz	30 GHz
Doppler shift (Hz)	2.25	22.5	34

Doppler shift is higher than in the previous case, though still very low compared to the case of Non GEO satellites.

When satellite is in near GEO orbit with inclination up to 6° , the Doppler shift can reach around 300 Hz at 2 GHz, then 3000 Hz at 20 GHz and 4500 Hz at 30 GHz, which are still compatible with OFDM.

5.3.3 Aerial vehicle

The altitude of aerial vehicle also called UAS (Unmanned Aircraft Systems) can be between 8 and 50 km, including HAPS. HAPS is a station located on an aerial object at an altitude of 20 to 50 km and at a specified, nominal, fixed point relative to the Earth.

The general UAS based system architectures are presented in the following picture.

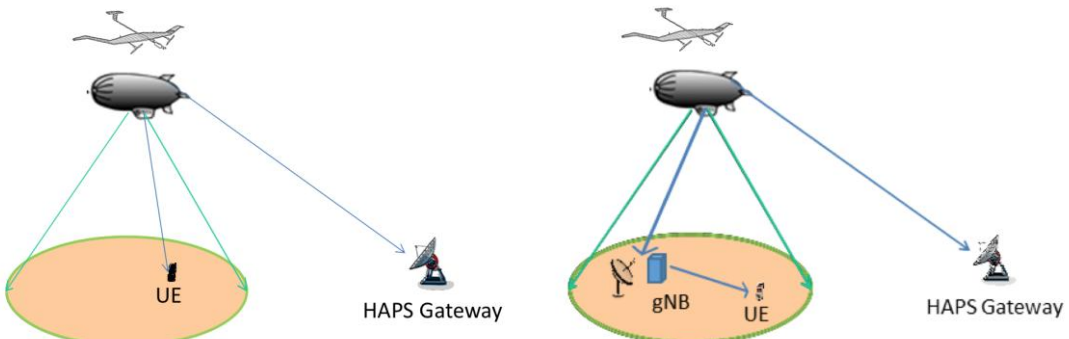


Figure 5.3.3-1: UAS based system architectures

The coverage can be divided into small cells, and usually the minimum elevation angle for a Mobile Terminal is 5°.

The platform can move around its nominal position within a few kilometres at a maximum tangential velocity of 15 m/s.

This can result in maximum Doppler shift (in absolute value) of 100 Hz @ 2GHz, 1000 Hz @ 20 GHz and 1500 Hz @ 30 GHz due to Haps motion.

In S band, at 100 km/h a car will suffer a Doppler shift of +/- 185 Hz maximum

The Doppler variation can be evaluated with a car moving from one edge to another at 100 km/h , covering 450 km . The Doppler variation will be around -0.0025 Hz/s. So no impact on demodulation

At 5° elevation angle the distance to the aerial vehicle is 229 km, and if we suppose the Gateway is at same distance

- One way delay is around 1.526 ms
- Round Trip Time is 3.053 ms
- Differential delay between nadir and Edge of Coverage: 0.697 ms

5.3.4 Non geostationary satellites

The Non-Geostationary case comprises three examples

- LEO at 600 km
- LEO at 1500 km
- MEO at 10000 km

5.3.4.1 Propagation delay

In the case of bent pipe satellites, one way propagation delay is the sum of feeder link propagation delay and user link propagation delay, thus the propagation delay between Gateway and UE.

In the case of regenerative satellite, one way propagation delay is the satellite to UE propagation delay.

In both cases the transit time and/or processing time are not taken into account.

In the case of bent pipe satellite, the Round Trip Time is the physical path duration of the path : Gateway-Satellite-UE-Satellite-Gateway, that is in fact twice the one way propagation delay.

In the case of regenerative satellite, the round trip delay is the delay corresponding to the following path :satellite-UE-satellite.

In the computation, Gateway is set at 5° (TBC) elevation angle, and terminal can be set at various elevation angles, but we consider that the reference case is 10° elevation angle for the propagation delay computation.

The following table summarises the different situations and the different distances in km and the different propagation delays in ms.

The results for the three cases of NGSO satellites are summarized in the next table.

Table 5.3.4.1-1: Propagation delays for different NGSO satellites (altitude and payload types)

Elevation angle	Path	LEO at 600 km		LEO at 1500 km		MEO at 10000 km	
		Distance D (km)	Delay (ms)	Distance D (km)	Delay (ms)	Distance D (km)	Delay (ms)
UE: 10°	satellite - UE	1932.24	6,440	3647.5	12,158	14018.16	46.727
GW: 5°	satellite - gateway	2329.01	7.763	4101.6	13.672	14539.4	48.464
90°	satellite - UE	600	2	1500	5	10000	33.333
Bent pipe satellite							
One way delay	Gateway-satellite_UE	4261.2	14.204	7749.2	25.83	28557.6	95.192
Round Trip Delay	Twice	8522.5	28.408	15498.4	51.661	57115.2	190.38
Regenerative satellite							
One way delay	Satellite -UE	1932.24	6.44	3647.5	12.16	14018.16	46.73
Round Trip Delay	Satellite-UE-Satellite	3864.48	12.88	7295	24.32	28036.32	93.45

5.3.4.2 Differential delay

In this clause, we compute the differential delays between some specific positions : for instance at nadir and Edge of Coverage.

The path to gateway is supposed to be the same for all terminals.

Table 5.3.4.2-1: Differential Delay for LEO satellite

	LEO 600 km		LEO 1500 km		MEO 10000 km	
	Delta Distance	Delta Delay	Delta Distance	Delta Delay	Delta Distance	Delta Delay
Differential One way delay between nadir and EOC paths	1332.2 km	4.44 ms	2147.5 km	7.158 ms	4018.16 km	13.4 ms
Percentage of the maximum delay (bent pipe)		31.26 %		27.8 %		14.1 %
Percentage of the maximum delay (regenerative satellite)		67 %		58.9 %		28.7 %

5.3.4.3 Doppler Shift and variation rate

The following picture summarizes the methodology used for Non Geostationary systems. We evaluate the Doppler shift which is maximum when the UE is located in the orbital plane.

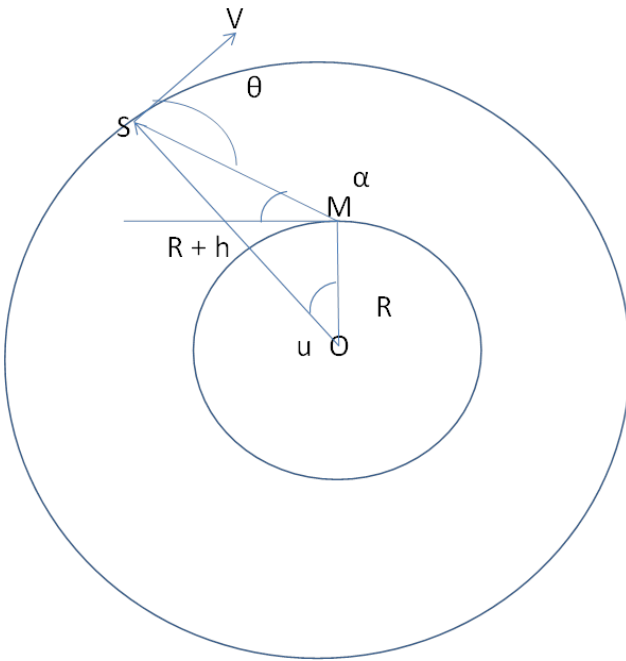


Figure 5.3.4.3-1: System Geometry for Doppler computation

The picture describing the system geometry shows the satellite "S" on its circular orbit. The vector V corresponds to the orbital speed vector.

The Doppler shift is computed for a Mobile Terminal "M" located in the orbital plan, and corresponds to the maximum value.

One of the impacting factors on the Doppler shift value is the angle between \overrightarrow{SM} and the speed vector \vec{V} . Angle called θ .

- The satellite is at an altitude h , and R is the earth radius.
- The satellite has the velocity \vec{V} , and the transmitted frequency is F_c .
- The Doppler shift value F_d due to satellite motion is expressed by the formula

$$F_d = \frac{F_c}{c} \times V \times \cos \theta = \frac{F_c}{c} \times V \times \frac{\sin u}{\sqrt{1+\gamma^2 - 2\gamma \cos u}}$$

- Where
 - θ is the angle between satellite velocity and \overrightarrow{SM} .
 - u the angle between \overrightarrow{OM} and \overrightarrow{OS}
 - \overrightarrow{OM} is the vector between earth centre and point on earth
 - \overrightarrow{OS} is the vector between earth centre and the satellite
 - angle u is varying with the satellite motion: $u(t) = V*t/(R+h)$ with t the time
 - α is the elevation angle to the satellite of the UT in M.
 - γ can be computed as follow:
- $\gamma = \frac{R+h}{R}$
- The Doppler formula is obtained after some computation.

At this altitude the speed of the satellite in circular orbit is 7.5622 km.s^{-1} . So we can use non-relativistic approximation to compute Doppler shift.

Also at first order we neglect the speed of earth which is 327 m/s at 45° latitude and 464 m/s at the equator.

For all Non GSO cases, the satellite speeds are the following

- At 600 km : $V = 7.5622 \text{ km.s}^{-1}$
- At 1500 km : $V = 7.1172 \text{ km.s}^{-1}$
- At 10000 km : $V = 4.9301 \text{ km.s}^{-1}$

5.3.4.3.1 Case at 2 GHz

Both (Downlink) D/L and (Uplink) U/L the signal is around 2GHz and we limit the curves at 2 GHz.

If we consider now a moving UE at 1000 km/h, and moving in the same direction than the satellite, we have determined the worst case impact in the following graph. We can define the bounds by adding the Doppler shift due to the satellite motion and the Doppler shift due to the UE motion.

All the curves are gathered in the next graphs, showing clearly the boundaries of the Doppler shift depending on the sense of motion between the satellites and the UE.

Three NON GSO satellites cases are provided.

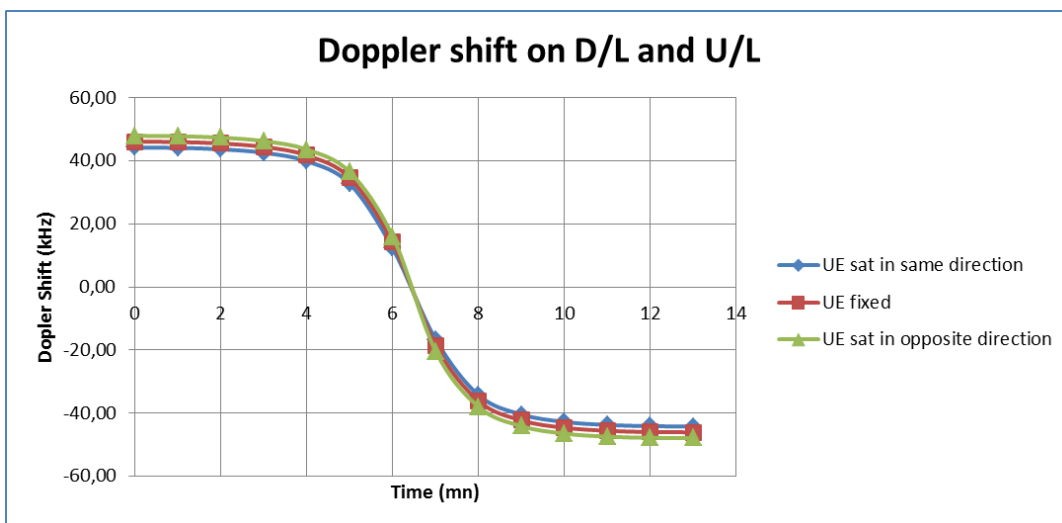


Figure 5.3.4.3.1-1: Case with 2 GHz signal at 600 km on D/L and U/L: fixed UE and UE in motion

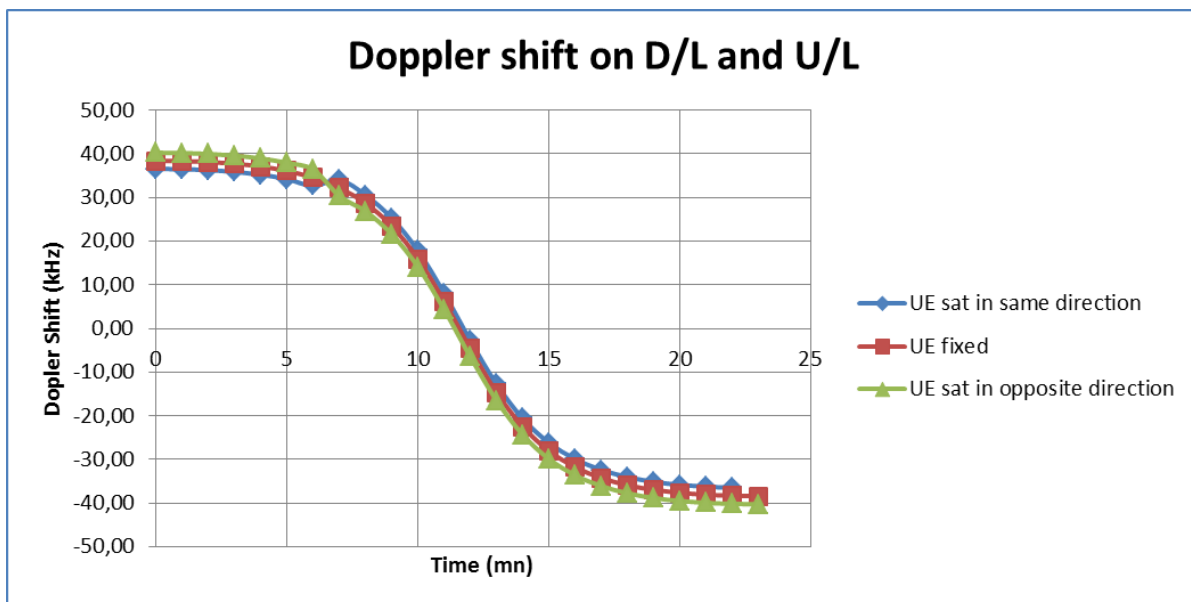


Figure 5.3.4.3.1-2: Case with 2 GHz signal at 1500 km: fixed UE and UE in motion

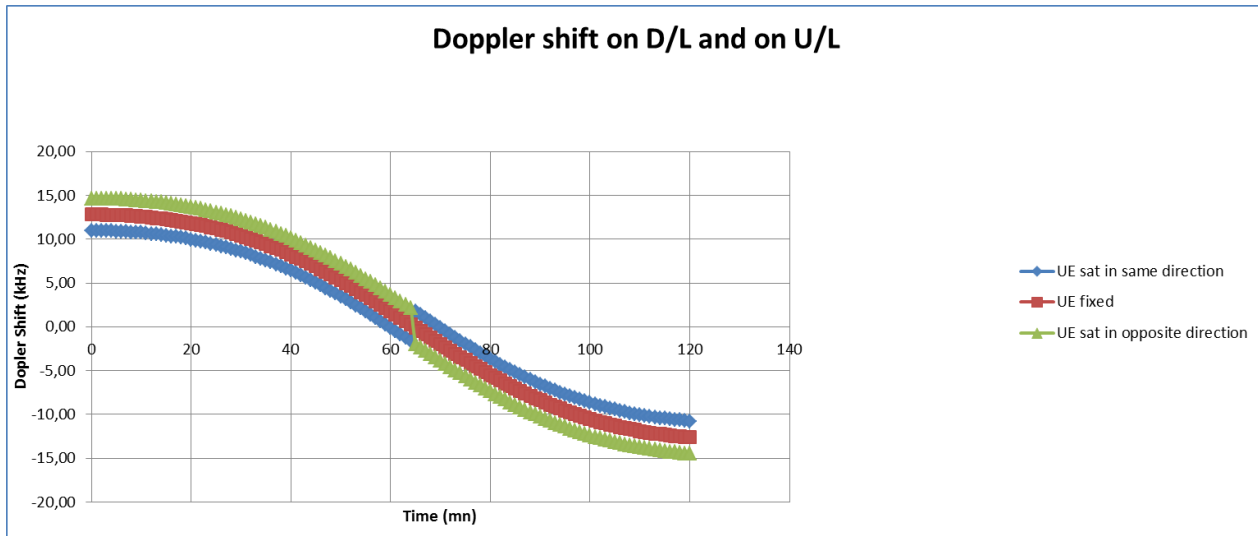


Figure 5.3.4.3.1-3: Case with 2 GHz signal at 10000 km: fixed UE and UE in motion

5.3.4.3.2 Case in Ka band

There are two cases

- Downlink at 20 GHz
- Uplink at 30 GHz

If we consider now a moving UE at 1000 km/h, and moving in the same direction than the satellite, we have determined the worst case impact in the following graph.

This impact is at maximum 18 kHz in one sense or the other at 20 GHz, and 27 kHz at 30 GHz, all the curves are gathered in the next graph, showing clearly the boundaries of the Doppler shift depending on the sense of motion between the satellite and the UE.

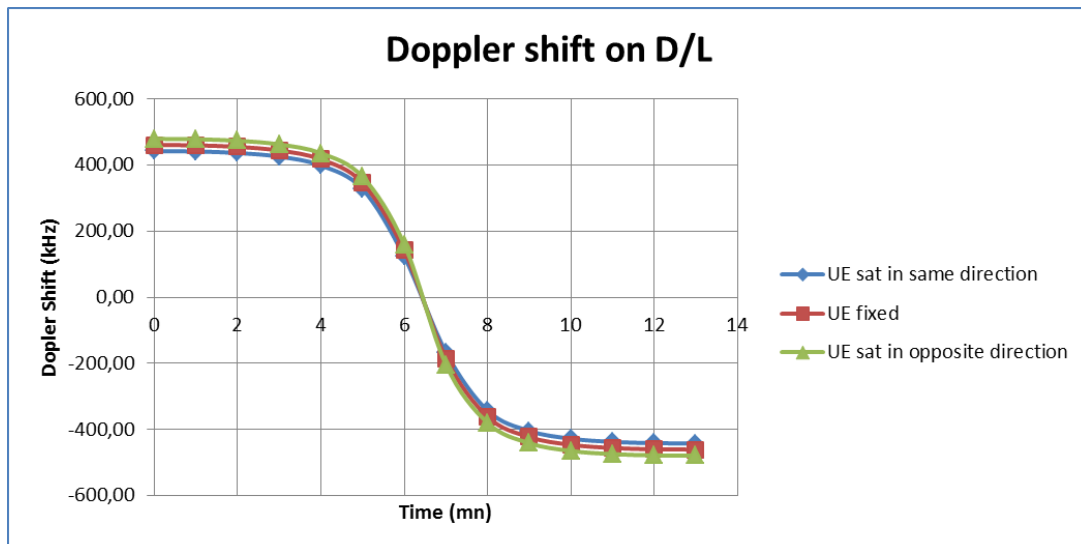


Figure 5.3.4.3.2-1: Case with 20 GHz signal at 600 km on D/L: fixed UE and UE in motion

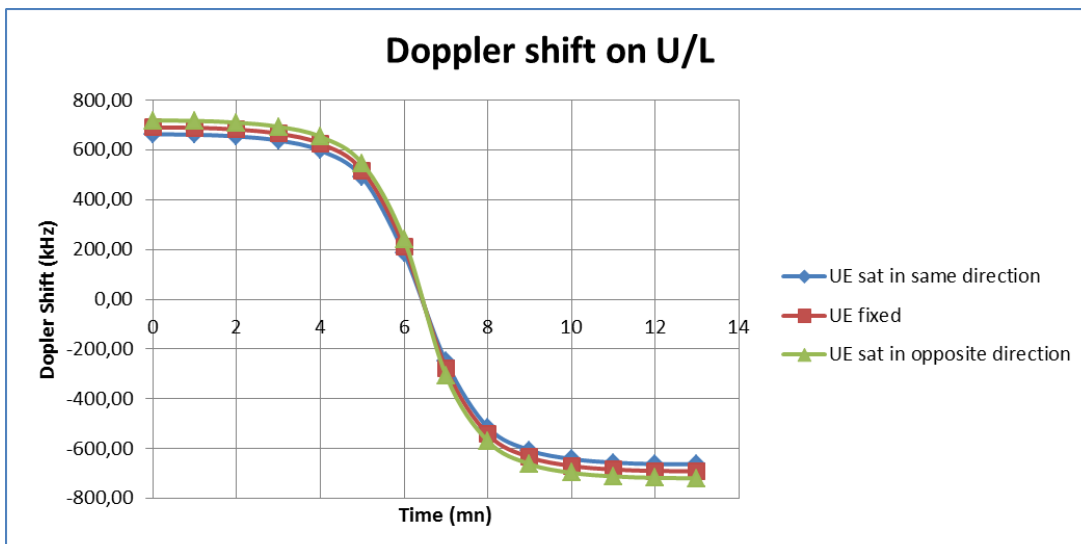


Figure 5.3.4.3.2-2 Case with 30 GHz signal at 600 km on D/L: fixed UE and UE in motion

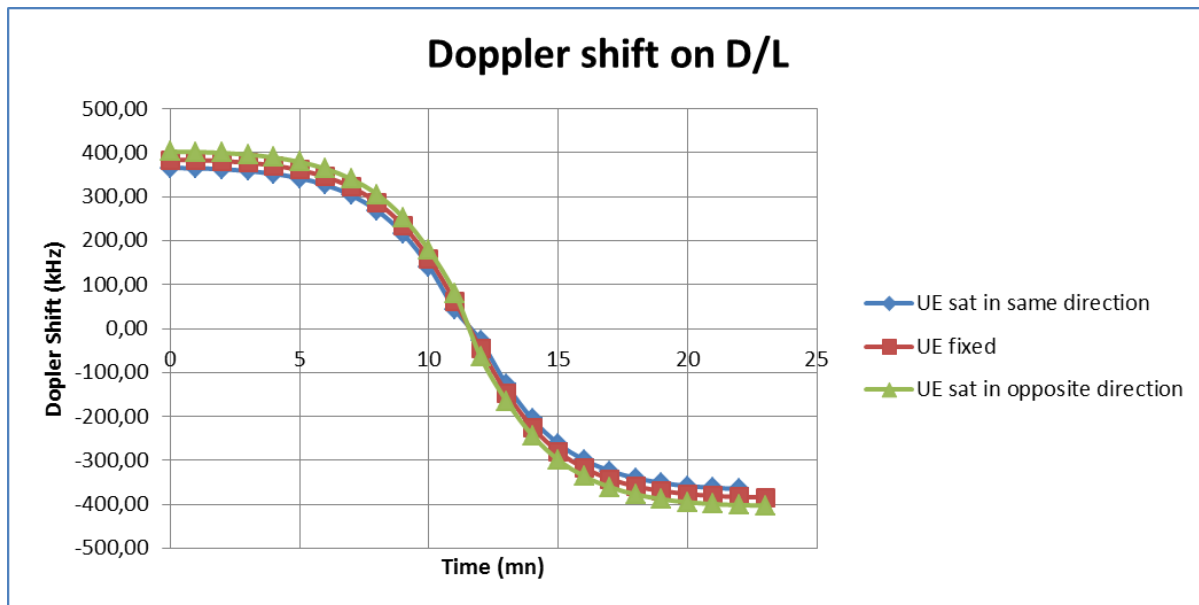


Figure 5.3.4.3.2-3: Case with 20 GHz signal at 1500 km on D/L: fixed UE and UE in motion

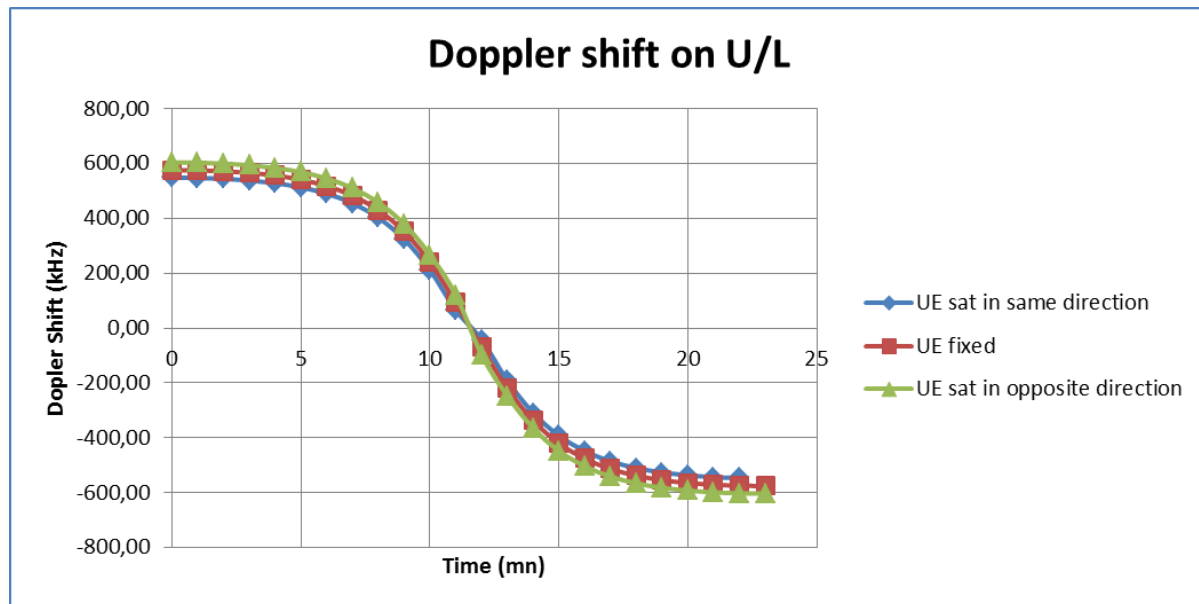


Figure 5.3.4.3.2-4: Case with 30 GHz signal at 1500 km on D/L: fixed UE and UE in motion

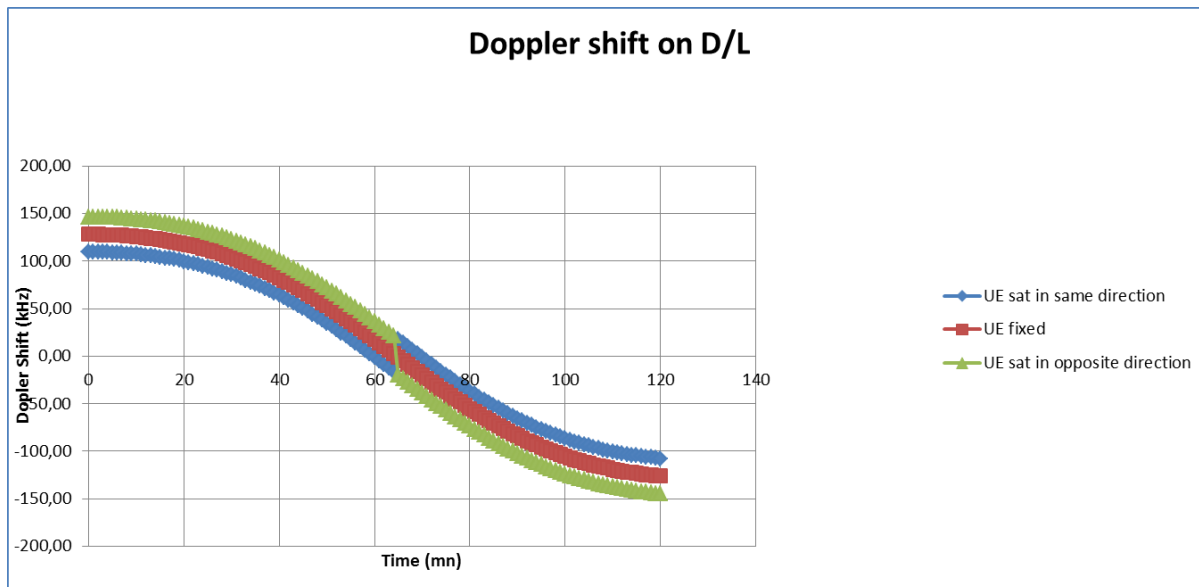


Figure 5.3.4.3.2-5: Case with 20 GHz signal at 10000 km on D/L: fixed UE and UE in motion

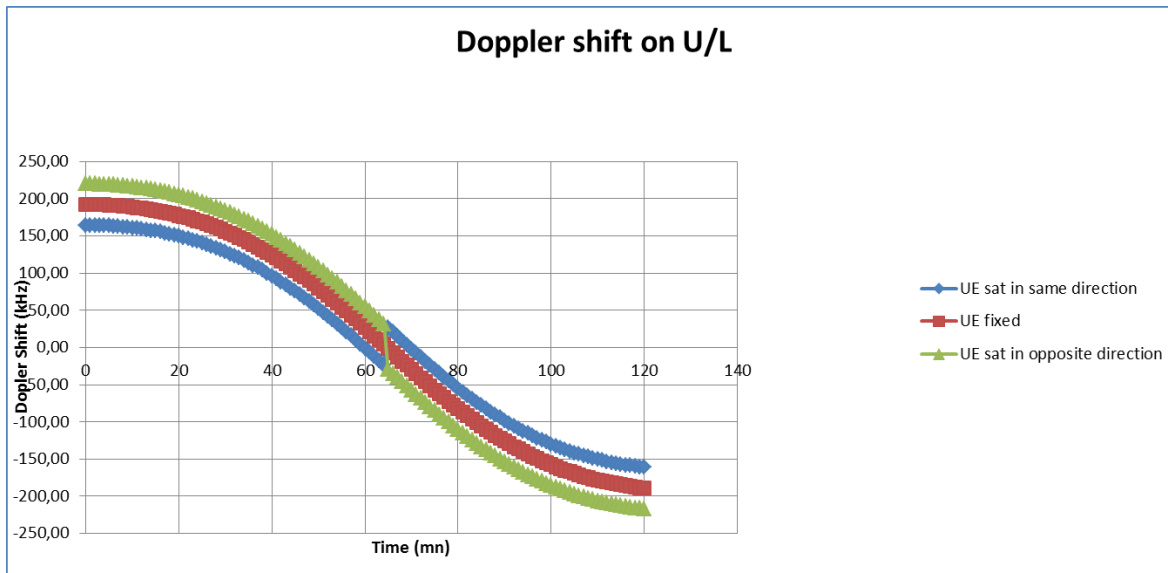


Figure 5.3.4.3.2-6: Case with 30 GHz signal at 10000 km on D/L: fixed UE and UE in motion

The different cases are summarized here below with the ratio of maximum Doppler shift in absolute value to the central frequency.

Table 5.3.4.3.2-7: Summary of Doppler shift and shift variation for different altitudes

Frequency (GHz)	Max Doppler	Relative Doppler	Max Doppler shift variation	
2	+/- 48 kHz	0.0024 %	- 544 Hz/s	LEO at 600 km altitude
20	+/- 480 kHz	0.0024 %	-5.44 kHz/s	
30	+/- 720 kHz	0.0024 %	-8.16 kHz/s	
2	+/- 40 kHz	0.002 %	-180 Hz/s	LEO at 1500 km altitude
20	+/- 400 kHz	0.002 %	-1.8 kHz/s	
30	+/- 600 kHz	0.002 %	-2.7 kHz/s	
2	+/- 15 kHz	0.00075 %	-6 Hz/s	MEO at 10000 km altitude
20	+/- 150 kHz	0.00075 %	-60 Hz/s	
30	+/- 225 kHz	0.00075 %	-90 Hz/s	

Note that the Maximum Doppler shift variation in absolute value is always negative and observed when the Doppler shift is zero.

5.3.4.4 Doppler Shift and variation rate

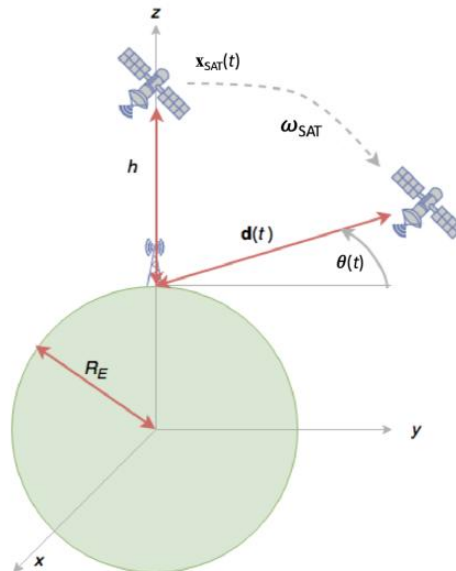
The following picture summarizes the methodology used to compute Doppler shift for Non Geostationary satellite systems. It assumes a Cartesian coordinate system such that the moving satellite and the receiver are on the y-z plane. The Doppler shift experienced by a stationary receiver can be computed as follows as a function of time:

$$f_d(t) = \frac{f_0}{c} \frac{\mathbf{d}(t)}{|\mathbf{d}(t)|} \frac{\partial \mathbf{x}_{SAT}(t)}{\partial t}$$

where f_0 is the carrier frequency, $\mathbf{d}(t)$ is the distance vector between the satellite and the receiver, and $\mathbf{x}_{SAT}(t)$ is the vector of the satellite position. These vectors can be expressed as:

$$\begin{aligned}\mathbf{d}(t) &= [0 \quad (R_E + h) \sin(\omega_{SAT} t) \quad (R_E + h) \cos(\omega_{SAT} t) - R_E]^T \\ \mathbf{x}_{SAT}(t) &= [0 \quad (R_E + h) \sin(\omega_{SAT} t) \quad (R_E + h) \cos(\omega_{SAT} t)]^T\end{aligned}$$

where R_E is the Earth radius, h is the satellite altitude, and ω_{SAT} is the satellite angular velocity.

**Figure 5.3.4.4-1: System geometry for Doppler computation (Satellite moves in the Y-Z plane)**

After some mathematical manipulation [7], the Doppler shift as a function of the elevation angle is computed in a closed-form expression as follows:

$$f_d(t) = \frac{f_0}{c} \omega_{SAT} R_E \cos[\theta(t)]$$

where the angular velocity is $\omega_{SAT} = \sqrt{\frac{GM_E}{(R_E+h)^3}}$, with G the gravitational constant and M_E the Earth mass.

If the receiver is placed on board an aircraft or a high speed train, there will be an additional term of Doppler shift resulting from its own velocity. In case of Non Geostationary satellites, the Doppler shift due to satellite movement is much higher than the one caused by UE movement. For GEO and HAPS, the Doppler shift component is mainly caused by the UE movement.

5.3.5 Synthesis for each scenarios

Following table summarises the different Doppler shift, Doppler Shift variation and propagation delays. The main impairments are the Doppler shifts and Doppler variation in deployment scenarios D3 and D4. (Non-geostationary platforms at 600 km).

Table 5.3.5-1: Summary of Doppler shift, Doppler Shift variation and propagation delay for LEO at 600 km, GEO and HAPS

	Deployment-D1	Deployment-D2	Deployment-D3	Deployment-D4	Deployment-D5	Cellular (10 km Radius)
Platform orbit and altitude when relevant	GEO at 35 786 km	GEO at 35 786 km	Non-GEO down to 600 km	Non-GEO down to 600 km	Airborne vehicle up to 20 km	
Frequency band	Ka band	S band	S band	Ka band	S band (Below 6 GHz)	S band
Max One way Propagation delay (ms)	Bentpipe: 272.37 ms gNB on board: 135.28 ms	272.37 ms	14.204 ms	14.204 ms	1.526 ms	0.03333 ms
Max Differential delay (ms)	16 (between Edge of satellite coverage and Nadir)	16 (between Edge of satellite coverage and Nadir)	4.44 (between Edge of satellite coverage and Nadir)	4.44 (between Edge of satellite coverage and Nadir)	0.697 (between Edge of satellite coverage and Nadir)	0.00333 (between cell centre and cell edge) equal to maximum delay
Max Doppler shift in kHz	For plane @ 20 GHz: +/- 18.51 kHz @ 30 GHz: +/- 27.7 kHz	For plane 1.851 kHz @ 20 GHz	+/- 48 kHz	@ 20 GHz : +/- 480 kHz @ 30 GHz : +/- 720 kHz	@ 2 GHz: +/- 100 Hz mainly due to platform motion	In case of UE on board a high speed train: +/- 925 Hz
% of the carrier frequency (Ratio of Doppler Shift over the central signal frequency)	10^{-4} %	10^{-4} %	0.0024%	0.0024%		
Max Doppler variation in Hz/s.	Negligible	Negligible	-544 Hz/s @ 2 GHz	-5.44 kHz/s @ 20GHz (Downlink) -8.16 kHz/s @ 30 GHz (uplink)	Negligible	Negligible

NOTE : In some cases like UE on board an aircraft during taking off, the acceleration can add a supplementary Doppler variation in absolute value of respectively 262 Hz/s @ 20 Ghz, and 393 Hz/s @ 30 GHz.

6 Non-Terrestrial Networks channel models

6.1. Status/expectation of existing information for satellite/HAPS channels

6.1.1 Channel modeling works outside of 3GPP

ITU recommendations are encompassing most recent works and measurements on satellite channel models.

- ITU-R P.681 [10] defines the Land Mobile Satellite channel with measurements up to 20 GHz
- ITU-R P.618 [11] describes atmospheric effects such as gas attenuation, scintillation, rain and cloud attenuation.

6.1.2 Targeted user environment

Only outdoor conditions are considered for satellite operations, since performance requirements are not expected to be met with the available link budget for indoor communications.

Since HAPS are closer to the Earth, resulting in less path loss than in satellite access networks, additional indoor conditions are also considered for HAPS.

Several user environments will be considered, depending on the frequency band: open, rural, suburban, urban and dense urban. In open environments (such as fixed terminals or terminals mounted on boats/aircrafts), an AWGN channel is assumed.

6.1.3 Modeling objectives

The requirements for channel modelling are as follows:

- Support a frequency range from 0.5 GHz up to 100 GHz. Two frequency bands are targeted in particular: below 6 GHz and Ka bands. For Ka band communications, the uplink frequency is around 30 GHz while the downlink frequency is around 20 GHz.
- Accommodate UE mobility. For satellite channel models, mobility speed up to 1000 km/h is supported; this corresponds to aircrafts that can be served by satellite access. For HAPS channel models, mobility speed up to around 500 km/h is supported, corresponding to high speed trains.

6.2 Differences between satellite/HAPS and cellular channel modelling

Figures 6.2-1 and 6.2-2 compare the macro-cellular and satellite access links in NLOS and LOS cases, respectively. The terrestrial propagation is quite similar: multipath propagation is caused by objects near the user. However, the angular spread from satellite is almost zero (due to its distant location) while it can still be several degrees from the base station.

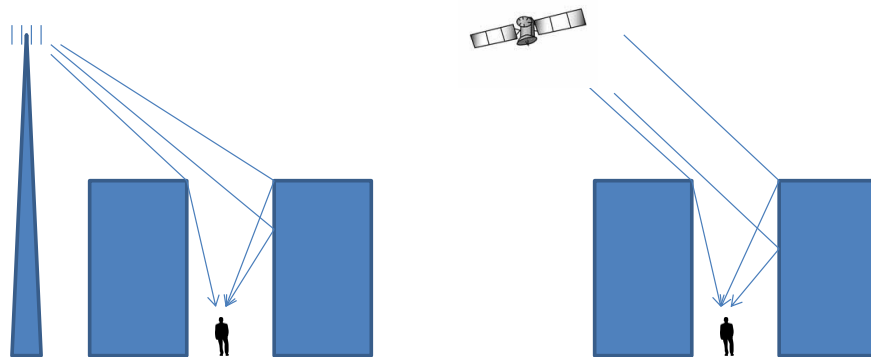


Figure 6.2-1: Macro-cellular vs. satellite channel, NLOS

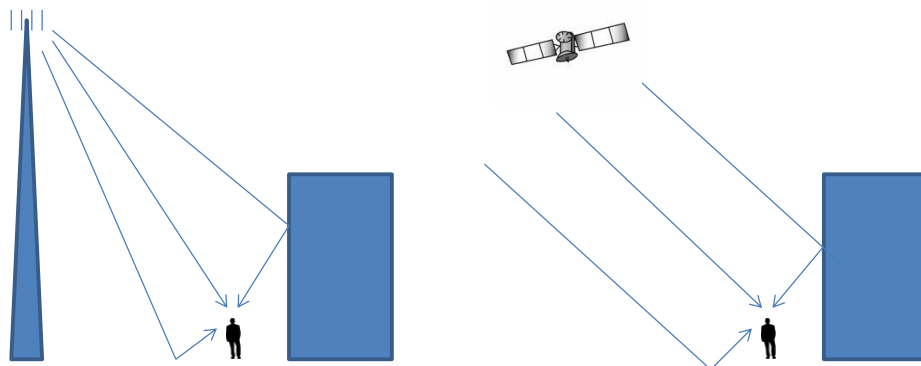


Figure 6.2-2: Macro-cellular vs. satellite channel, LOS

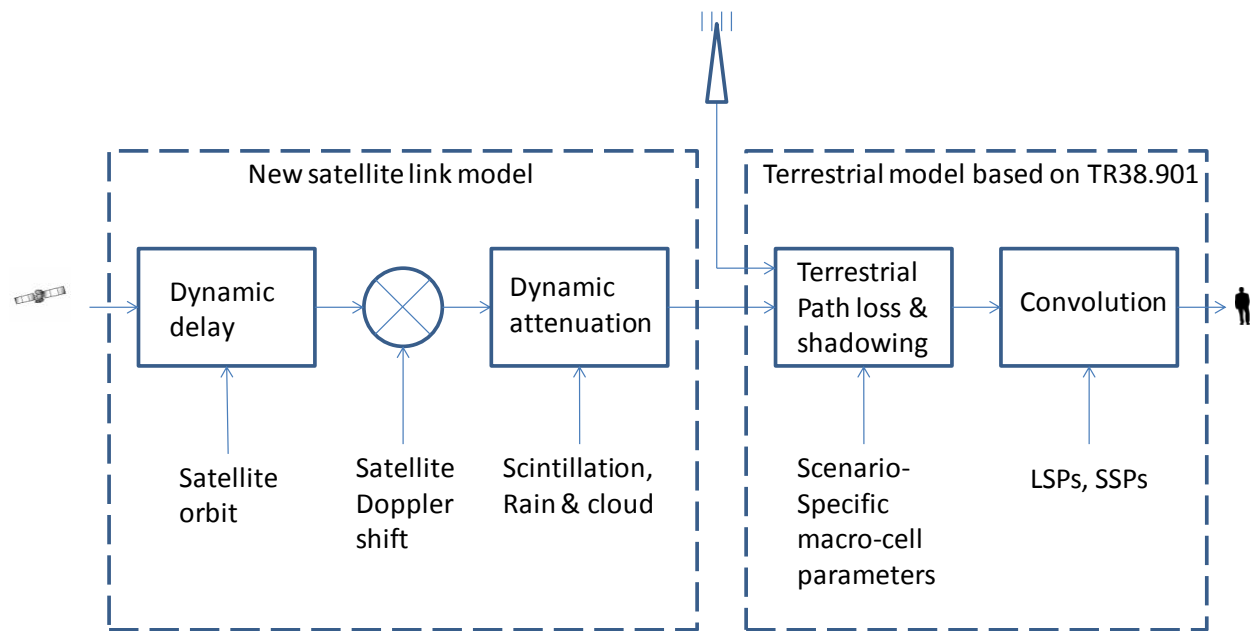


Figure 6.2-3: Combined satellite and terrestrial channels (conceptual drawing).

6.3 Coordinate system

A three-dimensional global coordinate system is considered, described as "Earth Centred Earth fixed". The Earth is approximated as a true sphere with radius of 6371 km. The coordinates' origin O lies in the center of the earth, x-y plane locates in the equator plane with x-axis pointing to 0 degree longitude, y axis pointing to 90 degree longitude, and z-axis pointing to geographical north pole from the origin O.

A UE or a satellite position is described by a set of three parameters (x, y, z) , with $\sqrt{x^2 + y^2 + z^2} = 6371 \text{ km}$ for all UEs and $\sqrt{x^2 + y^2 + z^2} > 6371 \text{ km}$ for all satellites.

The proposed coordinate system is illustrated in Figure 6.3-1 for a non-GEO satellite constellation.

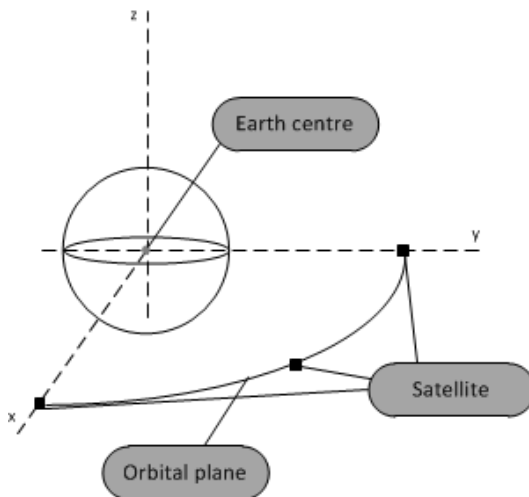


Figure 6.3-1: Illustration of the coordinate system

6.4 Antenna modelling

6.4.1 HAPS/Satellite antenna

Satellite antenna pattern

The following normalized antenna gain pattern, corresponding to a typical reflector antenna with a circular aperture, is considered

$$\begin{aligned} 1 &\quad \text{for } \theta = 0 \\ 4 \left| \frac{J_1(ka \sin \theta)}{ka \sin \theta} \right|^2 &\quad \text{for } 0 < |\theta| \leq 90^\circ \end{aligned}$$

where $J_1(x)$ is the Bessel function of the first kind and first order with argument x , a is the radius of the antenna's circular aperture, $k = 2\pi f/c$ is the wave number, f is the frequency of operation, c is the speed of light in a vacuum and θ is the angle measured from the bore sight of the antenna's main beam. Note that ka equals to the number of wavelengths on the circumference of the aperture and is independent of the operating frequency.

The normalized gain pattern for $a = 10 c/f$ (aperture radius of 10 wavelengths) is shown in Figure 6.4.1-1.

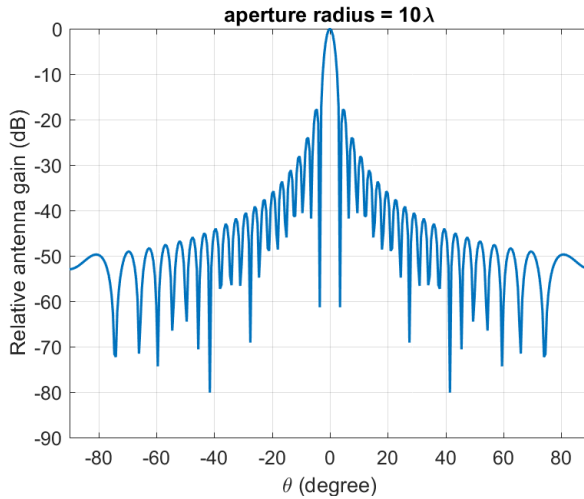


Figure 6.4.1-1: Satellite antenna gain pattern for aperture radius 10 wavelengths, $a=10 c/f$

HAPS antenna pattern

Two different antenna patterns are considered:

- The above antenna pattern defined for satellite scenarios, based on the Bessel function.
- The 3GPP antenna pattern defined for the base station in Section 7.3 of [12], corresponding to a uniform rectangular panel array with dual linear polarization.

6.4.2 UE antenna pattern

The following reference UE antenna patterns are adopted for fast fading:

- Quasi Isotropic - Linear polarisation (Quasi isotropic refers to dipole antenna which is omni-directional in one plane)
- Co-phased array - Dual Linear polarisation (one for below 6 GHz band and one for above 6 GHz band as described in [48])
- "VSAT type - circular polarization: fixed or tracking" UE antenna pattern (only in deployment scenarios featuring flat fading conditions)

6.5 Methodology to define channel models

6.5.1 System-level methodology

Only drop-based simulations are considered, similarly to [12].

The baseline model to generate channel coefficients is the one described in [12] for terrestrial links, and depicted in Figure 6.5.1-1.

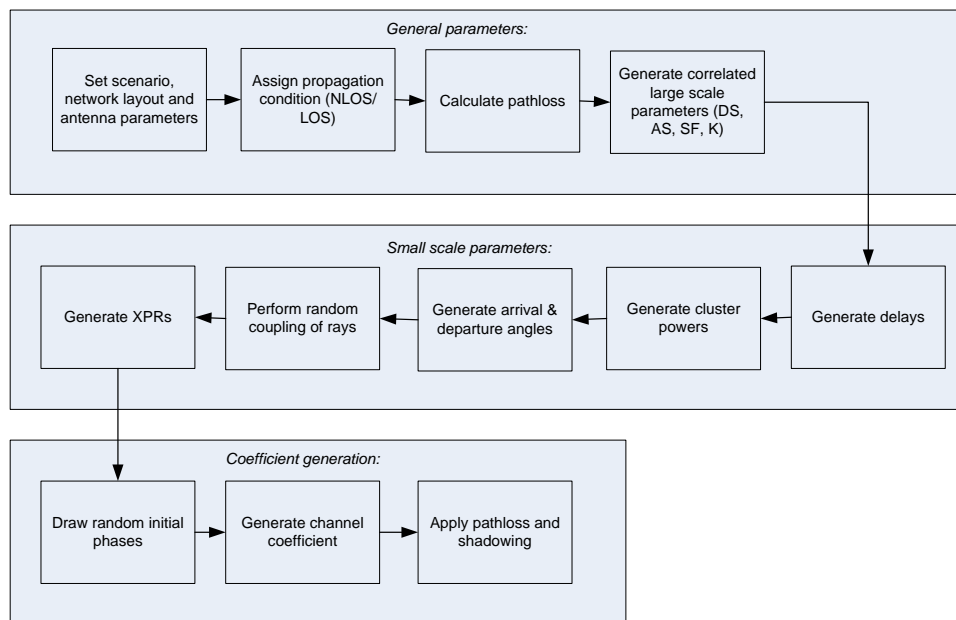


Figure 6.5.1-1: Channel coefficient generation procedure issued from [12]

An alternative and simplified model can be applied if all UE meet the flat fading criteria. In this case, the channel coefficients reduce to a single tap, since the channel is not frequency selective. This simplified model, derived from [10] is depicted in Figure 6.5.1-2.

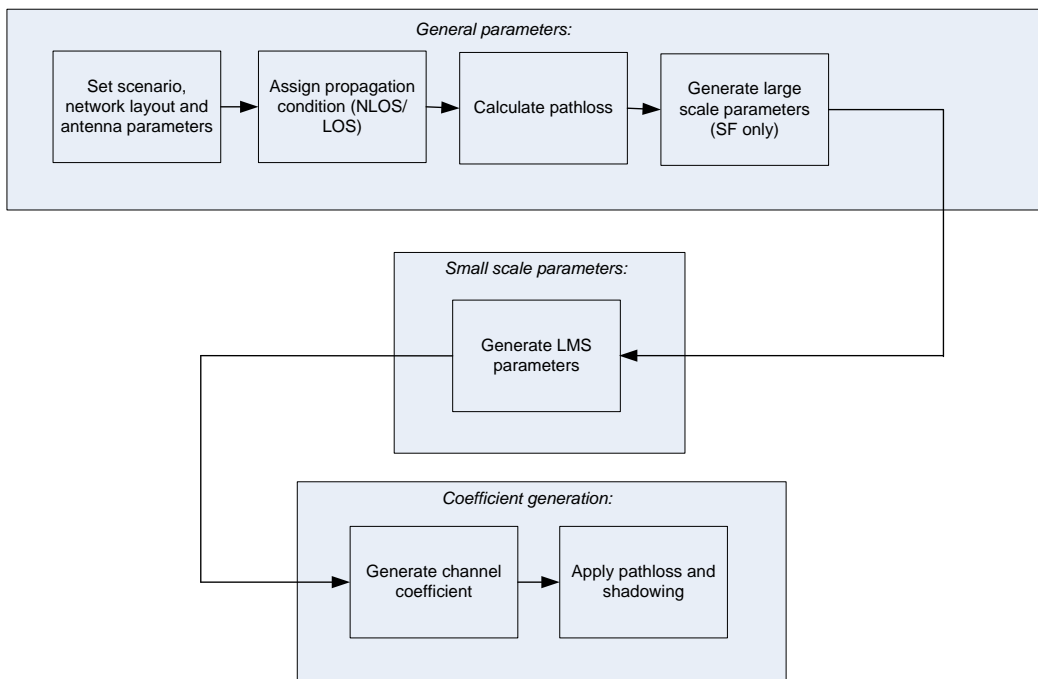


Figure 6.5.1-2: Simplified channel coefficient generation issued from [10]

6.5.2 Link-level methodology

Similarly to [12], reference CDL and TDL are considered for link-level simulations. For given environment and elevation angle, they are obtained from a single instance of the baseline model used for system level simulations (i.e. the one derived from [12]).

For flat fading conditions (including AWGN) no channel model is needed for link-level simulations.

6.6 Large scale model

6.6.1 LOS probability

Line-Of-Sight (LOS) probability depends on UE environment and elevation angle, and is obtained from Table 6.6.1-1. Reference elevation angles are considered from 10° to 90° with a 10° step. For an UE-to-satellite or UE-to-HAPS link, the LOS probability is taken from the nearest reference elevation angle.

Table 6.6.1-1 LOS probability

Elevation	Dense urban scenario	Urban scenario	Suburban and Rural scenarios
10°	28.2%	24.6%	78.2%
20°	33.1%	38.6%	86.9%
30°	39.8%	49.3%	91.9%
40°	46.8%	61.3%	92.9%
50°	53.7%	72.6%	93.5%
60°	61.2%	80.5%	94.0%
70°	73.8%	91.9%	94.9%
80°	82.0%	96.8%	95.2%
90°	98.1%	99.2%	99.8%

6.6.2 Path loss and Shadow fading

The signal path between a satellite or HAPS transmitter and an NTN terminal undergoes several stages of propagation and attenuation. The path loss (PL) is composed of components as follows:

$$PL = PL_b + PL_g + PL_s + PL_e, \quad (6.6-1)$$

where PL is the total path loss in dB,

PL_b is the basic path loss in dB,

PL_g is the attenuation due to atmospheric gasses in dB,

PL_s is the attenuation due to either ionospheric or tropospheric scintillation in dB,

PL_e is building entry loss in dB.

This section specifies the basic path loss model (PL_b) which accounts for the signal's free space propagation, clutter loss, and shadow fading. Attenuations due to building entry loss, atmospheric gasses and scintillation are described in Sections 6.6.3, 6.6.4 and 6.6.6, respectively.

The free space path loss (FSPL) in dB for a separation distance d in meter and frequency f_c in GHz is given by

$$FSPL(d, f_c) = 32.45 + 20\log_{10}(f_c) + 20\log_{10}(d) \quad (6.6-2)$$

For a ground terminal, the distance d (a.k.a. slant range), as shown in Figure 6.6.2-1, can be determined by the satellite/HAPS altitude h_0 and elevation angle α by

$$d = \sqrt{R_E^2 \sin^2 \alpha + h_0^2 + 2h_0 R_E} - R_E \sin \alpha, \quad (6.6-3)$$

where R_E denotes Earth radius.

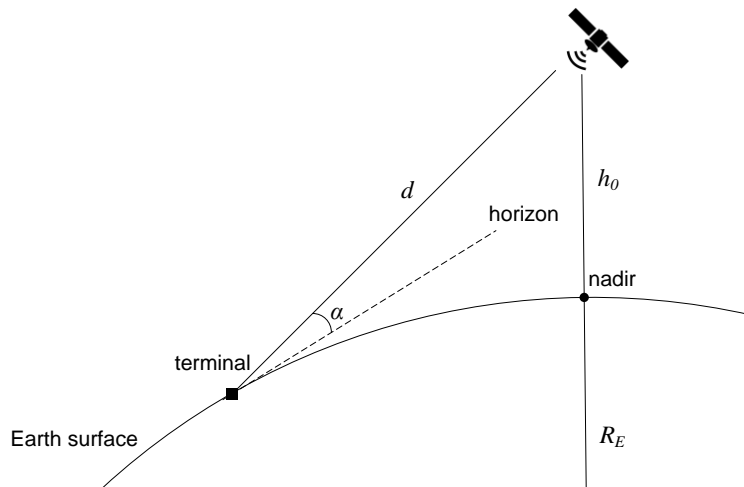


Figure 6.6.2-1: Slant range d between a satellite and a ground terminal

Clutter loss (CL) models the attenuation of signal power caused by surrounding buildings and objects on the ground. It depends on the elevation angle α , the carrier frequency f_c , and the environment. Shadow fading (SF) is modeled by a log-normal distribution, which when expressed in decibel unit, is a zero-mean normal distribution with a standard deviation σ_{SF}^2 , i.e., $N(0, \sigma_{SF}^2)$.

The basic path loss in dB unit is modeled as

$$PL_b = FSPL(d, f_c) + SF + CL(\alpha, f_c), \quad (6.6-4)$$

where $FSPL(d, f_c)$ is the free space path loss, $CL(\alpha, f_c)$ is clutter loss, and SF is shadow fading loss represented by a random number generated by the normal distribution, i.e., $SF \sim N(0, \sigma_{SF}^2)$. When the UE is in LOS condition, clutter loss is negligible and should be set to 0 dB in the basic path loss model.

The values of σ_{SF}^2 and CL are given in tables 6.6.2-1 to 6.6.2-3 at reference elevation angles for different scenarios. The UE in a particular scenario should take the values corresponding to the reference angle nearest to its elevation angle α .

Table 6.6.2-1: Shadow fading and clutter loss for dense urban scenario

Elevation	S-band			Ka-band		
	LOS		NLOS	LOS		NLOS
	σ_{SF} (dB)	σ_{SF} (dB)	CL (dB)	σ_{SF} (dB)	σ_{SF} (dB)	CL (dB)
10°	3.5	15.5	34.3	2.9	17.1	44.3
20°	3.4	13.9	30.9	2.4	17.1	39.9
30°	2.9	12.4	29.0	2.7	15.6	37.5
40°	3.0	11.7	27.7	2.4	14.6	35.8
50°	3.1	10.6	26.8	2.4	14.2	34.6
60°	2.7	10.5	26.2	2.7	12.6	33.8
70°	2.5	10.1	25.8	2.6	12.1	33.3
80°	2.3	9.2	25.5	2.8	12.3	33.0
90°	1.2	9.2	25.5	0.6	12.3	32.9

Table 6.6.2-2: Shadow fading and clutter loss for urban scenario

Elevation	S-band			Ka-band		
	LOS		NLOS	LOS		NLOS
	σ_{SF} (dB)	σ_{SF} (dB)	CL (dB)	σ_{SF} (dB)	σ_{SF} (dB)	CL (dB)
10°	4	6	34.3	4	6	44.3
20°	4	6	30.9	4	6	39.9
30°	4	6	29.0	4	6	37.5
40°	4	6	27.7	4	6	35.8
50°	4	6	26.8	4	6	34.6
60°	4	6	26.2	4	6	33.8
70°	4	6	25.8	4	6	33.3
80°	4	6	25.5	4	6	33.0
90°	4	6	25.5	4	6	32.9

Table 6.6.2-3: Shadow fading and clutter loss for suburban and rural scenarios

Elevation	S-band			Ka-band		
	LOS		NLOS	LOS		NLOS
	σ_{SF} (dB)	σ_{SF} (dB)	CL (dB)	σ_{SF} (dB)	σ_{SF} (dB)	CL (dB)
10°	1.79	8.93	19.52	1.9	10.7	29.5
20°	1.14	9.08	18.17	1.6	10.0	24.6
30°	1.14	8.78	18.42	1.9	11.2	21.9
40°	0.92	10.25	18.28	2.3	11.6	20.0
50°	1.42	10.56	18.63	2.7	11.8	18.7
60°	1.56	10.74	17.68	3.1	10.8	17.8
70°	0.85	10.17	16.50	3.0	10.8	17.2
80°	0.72	11.52	16.30	3.6	10.8	16.9
90°	0.72	11.52	16.30	0.4	10.8	16.8

6.6.3 O2I penetration loss

For an indoor Earth-based station, account must be taken of the additional loss between the station and the adjacent outdoor path. The additional loss varies greatly with the location and construction details of buildings, and a statistical evaluation is required. Recommendation ITU-R P.2109 gives a suitable building entry/exit-loss model for this purpose.

Experimental results, such as those collated in Report ITU-R P.2346, shows that, when characterised in terms of entry loss, buildings fall into two distinct populations: where modern, thermally-efficient building methods are used (metallised glass, foil-backed panels) building entry loss is generally significantly higher than for 'traditional' buildings without such materials. The model therefore gives predictions for these two cases.

This classification, of 'thermally efficient' and 'traditional', refers purely to the thermal efficiency of construction materials. No assumption should be made on the year of construction, type (single or multi-floors), heritage or building method.

For building entry loss, it is important to consider the thermal efficiency of the complete building (or the overall thermal efficiency). A highly thermally efficient main structure with poorly insulated windows (e.g. single glazed with thin glass) can make the building thermally inefficient and vice versa.

Thermal transmittance, commonly referred as U-value, provides a quantifiable description of thermal efficiency. Low U-values represent high thermal efficiency. Typically, the presence of metallised glass windows, insulated cavity walls, thick reinforced concrete and metal foil back cladding is a good indication of a thermally efficient building.

NOTE: For example, U-values of < 0.3 and < 0.9 are representative of thermally efficient main structure and metallised glass, respectively.

Building entry loss will vary depending on building type, location within the building and movement in the building. The building entry loss distribution is given by a combination of two lognormal distributions. The building entry loss not exceeded for the probability, P , is given by:

$$L_{BEL}(P) = 10\log(10^{0.1A(P)} + 10^{0.1B(P)} + 10^{0.1C})dB \quad (6.6-5)$$

with:

$$\begin{aligned} A(P) &= F^{-1}(P)\sigma_1 + \mu_1 \\ B(P) &= F^{-1}(P)\sigma_2 + \mu_2 \\ C &= -3.0 \end{aligned}$$

$$\begin{aligned} \mu_1 &= L_h + L_e \\ \mu_2 &= w + x\log(f) \\ \sigma_1 &= u + v\log(f) \\ \sigma_2 &= y + z\log(f) \end{aligned}$$

where:

L_h is the median loss for horizontal paths, given by:

$$L_h = r + s\log(f) + t(\log(f))^2 \quad (6.6-6)$$

L_e is the correction for elevation angle of the path at the building façade:

$$L_e = 0.212\theta \quad (6.6-7)$$

and:

- f = frequency (GHz)
- θ = elevation angle of the path at the building façade (degrees)
- P = probability that loss is not exceeded ($0.0 < P < 1.0$)
- $F^{-1}(P)$ = inverse cumulative normal distribution as a function of probability.

and the coefficients are as given in Table 6.6.3-1:

Table 6.6.3-1: Model coefficients

Building type	r	s	t	u	v	w	x	y	z
Related to:	Median BEL (μ_1)			σ_1		μ_2		σ_2	
Traditional	12.64	3.72	0.96	9.6	2.0	9.1	-3.0	4.5	-2.0
Thermally-efficient	28.19	-3.00	8.48	13.5	3.8	27.8	-2.9	9.4	-2.1

6.6.4 Atmospheric absorption

Attenuation by atmospheric gases which is entirely caused by absorption depends mainly on frequency, elevation angle, altitude above sea level and water vapour density (absolute humidity). At frequencies below 10 GHz, it may normally be neglected. However, for elevation angles below 10 degrees it is recommended that the calculation is performed for any frequency above 1 GHz. Annex 1 of Recommendation ITU-R P.676 gives a complete method for calculating gaseous attenuation, while Annex 2 of the same Recommendation gives an approximate method for frequencies up to 350 GHz.

For system level simulations, the baseline method is as follows:

- The method of Annex 2 in ITU-R P.676 is considered (except for UE altitude higher than 10km and for frequencies within 0.5 GHz of the centres of resonance lines at any altitude).
- For all UEs, a geometric height of 0km is considered, corresponding to the sea level.
- For all UEs, dry air pressure, water-vapour density, water vapour partial pressure and temperature correspond to the mean annual global reference atmosphere given in Recommendation ITU-R P835.

For all UEs, this corresponds to the following values:

$$T = 288.15 \text{ K}$$

$$p = 1013.25 \text{ hPa}$$

$$\rho = 7.5 \text{ g/m}^3$$

$$e = \frac{\rho T}{216.5} = 9.98 \text{ hPa}$$

where T denotes the temperature, p the dry air pressure, ρ the water-vapour density and e the water vapour partial pressure.

Figure 6 of ITU-R P.676 shows the corresponding zenith attenuation $A_{zenith}(f)$ for frequencies between 1 and 350 GHz. For an elevation angle α , the corresponding attenuation $PL_A(\alpha, f)$ is given by:

$$PL_A(\alpha, f) = \frac{A_{zenith}(f)}{\sin(\alpha)} \quad (6.6-8)$$

6.6.5 Rain and cloud attenuation

Rain and cloud attenuation is considered as negligible for frequencies below 6 GHz. Section 2.2 of [11] describes a method to estimate the long-term statistics of attenuation due to rain, which are location specific.

For system-level simulations, the baseline is to consider clear sky conditions only.

Alternatively, the following procedure shall be followed to define rain and cloud attenuation (adaptation of [11] for drop-based simulations):

- For each UE, determine its CDF of rain and cloud attenuation (location specific) using Section 2.2 of [11].
- For each drop, draw the attenuation due to rain and cloud attenuation for each UE from its corresponding CDF

NOTE: The spatial correlation of rain and cloud attenuation is not taken into account in this procedure.

6.6.6 Scintillation

6.6.6.1 Ionospheric scintillation

Scintillation corresponds to rapid fluctuations of the received signal amplitude and phase. Ionosphere propagation shall only be considered for frequencies below 6 GHz.

These phenomena are among the most severe disruptions along a trans-ionospheric propagation path for signals below 3 GHz, and may be observed occasionally up to 10 GHz [13]. Scintillations depend on location, time-of-day (as observed in Figure 6.6.6.1-1), season, solar and geomagnetic activity. During nominal conditions, strong levels of scintillation are rarely observed in mid-latitudes, but they may be encountered daily during post-sunset hours in low latitude regions. At high (auroral and polar) latitudes, moderate to strong levels of scintillations have been observed.

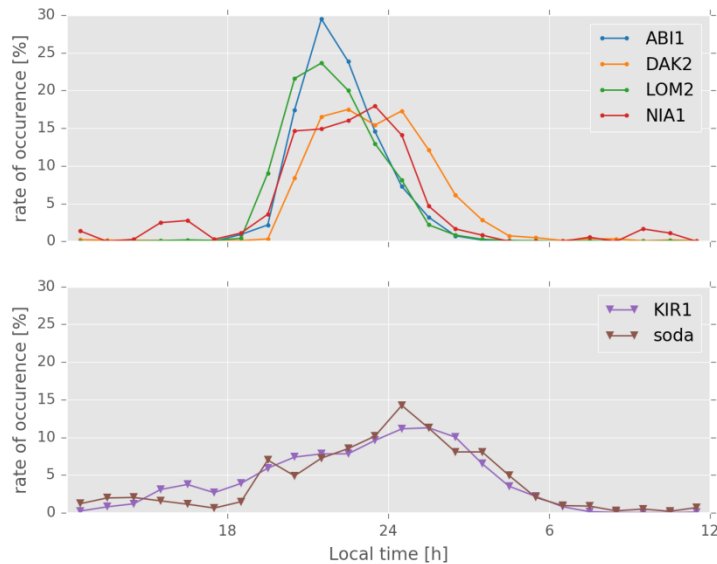


Figure 6.6.6.1-1: Occurrence of different scintillation events around the solar maximum of 2014 at low (top) and high (bottom) latitudes

6.6.6.1.1 Ionospheric scintillation indices

The most commonly used parameter to characterize intensity fluctuations (amplitude scintillations) is the amplitude scintillation index S_4 [4], defined by equation:

$$S_4 = \left(\frac{\langle I^2 \rangle - \langle I \rangle^2}{\langle I \rangle^2} \right)^{1/2} \quad (6.6-9)$$

where I is intensity (proportional to the square of the signal amplitude) and $\langle \cdot \rangle$ denotes averaging, usually over a period of 60 seconds. Likewise, phase scintillations are characterized by the standard deviation of the phase variations, the phase scintillation index σ_ϕ :

$$\sigma_\phi = \sqrt{\langle \phi^2 \rangle - \langle \phi \rangle^2} \quad (6.6-10)$$

where ϕ is carrier phase in radians and $\langle \cdot \rangle$ denotes averaging, usually over a period of 60 seconds. For convenience, scintillation strength can be classified into three regimes:

Table 6.6.6.1.1-1: Definition of scintillation regime based on S_4 values

Scintillation Regime	Amplitude Scintillation	Phase Scintillation (rad)
Weak	$S_4 < 0.3$	$\sigma_\phi < 0.25-0.3$
Moderate	$0.3 \leq S_4 \leq 0.6$	$0.25-0.3 \leq \sigma_\phi \leq 0.5-0.7$
Strong	$S_4 > 0.6$	$\sigma_\phi > 0.5-0.7$

6.6.6.1.2 Ionospheric scintillation location dependence

As previously mentioned, scintillation effects differ at low and high-latitudes, and they are not observed at mid-latitudes except for strong geomagnetic storms. At high-latitudes (e.g., above 60°), the effect mainly occurs from the high-latitude edge of the Van Allen outer belt into polar region. On the other hand, Equatorial scintillations occur around $\pm 20^\circ$ of latitude of the magnetic equator and they are due to large (~ 100 km) depleted ionization volumes driven through the F region, leaving a plume of small-scale (tens of cm to m) irregularities surrounding the depletion, which can extend well through F-layer peak. They are produced by convective plasma processes. Irregularities with this range of scales are not independent from larger-scale plasma structures to those of smaller-scale irregularities.

The cross-correlation between S_4 and σ_ϕ is markedly different between high geomagnetic latitudes and low latitudes. Amplitude scintillations dominate at low-latitudes, and phase scintillations dominate at high latitudes, however, they are not exclusively and both effects can be expected in the two regions.

6.6.6.1.3 Frequency scaling

For frequency scaling, typically the following relation on amplitude scintillation S_4 index is used:

$$S_{4,f_2} = S_{4,f_1} \left(\frac{f_2}{f_1} \right)^{-n} \quad (6.6-11)$$

with $n=1.5$ recommended for L-band frequencies. In [14], values of n derived from satellite measurement data between several pairs of frequencies from 30 MHz up to 6 GHz are presented, ranging from 1 to 2. This relationship is valid particularly for weak scattering assumptions (higher elevations and low to moderate S_4 values below 0.6). For high S_4 values ($S_4=1$), the relation saturates with n equal to 0.

For phase scintillations, an equivalent relation is used:

$$S_{\phi,f_2} = S_{\phi,f_1} \left(\frac{f_2}{f_1} \right)^{-n} \quad (6.6-12)$$

with $n=1$ recommended for L-band frequencies and also reaching saturation for high σ_ϕ values.

As an illustrative example, the frequency scaling between GPS L1, L2 and L5 bands (1.57542, 1.22760 and 1.17645 GHz, respectively) is presented in Figure 6.6.6.1.3-1, where scintillation events in two bands are compared against each other and against the theoretical values described by 6.6-11 and 6.6-12.

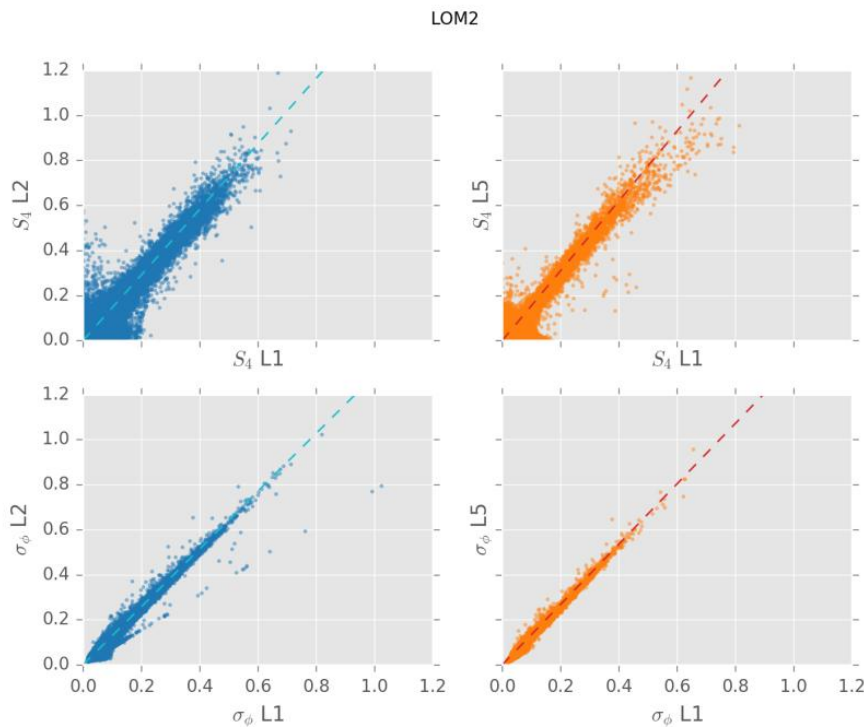


Figure 6.6.6.1.3-1: Frequency correlation of scintillation events observed in GPS L1, L2 and L5 bands

6.6.6.1.4 Model for ionospheric scintillation loss

The proposed method for the ionospheric scintillation loss is based on the so-called *Gigahertz scintillation model* ([13], Section 4.8), and it is valid only for the regions located approximately 20° north and south of the magnetic equator. At high-latitudes (e.g., above 60°), this model is not applicable, whereas for other latitude locations the ionospheric scintillation can be neglected.

To evaluate the scintillation effects that can be expected in a given situation the following steps may be used:

Step 1: Figure 6.6.6.1.4-1 provides scintillation occurrence statistics on equatorial ionospheric paths: peak-to-peak amplitude fluctuations, P_{fluc} , (dB), for 4 GHz reception from satellites in the East at elevation angles of about 20° (**P** solid curves) and in the West at about 30° elevation (**I** dotted curves). The data are given for different times of year and sunspot number.

Step 2: Since Figure 6.6.6.1.4-1 relates to 4 GHz, values for other frequencies are found by multiplying these values by $(f/4)^{-1.5}$ where f is the frequency of interest (GHz).

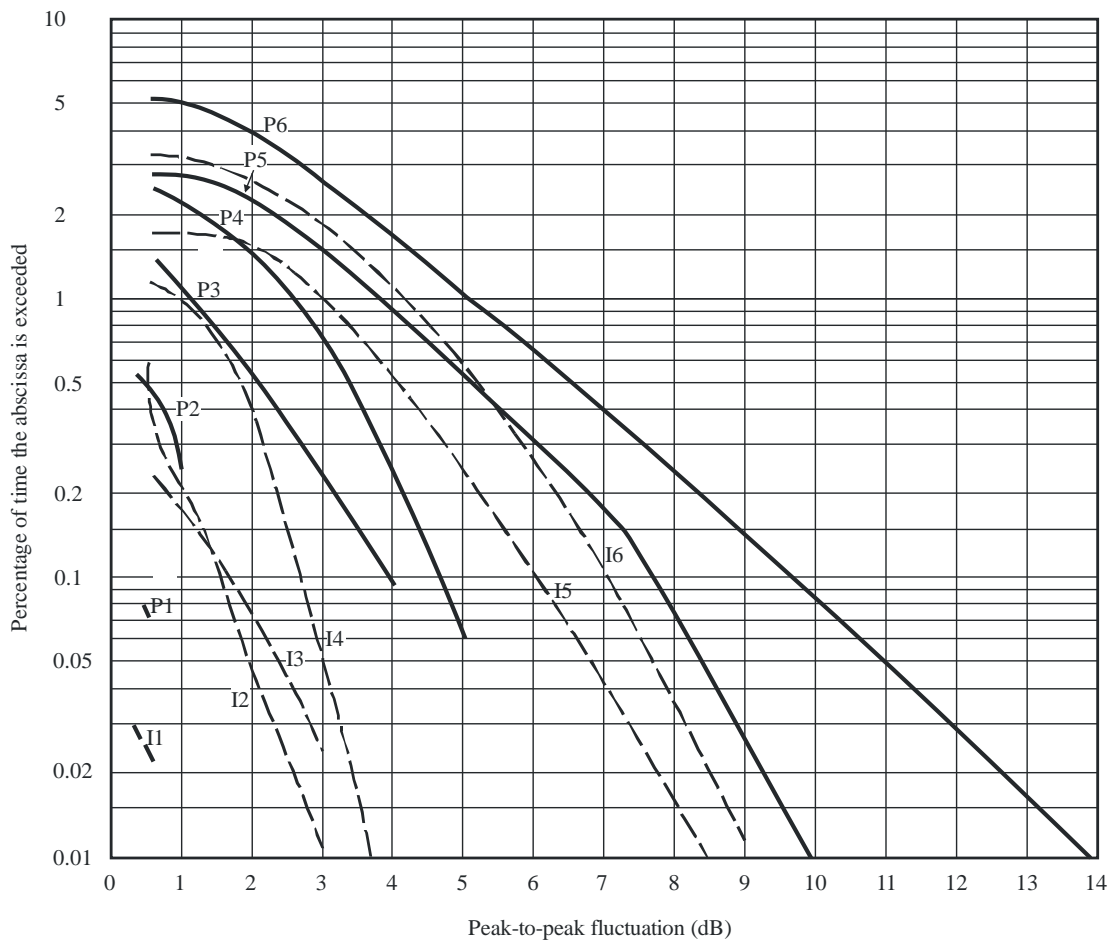
Step 3: Since one element of link budget calculations is related to signal loss due to ionospheric scintillation, A_{IS} , the following relationship is recommended:

$$A_{IS} = P_{fluc} / \sqrt{2} \quad \{\text{QUOTE } A_s = P_{fluc} / \sqrt{2} \} \quad (6.6-13)$$

NOTE: The most widely used parameter in describing amplitude scintillations phenomena is the amplitude index S_4 . It is adopted to define three main regime conditions (see Table 6.6.6.1.1-1), and it is related to P_{fluc} using the empirical approximation:

$$P_{fluc} = 27.5 S_4^{1.26} \quad (6.6-14)$$

where the empirical conversion table is presented in Table 1 of [13].



P0531-12

Figure 6.6.6.1.4-1: Annual statistics of peak-to-peak fluctuations observed at Hong Kong earth station (Curves I1, P1, I3-I6, P3-P6) and Taipei earth station (Curves P2 and I2). Extracted from [13].

For system-level simulations below 6 GHz, PL_s is equal to A_{IS} from Equation (6.6-13) for latitudes of maximum $\pm 20^\circ$.

For latitudes between $\pm 20^\circ$ and $\pm 60^\circ$ of latitude, $PL_s = 0$. Finally, for latitude above $\pm 60^\circ$, the presented ITU model is not applicable; nevertheless, in those regions the scintillation phenomena are mainly affecting the signal phase and having negligible effects on the signal amplitude. For such reasons, the choice of $PL_s = 0$ is also applied for latitude above $\pm 60^\circ$.

As baseline for system-level simulations below 6 GHz in the regions of maximum $\pm 20^\circ$, the additional path loss due to scintillation PL_s is equal to the ionospheric attenuation level at 99% of the P3 curve derived from Figure 6.6.6.1.4-1. For example, by applying the presented *Gigahertz scintillation model*, the attenuation at 2 GHz center frequency is summarized in the following equation:

$$A_{IS} = P_{fluc}(4\text{GHz}) \times \frac{0.5^{-1.5}}{\sqrt{2}} = 1.1 \times \frac{0.5^{-1.5}}{\sqrt{2}} = 2.2 \text{ dB}$$

6.6.6.2 Tropospheric scintillation

Scintillation corresponds to rapid fluctuations of the received signal amplitude and phase. Tropospheric propagation shall only be considered for frequencies above 6 GHz.

Tropospheric scintillation is a phenomenon that causes rapid amplitude and phase fluctuations of signals from satellite communication systems. Unlike, ionospheric scintillation, the effect of tropospheric scintillation increases with the carrier frequency of the signal, being especially significant above 10 GHz. In this case, the signal fluctuations are caused by sudden changes in the refractive index due to the variation of temperature, water vapor content, and barometric pressure.

Besides increasing with the carrier frequency, the effects of scintillation also increase with low elevation angles, due to the longer path of the signal, and wide beam width receiving antennas.

6.6.6.2.1 Model for Tropospheric scintillation loss

The ITU-R recommendation algorithm for fading prediction [11] permits an accurate prediction of the amplitude. This method consists in three parts:

- Prediction of the amplitude scintillation fading at free-space elevation angles $\geq 5^\circ$ (Section 2.4.1 in [13]).
- Prediction of the amplitude scintillation fading for fades ≥ 25 dB (section 2.4.2 in [13]).
- Prediction of the amplitude scintillation in the transition region between the above two distributions (section 2.4.3 in [13]).

An illustrative example of typical power attenuation levels as a function of the elevation angle is depicted in Figure 6.6.6.2.1-1. The user location is Toulouse (France), the carrier frequency is set to 20 GHz, and circular polarization is assumed. Even though tropospheric scintillation is latitude dependent, it is suggested to take this plot as a reference for satellite link margin computation.

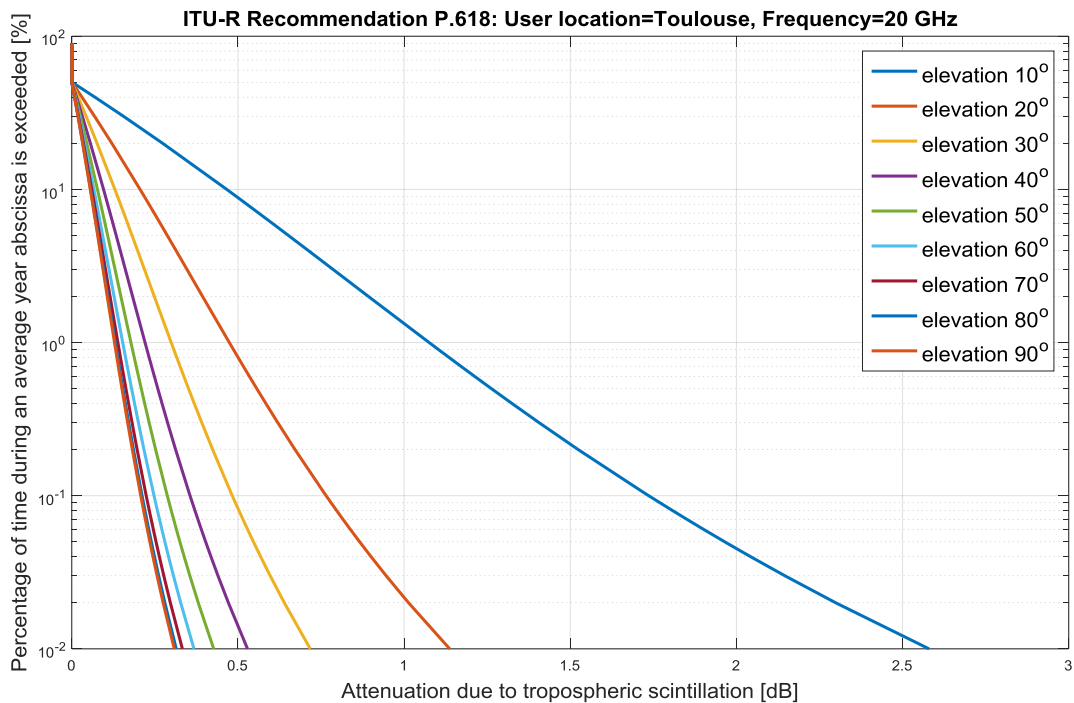


Figure 6.6.6.2.1-1: Complementary cumulative probability function of the tropospheric scintillation attenuation at 20 GHz in Toulouse (France).

As baseline for system-level simulations above 6 GHz, the fading due to scintillation PL_S is equal to the tropospheric attenuation level at 99% of the time derived from Figure 6.6.6.2.1-1 and summarized in Table 6.6.6.2.1-1. Alternatively, it can be drawn for each UE based on its corresponding CDF from Figure 6.6.6.2.1-1, assuming no correlation between different UE.

Table 6.6.6.2.1-1: Tropospheric attenuation in dB with 99% probability at 20 GHz in Toulouse

Elevation angle [deg]	Tropospheric attenuation, $P\{A_{IS} > x\} < 0.01$
10	1.08 dB
20	0.48 dB
30	0.30 dB
40	0.22 dB
50	0.17 dB
60	0.13 dB
70	0.12 dB
80	0.12 dB
90	0.12 dB

6.7 Fast fading model

The generic fast fading model in 3GPP is based on TR 38.901 [12]. For narrowband SISO simulations, an optional simplified channel model can be used as long as the flat fading assumption is valid.

Most literature on satellite channel models rely on flat fading models [15], [16], [17], i.e. non frequency selective channel models, the ITU two-state model described in [1] being the most up-to-date model.

The formula $B_C = \frac{1}{10\tau_{rms}}$ is defined to calculate the coherence bandwidth from the 95th percentile rms delay spread.

Coherence bandwidth depends on environment, antenna pattern and elevation. The channel is assumed to be flat if the UE bandwidth is lower than the coherence bandwidth of the channel. In satellite channels, where small fade margins are usually considered, τ_{rms} can be assessed only for cases where the fade event is below a given threshold (otherwise, system outage will occur regardless of channel dispersion).

In [47], values of τ_{rms} were estimated considering an omnidirectional UE antenna for suburban and urban environments, several elevation angles and fade margins. Based on these results, the ITU two-state model can at least (NOTE 1) be used as a simplified alternative to the TR 38.901 [12] methodology for satellite links if all of the following conditions are met:

- S-band scenario
- Minimum elevation angle is 20° or above
- Quasi-LOS conditions (i.e. fading margin is approx. 5dB maximum)
- Channel bandwidth is 5 MHz or below
- Environment is rural, suburban or urban

NOTE 1: Flat fading conditions are more easily achievable when using highly directive UE antennas located in less scattering environment, like on a rooftop or on an open field. In every case, the flat fading criterion described above shall be fulfilled.

6.7.1 Flat fading

We consider here the ITU two-state model. This model includes already the clutter loss and the shadow fading, so that the basis path loss is calculated as follows:

$$PL_b = FSPL(d, f_c) \quad (6.7-1)$$

In the two-state model, the signal level is statistically described with a good state (corresponding to LOS and slightly shadowed conditions) and a bad state (corresponding to severe shadowed conditions). The state duration is described by

a semi-Markov model. Within each state fading is described by a Loo distribution where the received signal is the sum of the direct path signal and the diffuse multipath.

The Loo distribution is therefore defined with the following parameters:

- Mean of the direct signal
- Standard deviation of the direct signal
- Mean of the multipath

The following procedure shall be followed for system-level evaluations:

Step 1: Set general parameters related to environment and satellite link as follows:

- Set the center frequency from 1.5 GHz to 20 GHz;
- Choose one of the following LMS scenarios available (in S band: urban, suburban, rural wooded, residential – in Ka band: suburban, rural wooded);
- Set the link elevation assuming a rounded value towards the closest available elevation for the frequency/environment chosen ($20^\circ, 30^\circ, 34^\circ, 45^\circ, 60^\circ, 70^\circ$);
- Give UE position, array orientation, speed and direction of motion in the global coordinate system.

Step 2: Determine the $(\mu, \sigma)_{G,B}$, $(\mu_{M_A}, \sigma_{M_A})_{G,B}$, $(g_1, g_2)_{G,B}$, $(h_1, h_2)_{G,B}$, $(dur_{min})_{G,B}$, (f_1, f_2) , $p_{B,min}$ and $p_{B,max}$ from the input parameters table provided in Annex 2 of [1] and summarized in Table 6.7.1-1.

Table 6.7.1-1: Model parameters of the 2-state model

Parameter	Description
$(\mu, \sigma)_{G,B}$	Mean and standard deviation of the log-normal law assumed for events duration (m)
$dur_{min,G,B}$	Minimum possible events duration (m)
$(\mu_{M_A}^{GB}, \sigma_{M_A}^{GB})$	Parameters of the $M_{A,G,B}$ distribution (M_A being the average value of the direct path amplitude A over one event) (dB)
$MP = h_{1G,B}M_A + h_{2G,B}$	Multipath power, $MP_{G,B}$ (one 1 st order polynomial for each state), (dB)
$\sum_{AG,B} = g_{1G,B}M_A + g_{2G,B}$	Standard deviation of A , $\sum_{AG,B}$ (one 1 st order polynomial for each state)
$L_{corrG,B}$ NOTE 2	Direct path amplitude correlation distance (m)
$f_1 \Delta M_A + f_2$	Transition length, L_{trans} (one single 1 st order polynomial), (m)
$[p_{B,min}, p_{B,max}]$	Probability range to consider for the $M_{A,B}$ distribution

NOTE 1: G stands for the GOOD state and B stands for the BAD state.

NOTE 2: Only for generative modelling.

Assign propagation condition (GOOD/BAD) states in the original procedure from [15].

NOTE: Unlike the frequency selective case, the LOS probability defined in clause 6.6.1 is not used when considering the flat fading model

The propagation conditions for different Earth-space links are uncorrelated.

The GOOD and BAD state probability is calculated as follows :

$$\langle dur \rangle_{G,B} = \exp(\mu_{G,B} + \frac{\sigma_{G,B}^2}{2}) \frac{1 - erf(\frac{\log dur_{min,B,G} - (\mu_{G,B} + \sigma_{G,B}^2 + \sigma_{G,B}^2)}{\sigma \sqrt{2}})}{1 - erf(\frac{\log dur_{min,B,G} - \mu_{G,B}}{\sigma \sqrt{2}})}$$
(6.7-2)

$$\langle dur \rangle_T = f_1 \times (\mu_{M_{A,G}} - \mu_{M_{A,B}} - \sigma_{M_{A,B}}^2 \times \frac{p_N(M_{A,\min}; \mu_{M_{A,B}}, \sigma_{M_{A,B}}) - p_N(M_{A,\max}; \mu_{M_{A,B}}, \sigma_{M_{A,B}})}{F_N(M_{A,\max}; \mu_{M_{A,B}}, \sigma_{M_{A,B}}) - F_N(M_{A,\min}; \mu_{M_{A,B}}, \sigma_{M_{A,B}})}) + f_2 \quad (6.7-3)$$

$$M_{A,\min/\max} = \mu_{M_{A,B}} + \sqrt{2}\sigma_{M_{A,B}} \operatorname{erf}^{-1}(2p_{B,\min/\max} - 1) \quad (6.7-4)$$

$$P_G = \frac{\langle dur \rangle_G + \langle dur \rangle_T}{\langle dur \rangle_G + \langle dur \rangle_B + 2\langle dur \rangle_T} \quad (6.7-5)$$

- Where subscripts G, B and T stand respectively for good, bad and transition states, $\langle dur \rangle$ the mean duration of the considered state in meters, dur_{\min} the minimal state duration in meters, μ and σ respectively the mean and standard deviation of the assumed log-normal law in m.
- $p_N(x; \mu, \sigma)$ and $F_N(x; \mu, \sigma)$ are respectively the probability density function and the cumulative distribution function of a normal distribution with mean μ and standard deviation σ as defined in Recommendation ITU-R P.1057
- Where $\mu_{M_A GB}, \sigma_{M_A GB}$ are the parameters of the average value of the direct path amplitude A over one event, $[p_{B,\min}, p_{B,\max}]$ the probability range to consider for the $M_{A,B}$ distribution.

Step 3: Draw M_{A_i} , the mean power of the direct signal, as a normally distributed parameter function of $(\mu_{M_A}, \sigma_{M_A})_{G,B}$ expressed in dB.

$$M_{A_i} \sim N(\mu_{M_{A_i}}, \sigma_{M_{A_i}})$$

Compute Σ_{Ai} and MP_i , respectively the standard deviation of the direct signal and the mean multipath power both expressed in dB where suscript i designate the good or bad state, as follow:

$$\Sigma_{Ai} = g_{1i}M_{Ai} + g_{2i} \quad (6.7-6)$$

$$MP_i = h_{1i}M_{Ai} + h_{2i} \quad (6.7-7)$$

Step 4: Draw the power of the direct signal P_D following the normally distribution (M_{A_i}, Σ_{A_i}) and derive the K factor as $P_D - MP_i$ (all expressed in dB).

For each UE, the channel is therefore characterized by a single Rice distributed tap.

Note that the above procedure is only valid for simulation durations up to a few TTIs. It is further assumed that no state change occurs during the simulation duration.

For longer simulations, the procedure described in clause 6.2 from [10] must be applied, as the K factor must not be considered as constant.

Note that individual fading values at a given time may directly be obtained after step 3 of the above procedure, based on the Loo distribution:

$$p_{Loo}(x) = \frac{8.686x}{\sum_{Ai} \sigma_i^2 \sqrt{2\pi}} \int_0^\infty \frac{1}{a} \exp\left(-\frac{(20\log_{10}(a) - M_{Ai})^2}{2\sum_{Ai}^2} - \frac{x^2 - a^2}{2\sigma_i^2}\right) I_0\left(\frac{xa}{\sigma_i^2}\right) da \quad (6.7-8)$$

With $2\sigma_i^2$ being the multipath mean received power expressed in dB, i.e. $MP_i = 10\log(2\sigma_i^2)$

Similarly to [10], a Jake's Doppler spectrum is considered for UE mobility.

Additional Doppler shift due to satellite motion should be taken into account according to the following formula:

$$f_{d,shift} = (v_{sat}/c) \times \left(\frac{R}{R+h} \cos \alpha_{model} \right) \times f_c,$$

Where v_{sat} denotes the satellite speed, c denotes the speed of light, R denotes the earth radius, h denotes the satellite altitude, α_{model} denotes the satellite elevation angle, and f_c denotes the carrier frequency.

The satellite speed, satellite elevation angle and UE speed should be considered to be constant during the simulation duration, if limited to few TTIs.

6.7.2 Frequency selective fading

In the fast fading model, the process in 7.5 of TR 38.901 [12] is used. This section is not a stand-alone description of the fast fading model, but it describes the differences between the channel models used for terrestrial and satellite/HAPS communications. As can be seen from Figure 6.7.2-1, there is not much difference in local scattering between the HAPS and satellite cases. Therefore, the same fast fading parameters can be used for the both cases, including different satellite orbits as well. The critical parameter is the elevation angle of the LOS path of the satellite/HAPS vs. ground horizon.

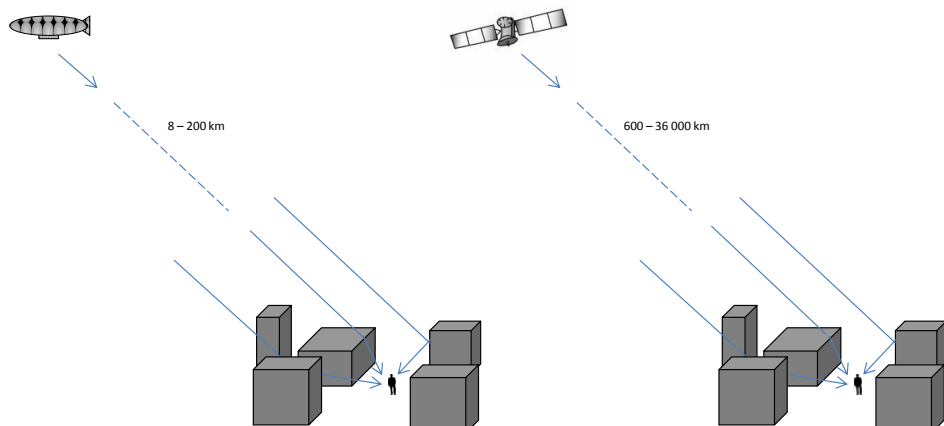


Figure 6.7.2-1: HAPS to UE vs. satellite to UE propagation

Instead of the parameterization tables in TR 38.901 [12] (Table 7.5-6 Part-1 and Part-2) the following tables shall be used.

NOTE 1: Some channel models may lead to pessimistic results of the performance of satellite/HAPS to UE link especially in the higher elevations due to the high number of clusters and low K factor.

NOTE 2: In some cases, the correlation distances are shorter in real world conditions.

Angular scaling factors in cluster generation need to be added to the NTN scenarios that have lower number of clusters than the scenarios described in TR 38.901 [12] (Table 6.7.2-1aa below corresponds to Table 7.5-2 in TR 38.901 [12] and Table 6.7.2-1ab below corresponds to Table 7.5-3 in TR 38.901 [12]).

Table 6.7.2-1aa: Scaling factors for AOA, AOD generation

# clusters	2	3	4	5	8	10	11	12	14	15	16	19	20
C_{ϕ}^{NLOS}	0.501	0.680	0.779	0.860	1.018	1.090	1.123	1.146	1.190	1.211	1.226	1.273	1.289

Table 6.7.2-1ab: Scaling factors for ZOA, ZOD generation

# clusters	2	3	4	8	10	11	12	15	19	20
C_{θ}^{NLOS}	0.430	0.594	0.697	0.889	0.957	1.031	1.104	1.1088	1.184	1.178

Table 6.7.2-1a: Channel model parameters for Dense Urban Scenario (LOS) in S band

Scenarios		Dense Urban LOS								
		10°	20°	30°	40°	50°	60°	70°	80°	90°
Delay spread (DS) lgDS= $\log_{10}(DS/1s)$	μ_{gDS}	-7.12	-7.28	-7.45	-7.73	-7.91	-8.14	-8.23	-8.28	-8.36
	σ_{gDS}	0.80	0.67	0.68	0.66	0.62	0.51	0.45	0.31	0.08
AOD spread (ASD) lgASD= $\log_{10}(ASD/1^\circ)$	μ_{gASD}	-3.06	-2.68	-2.51	-2.40	-2.31	-2.20	-2.00	-1.64	-0.63
	σ_{gASD}	0.48	0.36	0.38	0.32	0.33	0.39	0.40	0.32	0.53
AOA spread (ASA) lgASA= $\log_{10}(ASA/1^\circ)$	μ_{gASA}	0.94	0.87	0.92	0.79	0.72	0.60	0.55	0.71	0.81
	σ_{gASA}	0.70	0.66	0.68	0.64	0.63	0.54	0.52	0.53	0.62
ZOA spread (ZSA) lgZSA= $\log_{10}(ZSA/1^\circ)$	μ_{gZSA}	0.82	0.50	0.82	1.23	1.43	1.56	1.66	1.73	1.79
	σ_{gZSA}	0.03	0.09	0.05	0.03	0.06	0.05	0.05	0.02	0.01
ZOD spread (ZSD) lgZSD= $\log_{10}(ZSD/1^\circ)$	μ_{gZSD}	-2.52	-2.29	-2.19	-2.24	-2.30	-2.48	-2.64	-2.68	-2.61
	σ_{gZSD}	0.50	0.53	0.58	0.51	0.46	0.35	0.31	0.39	0.28
Shadow fading (SF) [dB]	σ_{SF}	See Table 6.6.2-1								
K-factor (K) [dB]	μ_K	4.4	9.0	9.3	7.9	7.4	7.0	6.9	6.5	6.8
	σ_K	3.3	6.6	6.1	4.0	3.0	2.6	2.2	2.1	1.9
Cross-Correlations	ASD vs DS	0.4	0.4	0.4	0.4	0.4	0.4	0.4	0.4	0.4
	ASA vs DS	0.8	0.8	0.8	0.8	0.8	0.8	0.8	0.8	0.8
	ASA vs SF	-0.5	-0.5	-0.5	-0.5	-0.5	-0.5	-0.5	-0.5	-0.5
	ASD vs SF	-0.5	-0.5	-0.5	-0.5	-0.5	-0.5	-0.5	-0.5	-0.5
	DS vs SF	-0.4	-0.4	-0.4	-0.4	-0.4	-0.4	-0.4	-0.4	-0.4
	ASD vs ASA	0	0	0	0	0	0	0	0	0
	ASD vs K	0	0	0	0	0	0	0	0	0
	ASA vs K	-0.2	-0.2	-0.2	-0.2	-0.2	-0.2	-0.2	-0.2	-0.2
	DS vs K	-0.4	-0.4	-0.4	-0.4	-0.4	-0.4	-0.4	-0.4	-0.4
	SF vs K	0	0	0	0	0	0	0	0	0
Cross-Correlations	ZSD vs SF	0	0	0	0	0	0	0	0	0
	ZSA vs SF	-0.8	-0.8	-0.8	-0.8	-0.8	-0.8	-0.8	-0.8	-0.8
	ZSD vs K	0	0	0	0	0	0	0	0	0
	ZSA vs K	0	0	0	0	0	0	0	0	0
	ZSD vs DS	-0.2	-0.2	-0.2	-0.2	-0.2	-0.2	-0.2	-0.2	-0.2
	ZSA vs DS	0	0	0	0	0	0	0	0	0
	ZSD vs ASD	0.5	0.5	0.5	0.5	0.5	0.5	0.5	0.5	0.5
	ZSA vs ASD	0	0	0	0	0	0	0	0	0
	ZSD vs ASA	-0.3	-0.3	-0.3	-0.3	-0.3	-0.3	-0.3	-0.3	-0.3
	ZSA vs ASA	0.4	0.4	0.4	0.4	0.4	0.4	0.4	0.4	0.4
Delay scaling parameter r_t		2.5	2.5	2.5	2.5	2.5	2.5	2.5	2.5	2.5
XPR [dB]	μ_{XPR}	24.4	23.6	23.2	22.6	21.8	20.5	19.3	17.4	12.3
	σ_{XPR}	3.8	4.7	4.6	4.9	5.7	6.9	8.1	10.3	15.2

Number of clusters N	3	3	3	3	3	3	3	3	3
Number of rays per cluster M	20	20	20	20	20	20	20	20	20
Cluster DS (C_{DS}) in [ns]	3.9	3.9	3.9	3.9	3.9	3.9	3.9	3.9	3.9
Cluster ASD (C_{ASD}) in [deg]	0	0	0	0	0	0	0	0	0
Cluster ASA (C_{ASA}) in [deg]	11	11	11	11	11	11	11	11	11
Cluster ZSA (C_{ZSA}) in [deg]	7	7	7	7	7	7	7	7	7
Per cluster shadowing std ζ [dB]	3	3	3	3	3	3	3	3	3
Correlation distance in the horizontal plane [m]	DS	30	30	30	30	30	30	30	30
	ASD	18	18	18	18	18	18	18	18
	ASA	15	15	15	15	15	15	15	15
	SF	37	37	37	37	37	37	37	37
	K	12	12	12	12	12	12	12	12
	ZSA	15	15	15	15	15	15	15	15
	ZSD	15	15	15	15	15	15	15	15

f_c is carrier frequency in GHz; d_{20} is BS-UT distance in km.

NOTE 1: DS = rms delay spread, ASD = rms azimuth spread of departure angles, ASA = rms azimuth spread of arrival angles, ZSD = rms zenith spread of departure angles, ZSA = rms zenith spread of arrival angles, SF = shadow fading, and K = Ricean K-factor.

NOTE 2: The sign of the shadow fading is defined so that positive SF means more received power at UT than predicted by the path loss model.

NOTE 3: All large scale parameters are assumed to have no correlation between different floors.

NOTE 4: The following notation for mean ($\mu_{lgX}=\text{mean}\{\log_{10}(X)\}$) and standard deviation ($\sigma_{lgX}=\text{std}\{\log_{10}(X)\}$) is used for logarithmized parameters X.

NOTE 5: For all considered scenarios the AOD/AOA distributions are modelled by a wrapped Gaussian distribution, the ZOD/ZOA distributions are modelled by a Laplacian distribution and the delay distribution is modelled by an exponential distribution.

NOTE 6: For UMa and frequencies below 6 GHz, use $f_c = 6$ when determining the values of the frequency-dependent LSP values

NOTE 7: For UMi and frequencies below 2 GHz, use $f_c = 2$ when determining the values of the frequency-dependent LSP values

NOTE 8: For satellite (e.g.GEO/LEO), the departure angle spreads are zeros, i.e. μ_{lgASD} and μ_{lgZSD} are $-\infty$, and corresponding standard deviations are zeros.

NOTE 9: The number of clusters is based on a limited data. The number may be different in the real field conditions.

Table 6.7.2-1b: Channel model parameters for Dense Urban Scenario (LOS) in Ka band

Scenarios	Dense Urban LOS									
	10°	20°	30°	40°	50°	60°	70°	80°	90°	
Delay spread (DS) $lgDS=\log_{10}(DS/1s)$	μ_{lgDS}	-7.43	-7.62	-7.76	-8.02	-8.13	-8.30	-8.34	-8.39	-8.45
	σ_{lgDS}	0.90	0.78	0.80	0.72	0.61	0.47	0.39	0.26	0.01
AOD spread (ASD) $lgASD=\log_{10}(ASD/1^\circ)$	μ_{lgASD}	-3.43	-3.06	-2.91	-2.81	-2.74	-2.72	-2.46	-2.30	-1.11
	σ_{lgASD}	0.54	0.41	0.42	0.34	0.34	0.70	0.40	0.78	0.51
AOA spread (ASA) $lgASA=\log_{10}(ASA/1^\circ)$	μ_{lgASA}	0.65	0.53	0.60	0.43	0.36	0.16	0.18	0.24	0.36
	σ_{lgASA}	0.82	0.78	0.83	0.78	0.77	0.84	0.64	0.81	0.65
ZOA spread (ZSA) $lgZSA=\log_{10}(ZSA/1^\circ)$	μ_{lgZSA}	0.82	0.47	0.80	1.23	1.42	1.56	1.65	1.73	1.79
	σ_{lgZSA}	0.05	0.11	0.05	0.04	0.10	0.06	0.07	0.02	0.01
ZOD spread (ZSD) $lgZSD=\log_{10}(ZSD/1^\circ)$	μ_{lgZSD}	-2.75	-2.64	-2.49	-2.51	-2.54	-2.71	-2.85	-3.01	-3.08
	σ_{lgZSD}	0.55	0.64	0.69	0.57	0.50	0.37	0.31	0.45	0.27
Shadow fading (SF) [dB]	σ_{SF}	See Table 6.6.2-1								
K-factor (K) [dB]	μ_K	6.1	13.7	12.9	10.3	9.2	8.4	8.0	7.4	7.6
	σ_K	2.6	6.8	6.0	3.3	2.2	1.9	1.5	1.6	1.3
Cross-Correlations	ASD vs DS	0.4	0.4	0.4	0.4	0.4	0.4	0.4	0.4	0.4
	ASA vs DS	0.8	0.8	0.8	0.8	0.8	0.8	0.8	0.8	0.8
	ASA vs SF	-0.5	-0.5	-0.5	-0.5	-0.5	-0.5	-0.5	-0.5	-0.5
	ASD vs SF	-0.5	-0.5	-0.5	-0.5	-0.5	-0.5	-0.5	-0.5	-0.5
	DS vs SF	-0.4	-0.4	-0.4	-0.4	-0.4	-0.4	-0.4	-0.4	-0.4
	ASD vs ASA	0	0	0	0	0	0	0	0	0
	ASD vs K	0	0	0	0	0	0	0	0	0
	ASA vs K	-0.2	-0.2	-0.2	-0.2	-0.2	-0.2	-0.2	-0.2	-0.2
	DS vs K	-0.4	-0.4	-0.4	-0.4	-0.4	-0.4	-0.4	-0.4	-0.4
	SF vs K	0	0	0	0	0	0	0	0	0
Cross-Correlations	ZSD vs SF	0	0	0	0	0	0	0	0	0

ZSA vs SF	-0.8	-0.8	-0.8	-0.8	-0.8	-0.8	-0.8	-0.8	-0.8	-0.8
ZSD vs K	0	0	0	0	0	0	0	0	0	0
ZSA vs K	0	0	0	0	0	0	0	0	0	0
ZSD vs DS	-0.2	-0.2	-0.2	-0.2	-0.2	-0.2	-0.2	-0.2	-0.2	-0.2
ZSA vs DS	0	0	0	0	0	0	0	0	0	0
ZSD vs ASD	0.5	0.5	0.5	0.5	0.5	0.5	0.5	0.5	0.5	0.5
ZSA vs ASD	0	0	0	0	0	0	0	0	0	0
ZSD vs ASA	-0.3	-0.3	-0.3	-0.3	-0.3	-0.3	-0.3	-0.3	-0.3	-0.3
ZSA vs ASA	0.4	0.4	0.4	0.4	0.4	0.4	0.4	0.4	0.4	0.4
ZSD vs ZSA	0	0	0	0	0	0	0	0	0	0
Delay scaling parameter r_τ	2.5	2.5	2.5	2.5	2.5	2.5	2.5	2.5	2.5	2.5
XPR [dB]	μ_{XPR}	24.7	24.4	24.4	24.2	23.9	23.3	22.6	21.2	17.6
	σ_{XPR}	2.1	2.8	2.7	2.7	3.1	3.9	4.8	6.8	12.7
Number of clusters N	3	3	3	3	3	3	3	3	3	3
Number of rays per cluster M	20	20	20	20	20	20	20	20	20	20
Cluster DS (C_{DS}) in [ns]	1.6	1.6	1.6	1.6	1.6	1.6	1.6	1.6	1.6	1.6
Cluster ASD (C_{ASD}) in [deg]	0	0	0	0	0	0	0	0	0	0
Cluster ASA (C_{ASA}) in [deg]	11	11	11	11	11	11	11	11	11	11
Cluster ZSA (C_{ZSA}) in [deg]	7	7	7	7	7	7	7	7	7	7
Per cluster shadowing std ζ [dB]	3	3	3	3	3	3	3	3	3	3
Correlation distance in the horizontal plane [m]	DS	30	30	30	30	30	30	30	30	30
	ASD	18	18	18	18	18	18	18	18	18
	ASA	15	15	15	15	15	15	15	15	15
	SF	37	37	37	37	37	37	37	37	37
	K	12	12	12	12	12	12	12	12	12
	ZSA	15	15	15	15	15	15	15	15	15
	ZSD	15	15	15	15	15	15	15	15	15

f_c is carrier frequency in GHz; d_{2D} is BS-UT distance in km.

NOTE 1: DS = rms delay spread, ASD = rms azimuth spread of departure angles, ASA = rms azimuth spread of arrival angles, ZSD = rms zenith spread of departure angles, ZSA = rms zenith spread of arrival angles, SF = shadow fading, and K = Ricean K-factor.

NOTE 2: The sign of the shadow fading is defined so that positive SF means more received power at UT than predicted by the path loss model.

NOTE 3: All large scale parameters are assumed to have no correlation between different floors.

NOTE 4: The following notation for mean ($\mu_{\lg X}=\text{mean}\{\log_{10}(X)\}$) and standard deviation ($\sigma_{\lg X}=\text{std}\{\log_{10}(X)\}$) is used for logarithmized parameters X.

NOTE 5: For all considered scenarios the AOD/AOA distributions are modelled by a wrapped Gaussian distribution, the ZOD/ZOA distributions are modelled by a Laplacian distribution and the delay distribution is modelled by an exponential distribution.

NOTE 6: For UMA and frequencies below 6 GHz, use $f_c=6$ when determining the values of the frequency-dependent LSP values

NOTE 7: For UMi and frequencies below 2 GHz, use $f_c=2$ when determining the values of the frequency-dependent LSP values

NOTE 8: For satellite (e.g.GEO/LEO), the departure angle spreads are zeros, i.e. $\mu_{\lg \text{ASD}}$ and $\mu_{\lg \text{ZSD}}$ are $-\infty$, and corresponding standard deviations are zeros.

NOTE 9: The number of clusters is based on a limited data. The number may be different in the real field conditions.

Table 6.7.2-2a: Channel model parameters for Dense Urban Scenario (NLOS) in S band

Scenarios	Dense Urban NLOS									
	10°	20°	30°	40°	50°	60°	70°	80°	90°	
Delay spread (DS) $\lg DS = \log_{10}(DS/1s)$	$\mu_{\lg DS}$	-6.84	-6.81	-6.94	-7.14	-7.34	-7.53	-7.67	-7.82	-7.84
	$\sigma_{\lg DS}$	0.82	0.61	0.49	0.49	0.51	0.47	0.44	0.42	0.55
AOD spread (ASD) $\lg ASD = \log_{10}(ASD/1^\circ)$	$\mu_{\lg ASD}$	-2.08	-1.68	-1.46	-1.43	-1.44	-1.33	-1.31	-1.11	-0.11
	$\sigma_{\lg ASD}$	0.87	0.73	0.53	0.50	0.58	0.49	0.65	0.69	0.53
AOA spread (ASA) $\lg ASA = \log_{10}(ASA/1^\circ)$	$\mu_{\lg ASA}$	1.00	1.44	1.54	1.53	1.48	1.39	1.42	1.38	1.23
	$\sigma_{\lg ASA}$	1.60	0.87	0.64	0.56	0.54	0.68	0.55	0.60	0.60
ZOA spread (ZSA) $\lg ZSA = \log_{10}(ZSA/1^\circ)$	$\mu_{\lg ZSA}$	1.00	0.94	1.15	1.35	1.44	1.56	1.64	1.70	1.70
	$\sigma_{\lg ZSA}$	0.63	0.65	0.42	0.28	0.25	0.16	0.18	0.09	0.17
ZOD spread (ZSD) $\lg ZSD = \log_{10}(ZSD/1^\circ)$	$\mu_{\lg ZSD}$	-2.08	-1.66	-1.48	-1.46	-1.53	-1.61	-1.77	-1.90	-1.99
	$\sigma_{\lg ZSD}$	0.58	0.50	0.40	0.37	0.47	0.43	0.50	0.42	0.50
Shadow fading (SF) [dB]	σ_{SF}	See Table 6.6.2-1								
Cross-Correlations	ASD vs DS	0.4	0.4	0.4	0.4	0.4	0.4	0.4	0.4	0.4
	ASA vs DS	0.6	0.6	0.6	0.6	0.6	0.6	0.6	0.6	0.6

	<i>ASA vs SF</i>	0	0	0	0	0	0	0	0
	<i>ASD vs SF</i>	-0.6	-0.6	-0.6	-0.6	-0.6	-0.6	-0.6	-0.6
	<i>DS vs SF</i>	-0.4	-0.4	-0.4	-0.4	-0.4	-0.4	-0.4	-0.4
	<i>ASD vs ASA</i>	0.4	0.4	0.4	0.4	0.4	0.4	0.4	0.4
	<i>ASD vs K</i>	N/A							
	<i>ASA vs K</i>	N/A							
	<i>DS vs K</i>	N/A							
	<i>SF vs K</i>	N/A							
Cross-Correlations	<i>ZSD vs SF</i>	0	0	0	0	0	0	0	0
	<i>ZSA vs SF</i>	-0.4	-0.4	-0.4	-0.4	-0.4	-0.4	-0.4	-0.4
	<i>ZSD vs K</i>	N/A							
	<i>ZSA vs K</i>	N/A							
	<i>ZSD vs DS</i>	-0.5	-0.5	-0.5	-0.5	-0.5	-0.5	-0.5	-0.5
	<i>ZSA vs DS</i>	0	0	0	0	0	0	0	0
	<i>ZSD vs ASD</i>	0.5	0.5	0.5	0.5	0.5	0.5	0.5	0.5
	<i>ZSA vs ASD</i>	-0.1	-0.1	-0.1	-0.1	-0.1	-0.1	-0.1	-0.1
	<i>ZSD vs ASA</i>	0	0	0	0	0	0	0	0
	<i>ZSA vs ASA</i>	0	0	0	0	0	0	0	0
	<i>ZSD vs ZSA</i>	0	0	0	0	0	0	0	0
	Delay scaling parameter r_e	2.3	2.3	2.3	2.3	2.3	2.3	2.3	2.3
XPR [dB]	μ_{XPR}	23.8	21.9	19.7	18.1	16.3	14.0	12.1	8.7
	σ_{XPR}	4.4	6.3	8.1	9.3	11.5	13.3	14.9	17.0
Number of clusters N		4	4	4	4	4	4	4	4
Number of rays per cluster M		20	20	20	20	20	20	20	20
Cluster DS (C_{DS}) in [ns]		3.9	3.9	3.9	3.9	3.9	3.9	3.9	3.9
Cluster ASD (C_{ASD}) in [deg]		0	0	0	0	0	0	0	0
Cluster ASA (C_{ASA}) in [deg]		15	15	15	15	15	15	15	15
Cluster ZSA (C_{ZSA}) in [deg]		7	7	7	7	7	7	7	7
Per cluster shadowing std ζ [dB]		3	3	3	3	3	3	3	3
Correlation distance in the horizontal plane [m]	DS	40	40	40	40	40	40	40	40
	ASD	50	50	50	50	50	50	50	50
	ASA	50	50	50	50	50	50	50	50
	SF	50	50	50	50	50	50	50	50
	K	N/A							
	ZSA	50	50	50	50	50	50	50	50
	ZSD	50	50	50	50	50	50	50	50
f_c is carrier frequency in GHz; d_{2D} is BS-UT distance in km.									
NOTE 1: DS = rms delay spread, ASD = rms azimuth spread of departure angles, ASA = rms azimuth spread of arrival angles, ZSD = rms zenith spread of departure angles, ZSA = rms zenith spread of arrival angles, SF = shadow fading, and K = Ricean K-factor.									
NOTE 2: The sign of the shadow fading is defined so that positive SF means more received power at UT than predicted by the path loss model.									
NOTE 3: All large scale parameters are assumed to have no correlation between different floors.									
NOTE 4: The following notation for mean ($\mu_{\log X} = \text{mean}\{\log_{10}(X)\}$) and standard deviation ($\sigma_{\log X} = \text{std}\{\log_{10}(X)\}$) is used for logarithmized parameters X.									
NOTE 5: For all considered scenarios the AOD/AOA distributions are modelled by a wrapped Gaussian distribution, the ZOD/ZOA distributions are modelled by a Laplacian distribution and the delay distribution is modelled by an exponential distribution.									
NOTE 6: For UMa and frequencies below 6 GHz, use $f_c = 6$ when determining the values of the frequency-dependent LSP values									
NOTE 7: For UMi and frequencies below 2 GHz, use $f_c = 2$ when determining the values of the frequency-dependent LSP values									
NOTE 8: For satellite (e.g.GEO/LEO), the departure angle spreads are zeros, i.e. $\mu_{\log ASD}$ and $\mu_{\log ZSD}$ are $-\infty$, and corresponding standard deviations are zeros.									
NOTE 9: The number of clusters is based on a limited data. The number may be different in the real field conditions.									

Table 6.7.2-2b: Channel model parameters for Dense Urban Scenario (NLOS) in Ka band

Scenarios	Dense Urban NLOS								
	10°	20°	30°	40°	50°	60°	70°	80°	90°

Delay spread (DS) lgDS= $\log_{10}(DS/1s)$	μ_{lgDS}	-6.86	-6.84	-7.00	-7.21	-7.42	-7.86	-7.76	-8.07	-7.95
	σ_{lgDS}	0.81	0.61	0.56	0.56	0.57	0.55	0.47	0.42	0.59
AOD spread (ASD) lgASD= $\log_{10}(ASD/1^\circ)$	μ_{lgASD}	-2.12	-1.74	-1.56	-1.54	-1.45	-1.64	-1.37	-1.29	-0.41
	σ_{lgASD}	0.94	0.79	0.66	0.63	0.56	0.78	0.56	0.76	0.59
AOA spread (ASA) lgASA= $\log_{10}(ASA/1^\circ)$	μ_{lgASA}	1.02	1.44	1.48	1.46	1.40	0.97	1.33	1.12	1.04
	σ_{lgASA}	1.44	0.77	0.70	0.60	0.59	1.27	0.56	1.04	0.63
ZOA spread (ZSA) lgZSA= $\log_{10}(ZSA/1^\circ)$	μ_{lgZSA}	1.01	0.96	1.13	1.30	1.40	1.41	1.63	1.68	1.70
	σ_{lgZSA}	0.56	0.55	0.43	0.37	0.32	0.45	0.17	0.14	0.17
ZOD spread (ZSD) lgZSD= $\log_{10}(ZSD/1^\circ)$	μ_{lgZSD}	-2.11	-1.69	-1.52	-1.51	-1.54	-1.84	-1.86	-2.16	-2.21
	σ_{lgZSD}	0.59	0.51	0.46	0.43	0.45	0.63	0.51	0.74	0.61
Shadow fading (SF) [dB]	σ_{SF}	See Table 6.6.2-1								
Cross-Correlations	ASD vs DS	0.4	0.4	0.4	0.4	0.4	0.4	0.4	0.4	0.4
	ASA vs DS	0.6	0.6	0.6	0.6	0.6	0.6	0.6	0.6	0.6
	ASA vs SF	0	0	0	0	0	0	0	0	0
	ASD vs SF	-0.6	-0.6	-0.6	-0.6	-0.6	-0.6	-0.6	-0.6	-0.6
	DS vs SF	-0.4	-0.4	-0.4	-0.4	-0.4	-0.4	-0.4	-0.4	-0.4
	ASD vs ASA	0.4	0.4	0.4	0.4	0.4	0.4	0.4	0.4	0.4
	ASD vs K	N/A	N/A	N/A	N/A	N/A	N/A	N/A	N/A	N/A
	ASA vs K	N/A	N/A	N/A	N/A	N/A	N/A	N/A	N/A	N/A
	DS vs K	N/A	N/A	N/A	N/A	N/A	N/A	N/A	N/A	N/A
	SF vs K	N/A	N/A	N/A	N/A	N/A	N/A	N/A	N/A	N/A
Cross-Correlations	ZSD vs SF	0	0	0	0	0	0	0	0	0
	ZSA vs SF	-0.4	-0.4	-0.4	-0.4	-0.4	-0.4	-0.4	-0.4	-0.4
	ZSD vs K	N/A	N/A	N/A	N/A	N/A	N/A	N/A	N/A	N/A
	ZSA vs K	N/A	N/A	N/A	N/A	N/A	N/A	N/A	N/A	N/A
	ZSD vs DS	-0.5	-0.5	-0.5	-0.5	-0.5	-0.5	-0.5	-0.5	-0.5
	ZSA vs DS	0	0	0	0	0	0	0	0	0
	ZSD vs ASD	0.5	0.5	0.5	0.5	0.5	0.5	0.5	0.5	0.5
	ZSA vs ASD	-0.1	-0.1	-0.1	-0.1	-0.1	-0.1	-0.1	-0.1	-0.1
	ZSD vs ASA	0	0	0	0	0	0	0	0	0
	ZSA vs ASA	0	0	0	0	0	0	0	0	0
Delay scaling parameter r_t		2.3	2.3	2.3	2.3	2.3	2.3	2.3	2.3	2.3
XPR [dB]	μ_{XPR}	23.7	21.8	19.6	18.0	16.3	15.9	12.3	10.5	10.5
	σ_{XPR}	4.5	6.3	8.2	9.4	11.5	12.4	15.0	15.7	15.7
Number of clusters N		4	4	4	4	4	4	4	4	4
Number of rays per cluster M		20	20	20	20	20	20	20	20	20
Cluster DS (c_{DS}) in [ns]		3.9	3.9	3.9	3.9	3.9	3.9	3.9	3.9	3.9
Cluster ASD (c_{ASD}) in [deg]		0	0	0	0	0	0	0	0	0
Cluster ASA (c_{ASA}) in [deg]		15	15	15	15	15	15	15	15	15
Cluster ZSA (c_{ZSA}) in [deg]		7	7	7	7	7	7	7	7	7
Per cluster shadowing std ζ [dB]		3	3	3	3	3	3	3	3	3
Correlation distance in the horizontal plane [m]	DS	40	40	40	40	40	40	40	40	40
	ASD	50	50	50	50	50	50	50	50	50
	ASA	50	50	50	50	50	50	50	50	50
	SF	50	50	50	50	50	50	50	50	50
	K	N/A	N/A	N/A	N/A	N/A	N/A	N/A	N/A	N/A
	ZSA	50	50	50	50	50	50	50	50	50
	ZSD	50	50	50	50	50	50	50	50	50

f_c is carrier frequency in GHz; d_{2D} is BS-UT distance in km.

NOTE 1: DS = rms delay spread, ASD = rms azimuth spread of departure angles, ASA = rms azimuth spread of arrival angles, ZSD = rms zenith spread of departure angles, ZSA = rms zenith spread of arrival angles, SF = shadow fading, and K = Ricean K-factor.

NOTE 2: The sign of the shadow fading is defined so that positive SF means more received power at UT than predicted by the path loss model.

NOTE 3: All large scale parameters are assumed to have no correlation between different floors.

NOTE 4: The following notation for mean ($\mu_{\lg X} = \text{mean}\{\log_{10}(X)\}$) and standard deviation ($\sigma_{\lg X} = \text{std}\{\log_{10}(X)\}$) is used for logarithmized parameters X.

NOTE 5: For all considered scenarios the AOD/AOA distributions are modelled by a wrapped Gaussian distribution, the ZOD/ZOA distributions are modelled by a Laplacian distribution and the delay distribution is modelled by an exponential distribution.

NOTE 6: For UMa and frequencies below 6 GHz, use $f_c = 6$ when determining the values of the frequency-dependent LSP values

NOTE 7: For UMi and frequencies below 2 GHz, use $f_c = 2$ when determining the values of the frequency-dependent LSP values

NOTE 8: For satellite (e.g.GEO/LEO), the departure angle spreads are zeros, i.e. $\mu_{\lg \text{ASD}}$ and $\mu_{\lg \text{ZSD}}$ are $-\infty$, and corresponding standard deviations are zeros.

NOTE 9: The number of clusters is based on a limited data. The number may be different in the real field conditions.

Table 6.7.2-3a: Channel model parameters for Urban Scenario (LOS) at S band

Scenarios		Urban LOS								
		10°	20°	30°	40°	50°	60°	70°	80°	90°
Delay spread (DS) lgDS=	μ_{lgDS}	-7.97	-8.12	-8.21	-8.31	-8.37	-8.39	-8.38	-8.35	-8.34
lgDS= $\log_{10}(DS/1s)$	σ_{lgDS}	1	0.83	0.68	0.48	0.38	0.24	0.18	0.13	0.09
AOD spread (ASD) lgASD=	μ_{lgASD}	-2.6	-2.48	-2.44	-2.6	-2.71	-2.76	-2.78	-2.65	-2.27
lgASD= $\log_{10}(ASD/1^\circ)$	σ_{lgASD}	0.79	0.8	0.91	1.02	1.17	1.17	1.2	1.45	1.85
AOA spread (ASA) lgASA=	μ_{lgASA}	0.18	0.42	0.41	0.18	-0.07	-0.43	-0.64	-0.91	-0.54
lgASA= $\log_{10}(ASA/1^\circ)$	σ_{lgASA}	0.74	0.9	1.3	1.69	2.04	2.54	2.47	2.69	1.66
ZOA spread (ZSA) lgZSA=	μ_{lgZSA}	-0.63	-0.15	0.54	0.35	0.27	0.26	-0.12	-0.21	-0.07
lgZSA= $\log_{10}(ZSA/1^\circ)$	σ_{lgZSA}	2.6	3.31	1.1	1.59	1.62	0.97	1.99	1.82	1.43
ZOD spread (ZSD) lgZSD=	μ_{lgZSD}	-2.54	-2.67	-2.03	-2.28	-2.48	-2.56	-2.96	-3.08	-3
lgZSD= $\log_{10}(ZSD/1^\circ)$	σ_{lgZSD}	2.62	2.96	0.86	1.19	1.4	0.85	1.61	1.49	1.09
Shadow fading (SF) [dB]	σ_{SF}	See Table 6.6.2-2								
K-factor (K) [dB]	μ_K	31.83	18.78	10.49	7.46	6.52	5.47	4.54	4.03	3.68
	σ_K	13.84	13.78	10.42	8.01	8.27	7.26	5.53	4.49	3.14
Cross-Correlations	ASD vs DS	0.4	0.4	0.4	0.4	0.4	0.4	0.4	0.4	0.4
	ASA vs DS	0.8	0.8	0.8	0.8	0.8	0.8	0.8	0.8	0.8
	ASA vs SF	-0.5	-0.5	-0.5	-0.5	-0.5	-0.5	-0.5	-0.5	-0.5
	ASD vs SF	-0.5	-0.5	-0.5	-0.5	-0.5	-0.5	-0.5	-0.5	-0.5
	DS vs SF	-0.4	-0.4	-0.4	-0.4	-0.4	-0.4	-0.4	-0.4	-0.4
	ASD vs ASA	0	0	0	0	0	0	0	0	0
	ASD vs K	0	0	0	0	0	0	0	0	0
	ASA vs K	-0.2	-0.2	-0.2	-0.2	-0.2	-0.2	-0.2	-0.2	-0.2
	DS vs K	-0.4	-0.4	-0.4	-0.4	-0.4	-0.4	-0.4	-0.4	-0.4
	SF vs K	0	0	0	0	0	0	0	0	0
Cross-Correlations	ZSD vs SF	0	0	0	0	0	0	0	0	0
	ZSA vs SF	-0.8	-0.8	-0.8	-0.8	-0.8	-0.8	-0.8	-0.8	-0.8
	ZSD vs K	0	0	0	0	0	0	0	0	0
	ZSA vs K	0	0	0	0	0	0	0	0	0
	ZSD vs DS	-0.2	-0.2	-0.2	-0.2	-0.2	-0.2	-0.2	-0.2	-0.2
	ZSA vs DS	0	0	0	0	0	0	0	0	0
	ZSD vs ASD	0.5	0.5	0.5	0.5	0.5	0.5	0.5	0.5	0.5
	ZSA vs ASD	0	0	0	0	0	0	0	0	0
	ZSD vs ASA	-0.3	-0.3	-0.3	-0.3	-0.3	-0.3	-0.3	-0.3	-0.3
	ZSA vs ASA	0.4	0.4	0.4	0.4	0.4	0.4	0.4	0.4	0.4

	ZSD vs ZSA	0	0	0	0	0	0	0	0
Delay scaling parameter r_c		2.5	2.5	2.5	2.5	2.5	2.5	2.5	2.5
XPR [dB]	μ_{XPR}	8	8	8	8	8	8	8	8
	σ_{XPR}	4	4	4	4	4	4	4	4
Number of clusters N		4	3	3	3	3	3	3	3
Number of rays per cluster M		20	20	20	20	20	20	20	20
Cluster DS (C_{DS}) in [ns]		3.9	3.9	3.9	3.9	3.9	3.9	3.9	3.9
Cluster ASD (C_{ASD}) in [deg]		0.09	0.09	0.12	0.16	0.2	0.28	0.44	0.9
Cluster ASA (C_{ASA}) in [deg]		12.55	12.76	14.36	16.42	17.13	19.01	19.31	22.39
Cluster ZSA (C_{ZSA}) in [deg]		1.25	3.23	4.39	5.72	6.17	7.36	7.7	9.25
Per cluster shadowing std ζ [dB]		3	3	3	3	3	3	3	3
Correlation distance in the horizontal plane [m]	DS	30	30	30	30	30	30	30	30
	ASD	18	18	18	18	18	18	18	18
	ASA	15	15	15	15	15	15	15	15
	SF	37	37	37	37	37	37	37	37
	K	12	12	12	12	12	12	12	12
	ZSA	15	15	15	15	15	15	15	15
	ZSD	15	15	15	15	15	15	15	15
f_c is carrier frequency in GHz; d_{BD} is BS-UT distance in km.									
NOTE 1: DS = rms delay spread, ASD = rms azimuth spread of departure angles, ASA = rms azimuth spread of arrival angles, ZSD = rms zenith spread of departure angles, ZSA = rms zenith spread of arrival angles, SF = shadow fading, and K = Ricean K-factor.									
NOTE 2: The sign of the shadow fading is defined so that positive SF means more received power at UT than predicted by the path loss model.									
NOTE 3: All large scale parameters are assumed to have no correlation between different floors.									
NOTE 4: The following notation for mean ($\mu_{\log X} = \text{mean}\{\log_{10}(X)\}$) and standard deviation ($\sigma_{\log X} = \text{std}\{\log_{10}(X)\}$) is used for logarithmized parameters X.									
NOTE 5: For all considered scenarios the AOD/AOA distributions are modelled by a wrapped Gaussian distribution, the ZOD/ZOA distributions are modelled by a Laplacian distribution and the delay distribution is modelled by an exponential distribution.									
NOTE 6: For UMa and frequencies below 6 GHz, use $f_c = 6$ when determining the values of the frequency-dependent LSP values									
NOTE 7: For UMi and frequencies below 2 GHz, use $f_c = 2$ when determining the values of the frequency-dependent LSP values									
NOTE 8: For satellite (e.g.GEO/LEO), the departure angle spreads are zeros, i.e. $\mu_{\log ASD}$ and $\mu_{\log ZSD}$ are $-\infty$, and corresponding standard deviations are zeros.									
NOTE 9: The number of clusters is based on a limited data. The number may be different in the real field conditions.									

Table 6.7.2-3b: Channel model parameters for Urban Scenario (LOS) at Ka band

Scenarios		Urban LOS								
		10°	20°	30°	40°	50°	60°	70°	80°	90°
Delay spread (DS) $\lg DS = \log_{10}(DS/1s)$	$\mu_{\log DS}$	-8.52	-8.59	-8.51	-8.49	-8.48	-8.44	-8.4	-8.37	-8.35
	$\sigma_{\log DS}$	0.92	0.79	0.65	0.48	0.46	0.34	0.27	0.19	0.14
AOD spread (ASD) $\lg ASD = \log_{10}(ASD/1^\circ)$	$\mu_{\log ASD}$	-3.18	-3.05	-2.98	-3.11	-3.19	-3.25	-3.33	-3.22	-2.83
	$\sigma_{\log ASD}$	0.79	0.87	1.04	1.06	1.12	1.14	1.25	1.35	1.62
AOA spread (ASA) $\lg ASA = \log_{10}(ASA/1^\circ)$	$\mu_{\log ASA}$	-0.4	-0.15	-0.18	-0.31	-0.58	-0.9	-1.16	-1.48	-1.14
	$\sigma_{\log ASA}$	0.77	0.97	1.58	1.69	2.13	2.51	2.47	2.61	1.7
ZOA spread (ZSA) $\lg ZSA = \log_{10}(ZSA/1^\circ)$	$\mu_{\log ZSA}$	-0.67	-0.34	0.07	-0.08	-0.21	-0.25	-0.61	-0.79	-0.58
	$\sigma_{\log ZSA}$	2.22	3.04	1.33	1.45	1.62	1.06	1.88	1.87	1.19
ZOD spread (ZSD) $\lg ZSD = \log_{10}(ZSD/1^\circ)$	$\mu_{\log ZSD}$	-2.61	-2.82	-2.48	-2.76	-2.93	-3.05	-3.45	-3.66	-3.56
	$\sigma_{\log ZSD}$	2.41	2.59	1.02	1.27	1.38	0.96	1.51	1.49	0.89
Shadow fading (SF) [dB]	σ_{SF}	See Table 6.6.2-2								
K-factor (K) [dB]	μ_K	40.18	23.62	12.48	8.56	7.42	5.97	4.88	4.22	3.81
	σ_K	16.99	18.96	14.23	11.06	11.21	9.47	7.24	5.79	4.25
Cross-Correlations	ASD vs DS	0.4	0.4	0.4	0.4	0.4	0.4	0.4	0.4	0.4
	ASA vs DS	0.8	0.8	0.8	0.8	0.8	0.8	0.8	0.8	0.8
	ASA vs SF	-0.5	-0.5	-0.5	-0.5	-0.5	-0.5	-0.5	-0.5	-0.5

	<i>ASD</i> vs <i>SF</i>	-0.5	-0.5	-0.5	-0.5	-0.5	-0.5	-0.5	-0.5	-0.5
	<i>DS</i> vs <i>SF</i>	-0.4	-0.4	-0.4	-0.4	-0.4	-0.4	-0.4	-0.4	-0.4
	<i>ASD</i> vs <i>ASA</i>	0	0	0	0	0	0	0	0	0
	<i>ASD</i> vs <i>K</i>	0	0	0	0	0	0	0	0	0
	<i>ASA</i> vs <i>K</i>	-0.2	-0.2	-0.2	-0.2	-0.2	-0.2	-0.2	-0.2	-0.2
	<i>DS</i> vs <i>K</i>	-0.4	-0.4	-0.4	-0.4	-0.4	-0.4	-0.4	-0.4	-0.4
	<i>SF</i> vs <i>K</i>	0	0	0	0	0	0	0	0	0
Cross-Correlations	<i>ZSD</i> vs <i>SF</i>	0	0	0	0	0	0	0	0	0
	<i>ZSA</i> vs <i>SF</i>	-0.8	-0.8	-0.8	-0.8	-0.8	-0.8	-0.8	-0.8	-0.8
	<i>ZSD</i> vs <i>K</i>	0	0	0	0	0	0	0	0	0
	<i>ZSA</i> vs <i>K</i>	0	0	0	0	0	0	0	0	0
	<i>ZSD</i> vs <i>DS</i>	-0.2	-0.2	-0.2	-0.2	-0.2	-0.2	-0.2	-0.2	-0.2
	<i>ZSA</i> vs <i>DS</i>	0	0	0	0	0	0	0	0	0
	<i>ZSD</i> vs <i>ASD</i>	0.5	0.5	0.5	0.5	0.5	0.5	0.5	0.5	0.5
	<i>ZSA</i> vs <i>ASD</i>	0	0	0	0	0	0	0	0	0
	<i>ZSD</i> vs <i>ASA</i>	-0.3	-0.3	-0.3	-0.3	-0.3	-0.3	-0.3	-0.3	-0.3
	<i>ZSA</i> vs <i>ASA</i>	0.4	0.4	0.4	0.4	0.4	0.4	0.4	0.4	0.4
	<i>ZSD</i> vs <i>ZSA</i>	0	0	0	0	0	0	0	0	0
Delay scaling parameter r_t		2.5	2.5	2.5	2.5	2.5	2.5	2.5	2.5	2.5
XPR [dB]	μ_{XPR}	8	8	8	8	8	8	8	8	8
	σ_{XPR}	4	4	4	4	4	4	4	4	4
Number of clusters N		4	3	3	3	3	3	3	3	3
Number of rays per cluster M		20	20	20	20	20	20	20	20	20
Cluster <i>DS</i> (C_{DS}) in [ns]		1.6	1.6	1.6	1.6	1.6	1.6	1.6	1.6	1.6
Cluster <i>ASD</i> (C_{ASD}) in [deg]		0.09	0.09	0.11	0.15	0.18	0.27	0.42	0.86	2.55
Cluster <i>ASA</i> (C_{ASA}) in [deg]		11.78	11.6	13.05	14.56	15.35	16.97	17.96	20.68	25.08
Cluster <i>ZSA</i> (C_{ZSA}) in [deg]		1.14	2.78	3.87	4.94	5.41	6.31	6.66	7.31	9.23
Per cluster shadowing std ζ [dB]		3	3	3	3	3	3	3	3	3
Correlation distance in the horizontal plane [m]	<i>DS</i>	30	30	30	30	30	30	30	30	30
	<i>ASD</i>	18	18	18	18	18	18	18	18	18
	<i>ASA</i>	15	15	15	15	15	15	15	15	15
	<i>SF</i>	37	37	37	37	37	37	37	37	37
	<i>K</i>	12	12	12	12	12	12	12	12	12
	<i>ZSA</i>	15	15	15	15	15	15	15	15	15
	<i>ZSD</i>	15	15	15	15	15	15	15	15	15

f_c is carrier frequency in GHz; d_{2D} is BS-UT distance in km.
NOTE 1: DS = rms delay spread, ASD = rms azimuth spread of departure angles, ASA = rms azimuth spread of arrival angles, ZSD = rms zenith spread of departure angles, ZSA = rms zenith spread of arrival angles, SF = shadow fading, and K = Ricean K-factor.
NOTE 2: The sign of the shadow fading is defined so that positive SF means more received power at UT than predicted by the path loss model.
NOTE 3: All large scale parameters are assumed to have no correlation between different floors.
NOTE 4: The following notation for mean ($\mu_{lgX}=\text{mean}\{\log_{10}(X)\}$) and standard deviation ($\sigma_{lgX}=\text{std}\{\log_{10}(X)\}$) is used for logarithmized parameters X.
NOTE 5: For all considered scenarios the AOD/AOA distributions are modelled by a wrapped Gaussian distribution, the ZOD/ZOA distributions are modelled by a Laplacian distribution and the delay distribution is modelled by an exponential distribution.
NOTE 6: For UMa and frequencies below 6 GHz, use $f_c = 6$ when determining the values of the frequency-dependent LSP values
NOTE 7: For UMi and frequencies below 2 GHz, use $f_c = 2$ when determining the values of the frequency-dependent LSP values
NOTE 8: For satellite (e.g.GEO/LEO), the departure angle spreads are zeros, i.e. μ_{lgASD} and μ_{lgZSD} are $-\infty$, and corresponding standard deviations are zeros.
NOTE 9: The number of clusters is based on a limited data. The number may be different in the real field conditions.

Table 6.7.2-4a: Channel model parameters for Urban Scenario (NLOS) at S band

Scenarios		Urban NLOS								
		10°	20°	30°	40°	50°	60°	70°	80°	90°
Delay spread (DS) $lgDS=\log_{10}(DS/1s)$	μ_{lgDS}	-7.21	-7.63	-7.75	-7.97	-7.99	-8.01	-8.09	-7.97	-8.17
	σ_{lgDS}	1.19	0.98	0.84	0.73	0.73	0.72	0.71	0.78	0.67
AOD spread (ASD) $lgASD=\log_{10}(ASD/1^\circ)$	μ_{lgASD}	-1.55	-1.61	-1.73	-1.95	-1.94	-1.88	-2.1	-1.8	-1.77
	σ_{lgASD}	0.87	0.88	1.15	1.13	1.21	0.99	1.77	1.54	1.4
AOA spread (ASA) $lgASA=\log_{10}(ASA/1^\circ)$	μ_{lgASA}	0.17	0.32	0.52	0.61	0.68	0.64	0.58	0.71	0.49
	σ_{lgASA}	2.97	2.99	2.71	2.26	2.08	1.93	1.71	0.96	1.16
ZOA spread (ZSA) $lgZSA=\log_{10}(ZSA/1^\circ)$	μ_{lgZSA}	-0.97	0.49	1.03	1.12	1.3	1.32	1.35	1.31	1.5
	σ_{lgZSA}	2.35	2.11	1.29	1.45	1.07	1.2	1.1	1.35	0.56
ZOD spread (ZSD) $lgZSD=\log_{10}(ZSD/1^\circ)$	μ_{lgZSD}	-2.86	-2.64	-2.05	-2.18	-2.24	-2.21	-2.69	-2.81	-4.29
	σ_{lgZSD}	2.77	2.79	1.53	1.67	1.95	1.87	2.72	2.98	4.37
Shadow fading (SF) [dB]	σ_{SF}	See Table 6.6.2-2								
K-factor (K) [dB]	μ_K	N/A	N/A	N/A	N/A	N/A	N/A	N/A	N/A	N/A
	σ_K	N/A	N/A	N/A	N/A	N/A	N/A	N/A	N/A	N/A
Cross-Correlations	ASD vs DS	0.54	0.46	0.56	0.52	0.6	0.59	0.6	0.57	0.64
	ASA vs DS	0.38	0.36	0.27	0.29	0.21	0.24	0.22	0.24	0.24
	ASA vs SF	-0.05	-0.04	-0.04	-0.04	-0.03	-0.05	-0.02	-0.01	0
	ASD vs SF	-0.48	-0.53	-0.52	-0.52	-0.54	-0.51	-0.5	-0.48	-0.43
	DS vs SF	-0.22	-0.26	-0.21	-0.25	-0.21	-0.19	-0.19	-0.2	-0.2
	ASD vs ASA	0.41	0.4	0.33	0.37	0.23	0.23	0.22	0.23	0.21
	ASD vs K	N/A	N/A	N/A	N/A	N/A	N/A	N/A	N/A	N/A
	ASA vs K	N/A	N/A	N/A	N/A	N/A	N/A	N/A	N/A	N/A
	DS vs K	N/A	N/A	N/A	N/A	N/A	N/A	N/A	N/A	N/A
	SF vs K	N/A	N/A	N/A	N/A	N/A	N/A	N/A	N/A	N/A
Cross-Correlations	ZSD vs SF	-0.02	0	0.01	0	0.01	0.01	-0.02	-0.08	-0.12
	ZSA vs SF	-0.31	-0.33	-0.33	-0.33	-0.38	-0.39	-0.37	-0.37	-0.36
	ZSD vs K	N/A	N/A	N/A	N/A	N/A	N/A	N/A	N/A	N/A
	ZSA vs K	N/A	N/A	N/A	N/A	N/A	N/A	N/A	N/A	N/A

ZSD vs DS	0.69	0.72	0.68	0.68	0.64	0.65	0.64	0.61	0.53
ZSA vs DS	0.05	0.09	0.09	0.09	-0.03	-0.15	-0.13	-0.29	-0.19
ZSD vs ASD	0.52	0.48	0.6	0.56	0.62	0.6	0.65	0.59	0.64
ZSA vs ASD	0.05	0.11	0.13	0.14	-0.02	-0.11	-0.13	-0.26	-0.22
ZSD vs ASA	0.4	0.39	0.34	0.37	0.31	0.28	0.23	0.21	0.28
ZSA vs ASA	0.04	0.13	0.16	0.13	0.13	0.14	-0.02	-0.2	-0.46
ZSD vs ZSA	-0.03	0.04	0.07	0.07	-0.01	-0.12	-0.15	-0.34	-0.36
Delay scaling parameter r_t	2.3	2.3	2.3	2.3	2.3	2.3	2.3	2.3	2.3
XPR [dB]	7	7	7	7	7	7	7	7	7
	μ_{XPR}	3	3	3	3	3	3	3	3
Number of clusters N	3	3	3	3	3	3	2	2	2
Number of rays per cluster M	20	20	20	20	20	20	20	20	20
Cluster DS (C_{DS}) in [ns]	3.9	3.9	3.9	3.9	3.9	3.9	3.9	3.9	3.9
Cluster ASD (C_{ASD}) in [deg]	0.08	0.1	0.14	0.23	0.33	0.53	1	1.4	6.63
Cluster ASA (C_{ASA}) in [deg]	15.07	16.2	18.14	19.96	21.53	22.44	23.59	26.57	32.7
Cluster ZSA (C_{ZSA}) in [deg]	1.66	4.71	7.33	9.82	11.52	11.75	10.93	12.19	16.68
Per cluster shadowing std ζ [dB]	3	3	3	3	3	3	3	3	3
Correlation distance in the horizontal plane [m]	DS	40	40	40	40	40	40	40	40
	ASD	50	50	50	50	50	50	50	50
	ASA	50	50	50	50	50	50	50	50
	SF	50	50	50	50	50	50	50	50
	K	N/A	N/A	N/A	N/A	N/A	N/A	N/A	N/A
	ZSA	50	50	50	50	50	50	50	50
	ZSD	50	50	50	50	50	50	50	50
f_c is carrier frequency in GHz; d_{20} is BS-UT distance in km.									
NOTE 1: DS = rms delay spread, ASD = rms azimuth spread of departure angles, ASA = rms azimuth spread of arrival angles, ZSD = rms zenith spread of departure angles, ZSA = rms zenith spread of arrival angles, SF = shadow fading, and K = Ricean K-factor.									
NOTE 2: The sign of the shadow fading is defined so that positive SF means more received power at UT than predicted by the path loss model.									
NOTE 3: All large scale parameters are assumed to have no correlation between different floors.									
NOTE 4: The following notation for mean ($\mu_{\lg X} = \text{mean}\{\log_{10}(X)\}$) and standard deviation ($\sigma_{\lg X} = \text{std}\{\log_{10}(X)\}$) is used for logarithmized parameters X.									
NOTE 5: For all considered scenarios the AOD/AOA distributions are modelled by a wrapped Gaussian distribution, the ZOD/ZOA distributions are modelled by a Laplacian distribution and the delay distribution is modelled by an exponential distribution.									
NOTE 6: For UMa and frequencies below 6 GHz, use $f_c = 6$ when determining the values of the frequency-dependent LSP values									
NOTE 7: For UMi and frequencies below 2 GHz, use $f_c = 2$ when determining the values of the frequency-dependent LSP values									
NOTE 8: For satellite (e.g.GEO/LEO), the departure angle spreads are zeros, i.e. $\mu_{\lg \text{ASD}}$ and $\mu_{\lg \text{ZSD}}$ are $-\infty$, and corresponding standard deviations are zeros.									
NOTE 9: The number of clusters is based on a limited data. The number may be different in the real field conditions.									

Table 6.7.2-4b: Channel model parameters for Urban Scenario (NLOS) at Ka band

Scenarios	Urban NLOS								
	10°	20°	30°	40°	50°	60°	70°	80°	90°
Delay spread (DS) $\lg DS = \log_{10}(DS/1s)$	$\mu_{\lg DS}$	-7.24	-7.7	-7.82	-8.04	-8.08	-8.1	-8.16	-8.03
	$\sigma_{\lg DS}$	1.26	0.99	0.86	0.75	0.77	0.76	0.73	0.79
AOD spread (ASD) $\lg ASD = \log_{10}(ASD/1^\circ)$	$\mu_{\lg ASD}$	-1.58	-1.67	-1.84	-2.02	-2.06	-1.99	-2.19	-1.88
	$\sigma_{\lg ASD}$	0.89	0.89	1.3	1.15	1.23	1.02	1.78	1.55
AOA spread (ASA) $\lg ASA = \log_{10}(ASA/1^\circ)$	$\mu_{\lg ASA}$	0.13	0.19	0.44	0.48	0.56	0.55	0.48	0.53
	$\sigma_{\lg ASA}$	2.99	3.12	2.69	2.45	2.17	1.93	1.72	1.51

ZOA spread (ZSA) $\lg ZSA = \log_{10}(ZSA/1^\circ)$	$\mu_{\lg ZSA}$	-1.13	0.49	0.95	1.15	1.14	1.13	1.16	1.28	1.42
	$\sigma_{\lg ZSA}$	2.66	2.03	1.54	1.02	1.61	1.84	1.81	1.35	0.6
ZOD spread (ZSD) $\lg ZSD = \log_{10}(ZSD/1^\circ)$	$\mu_{\lg ZSD}$	-2.87	-2.68	-2.12	-2.27	-2.5	-2.47	-2.83	-2.82	-4.55
	$\sigma_{\lg ZSD}$	2.76	2.76	1.54	1.77	2.36	2.33	2.84	2.87	4.27
Shadow fading (SF) [dB]	σ_{SF}	See Table 6.6.2-2								
K-factor (K) [dB]	μ_K	N/A	N/A	N/A	N/A	N/A	N/A	N/A	N/A	N/A
	σ_K	N/A	N/A	N/A	N/A	N/A	N/A	N/A	N/A	N/A
Cross-Correlations	ASD vs DS	0.55	0.47	0.55	0.52	0.55	0.57	0.61	0.59	0.65
	ASA vs DS	0.38	0.37	0.29	0.3	0.23	0.21	0.23	0.23	0.36
	ASA vs SF	-0.05	-0.04	-0.04	-0.04	-0.03	-0.05	-0.03	-0.01	-0.03
	ASD vs SF	-0.48	-0.52	-0.52	-0.53	-0.57	-0.53	-0.5	-0.49	-0.38
	DS vs SF	-0.21	-0.25	-0.21	-0.26	-0.25	-0.2	-0.19	-0.2	-0.19
	ASD vs ASA	0.41	0.42	0.34	0.38	0.28	0.2	0.26	0.23	0.31
	ASD vs K	N/A	N/A	N/A	N/A	N/A	N/A	N/A	N/A	N/A
	ASA vs K	N/A	N/A	N/A	N/A	N/A	N/A	N/A	N/A	N/A
	DS vs K	N/A	N/A	N/A	N/A	N/A	N/A	N/A	N/A	N/A
	SF vs K	N/A	N/A	N/A	N/A	N/A	N/A	N/A	N/A	N/A
Cross-Correlations	ZSD vs SF	-0.02	0	0.01	0.01	0.03	0.03	-0.02	-0.05	-0.12
	ZSA vs SF	-0.31	-0.32	-0.33	-0.33	-0.41	-0.4	-0.36	-0.37	-0.33
	ZSD vs K	N/A	N/A	N/A	N/A	N/A	N/A	N/A	N/A	N/A
	ZSA vs K	N/A	N/A	N/A	N/A	N/A	N/A	N/A	N/A	N/A
	ZSD vs DS	0.68	0.72	0.68	0.67	0.65	0.67	0.63	0.61	0.54
	ZSA vs DS	0.06	0.1	0.11	0.13	-0.04	-0.14	-0.11	-0.24	-0.19
	ZSD vs ASD	0.52	0.48	0.59	0.55	0.54	0.6	0.64	0.6	0.6
	ZSA vs ASD	0.06	0.12	0.14	0.18	0.01	-0.1	-0.11	-0.24	-0.2
	ZSD vs ASA	0.4	0.41	0.34	0.38	0.31	0.25	0.23	0.22	0.29
	ZSA vs ASA	0.05	0.13	0.16	0.16	0.18	0.21	0.02	-0.13	-0.35
Delay scaling parameter r_c	ZSD vs ZSA	-0.02	0.04	0.09	0.11	0	-0.09	-0.15	-0.29	-0.33
	XPR [dB]	2.3	2.3	2.3	2.3	2.3	2.3	2.3	2.3	2.3
		7	7	7	7	7	7	7	7	7
Number of clusters N		3	3	3	3	3	3	2	2	2
Number of rays per cluster M		20	20	20	20	20	20	20	20	20
Cluster DS (C_{DS}) in [ns]		1.6	1.6	1.6	1.6	1.6	1.6	1.6	1.6	1.6
Cluster ASD (C_{ASD}) in [deg]		0.08	0.1	0.14	0.22	0.31	0.49	0.97	1.52	5.36
Cluster ASA (C_{ASA}) in [deg]		14.72	14.62	16.4	17.86	19.74	19.73	20.5	26.16	25.83
Cluster ZSA (C_{ZSA}) in [deg]		1.57	4.3	6.64	9.21	10.32	10.3	10.2	12.27	12.75
Per cluster shadowing std ζ [dB]		3	3	3	3	3	3	3	3	3
Correlation distance in the horizontal plane [m]	DS	40	40	40	40	40	40	40	40	40
	ASD	50	50	50	50	50	50	50	50	50
	ASA	50	50	50	50	50	50	50	50	50
	SF	50	50	50	50	50	50	50	50	50
	K	N/A	N/A	N/A	N/A	N/A	N/A	N/A	N/A	N/A
	ZSA	50	50	50	50	50	50	50	50	50
	ZSD	50	50	50	50	50	50	50	50	50

f_c is carrier frequency in GHz; d_{2D} is BS-UT distance in km.

NOTE 1: DS = rms delay spread, ASD = rms azimuth spread of departure angles, ASA = rms azimuth spread of arrival angles, ZSD = rms zenith spread of departure angles, ZSA = rms zenith spread of arrival angles, SF = shadow fading, and K = Ricean K-factor.

NOTE 2: The sign of the shadow fading is defined so that positive SF means more received power at UT than predicted by the path loss model.

NOTE 3: All large scale parameters are assumed to have no correlation between different floors.

NOTE 4: The following notation for mean ($\mu_{\lg X} = \text{mean}\{\log_{10}(X)\}$) and standard deviation ($\sigma_{\lg X} = \text{std}\{\log_{10}(X)\}$) is used for logarithmized parameters X.

NOTE 5: For all considered scenarios the AOD/AOA distributions are modelled by a wrapped Gaussian distribution, the ZOD/ZOA distributions are modelled by a Laplacian distribution and the delay distribution is modelled by an exponential distribution.

NOTE 6: For UMa and frequencies below 6 GHz, use $f_c = 6$ when determining the values of the frequency-dependent LSP values.

NOTE 7: For UMi and frequencies below 2 GHz, use $f_c = 2$ when determining the values of the frequency-dependent LSP values.

NOTE 8: For satellite (e.g.GEO/LEO), the departure angle spreads are zeros, i.e. $\mu_{\lg ASD}$ and $\mu_{\lg ZSD}$ are $-\infty$, and corresponding standard deviations are zeros.

NOTE 9: The number of clusters is based on a limited data. The number may be different in the real field conditions.

Table 6.7.2-5a: Channel model parameters for Suburban Scenario (LOS) in S band

Scenarios		Suburban LOS									
		10°	20°	30°	40°	50°	60°	70°	80°	90°	
Delay spread (DS) lgDS= $\log_{10}(DS/1s)$	μ_{lgDS}	-8.16	-8.56	-8.72	-8.71	-8.72	-8.66	-8.38	-8.34	-8.34	
	σ_{lgDS}	0.99	0.96	0.79	0.81	1.12	1.23	0.55	0.63	0.63	
AOD spread (ASD) lgASD= $\log_{10}(ASD/1^\circ)$	μ_{lgASD}	-3.57	-3.80	-3.77	-3.57	-3.42	-3.27	-3.08	-2.75	-2.75	
	σ_{lgASD}	1.62	1.74	1.72	1.60	1.49	1.43	1.36	1.26	1.26	
AOA spread (ASA) lgASA= $\log_{10}(ASA/1^\circ)$	μ_{lgASA}	0.05	-0.38	-0.56	-0.59	-0.58	-0.55	-0.28	-0.17	-0.17	
	σ_{lgASA}	1.84	1.94	1.75	1.82	1.87	1.92	1.16	1.09	1.09	
ZOA spread (ZSA) lgZSA= $\log_{10}(ZSA/1^\circ)$	μ_{lgZSA}	-1.78	-1.84	-1.67	-1.59	-1.55	-1.51	-1.27	-1.28	-1.28	
	σ_{lgZSA}	0.62	0.81	0.57	0.86	1.05	1.23	0.54	0.67	0.67	
ZOD spread (ZSD) lgZSD= $\log_{10}(ZSD/1^\circ)$	μ_{lgZSD}	-1.06	-1.21	-1.28	-1.32	-1.39	-1.36	-1.08	-1.31	-1.31	
	σ_{lgZSD}	0.96	0.95	0.49	0.79	0.97	1.17	0.62	0.76	0.76	
Shadow fading (SF) [dB]	σ_{SF}	Table 6.6.2-3									
K-factor (K) [dB]	μ_K	11.40	19.45	20.80	21.20	21.60	19.75	12.00	12.85	12.85	
	σ_K	6.26	10.32	16.34	15.63	14.22	14.19	5.70	9.91	9.91	
Cross-Correlations	ASD vs DS	0.4	0.4	0.4	0.4	0.4	0.4	0.4	0.4	0.4	
	ASA vs DS	0.8	0.8	0.8	0.8	0.8	0.8	0.8	0.8	0.8	
	ASA vs SF	-0.5	-0.5	-0.5	-0.5	-0.5	-0.5	-0.5	-0.5	-0.5	
	ASD vs SF	-0.5	-0.5	-0.5	-0.5	-0.5	-0.5	-0.5	-0.5	-0.5	
	DS vs SF	-0.4	-0.4	-0.4	-0.4	-0.4	-0.4	-0.4	-0.4	-0.4	
	ASD vs ASA	0	0	0	0	0	0	0	0	0	
	ASD vs K	0	0	0	0	0	0	0	0	0	
	ASA vs K	-0.2	-0.2	-0.2	-0.2	-0.2	-0.2	-0.2	-0.2	-0.2	
	DS vs K	-0.4	-0.4	-0.4	-0.4	-0.4	-0.4	-0.4	-0.4	-0.4	
	SF vs K	0	0	0	0	0	0	0	0	0	
Cross-Correlations	ZSD vs SF	0	0	0	0	0	0	0	0	0	
	ZSA vs SF	-0.8	-0.8	-0.8	-0.8	-0.8	-0.8	-0.8	-0.8	-0.8	
	ZSD vs K	0	0	0	0	0	0	0	0	0	
	ZSA vs K	0	0	0	0	0	0	0	0	0	
	ZSD vs DS	-0.2	-0.2	-0.2	-0.2	-0.2	-0.2	-0.2	-0.2	-0.2	
	ZSA vs DS	0	0	0	0	0	0	0	0	0	
	ZSD vs ASD	0.5	0.5	0.5	0.5	0.5	0.5	0.5	0.5	0.5	
	ZSA vs ASD	0	0	0	0	0	0	0	0	0	
	ZSD vs ASA	-0.3	-0.3	-0.3	-0.3	-0.3	-0.3	-0.3	-0.3	-0.3	
	ZSA vs ASA	0.4	0.4	0.4	0.4	0.4	0.4	0.4	0.4	0.4	
Delay scaling parameter r_τ	2.20	3.36	3.50	2.81	2.39	2.73	2.07	2.04	2.04	2.04	
	XPR [dB]	21.3	21.0	21.2	21.1	20.7	20.6	20.3	19.8	19.1	19.1
		7.6	8.9	8.5	8.4	9.2	9.8	10.8	12.2	13.0	13.0
Number of clusters N	3	3	3	3	3	3	2	2	2	2	
Number of rays per cluster M	20	20	20	20	20	20	20	20	20	20	
Cluster DS (C_{DS}) in [ns]	1.6	1.6	1.6	1.6	1.6	1.6	1.6	1.6	1.6	1.6	
Cluster ASD (C_{ASD}) in [deg]	0	0	0	0	0	0	0	0	0	0	
Cluster ASA (C_{ASA}) in [deg]	11	11	11	11	11	11	11	11	11	11	
Cluster ZSA (C_{ZSA}) in [deg]	7	7	7	7	7	7	7	7	7	7	
Per cluster shadowing std ζ [dB]	3	3	3	3	3	3	3	3	3	3	
Correlation distance in the horizontal plane [m]	DS	30	30	30	30	30	30	30	30	30	
	ASD	18	18	18	18	18	18	18	18	18	
	ASA	15	15	15	15	15	15	15	15	15	
	SF	37	37	37	37	37	37	37	37	37	
	K	12	12	12	12	12	12	12	12	12	
	ZSA	15	15	15	15	15	15	15	15	15	
	ZSD	15	15	15	15	15	15	15	15	15	

f_c is carrier frequency in GHz; d_{2D} is BS-UT distance in km.

- NOTE 1: DS = rms delay spread, ASD = rms azimuth spread of departure angles, ASA = rms azimuth spread of arrival angles, ZSD = rms zenith spread of departure angles, ZSA = rms zenith spread of arrival angles, SF = shadow fading, and K = Ricean K-factor.
- NOTE 2: The sign of the shadow fading is defined so that positive SF means more received power at UT than predicted by the path loss model.
- NOTE 3: All large scale parameters are assumed to have no correlation between different floors.
- NOTE 4: The following notation for mean ($\mu_{lgX}=\text{mean}\{\log_{10}(X)\}$) and standard deviation ($\sigma_{lgX}=\text{std}\{\log_{10}(X)\}$) is used for logarithmized parameters X.
- NOTE 5: For all considered scenarios the AOD/AOA distributions are modelled by a wrapped Gaussian distribution, the ZOD/ZOA distributions are modelled by a Laplacian distribution and the delay distribution is modelled by an exponential distribution.
- NOTE 6: For UMA and frequencies below 6 GHz, use $f_c = 6$ when determining the values of the frequency-dependent LSP values
- NOTE 7: For UMi and frequencies below 2 GHz, use $f_c = 2$ when determining the values of the frequency-dependent LSP values
- NOTE 8: For satellite (e.g.GEO/LEO), the departure angle spreads are zeros, i.e. μ_{lgASD} and μ_{lgZSD} are $-\infty$, and corresponding standard deviations are zeros.

Table 6.7.2-5b: Channel model parameters for Suburban Scenario (LOS) in Ka band

Scenarios		Suburban LOS									
		10°	20°	30°	40°	50°	60°	70°	80°	90°	
Delay spread (DS) lgDS= $\log_{10}(DS/1s)$	μ_{gDS}	-8.07	-8.61	-8.72	-8.63	-8.54	-8.48	-8.42	-8.39	-8.37	
	σ_{gDS}	0.46	0.45	0.28	0.17	0.14	0.15	0.09	0.05	0.02	
AOD spread (ASD) lgASD= $\log_{10}(ASD/1^\circ)$	μ_{gASD}	-3.55	-3.69	-3.59	-3.38	-3.23	-3.19	-2.83	-2.66	-1.22	
	σ_{gASD}	0.48	0.41	0.41	0.35	0.35	0.43	0.33	0.44	0.31	
AOA spread (ASA) lgASA= $\log_{10}(ASA/1^\circ)$	μ_{gASA}	0.89	0.31	0.02	-0.10	-0.19	-0.54	-0.24	-0.52	-0.15	
	σ_{gASA}	0.67	0.78	0.75	0.65	0.55	0.96	0.43	0.93	0.44	
ZOA spread (ZSA) lgZSA= $\log_{10}(ZSA/1^\circ)$	μ_{gZSA}	0.63	0.76	1.11	1.37	1.53	1.65	1.74	1.82	1.87	
	σ_{gZSA}	0.35	0.30	0.28	0.23	0.23	0.17	0.11	0.05	0.02	
ZOD spread (ZSD) lgZSD= $\log_{10}(ZSD/1^\circ)$	μ_{gZSD}	-3.37	-3.28	-3.04	-2.88	-2.83	-2.86	-2.95	-3.21	-3.49	
	σ_{gZSD}	0.28	0.27	0.26	0.21	0.18	0.17	0.10	0.07	0.24	
Shadow fading (SF) [dB]	σ_{SF}	Table 6.6.2-3									
K-factor (K) [dB]	μ_K	8.9	14.0	11.3	9.0	7.5	6.6	5.9	5.5	5.4	
	σ_K	4.4	4.6	3.7	3.5	3.0	2.6	1.7	0.7	0.3	
Cross-Correlations	ASD vs DS	0.4	0.4	0.4	0.4	0.4	0.4	0.4	0.4	0.4	
	ASA vs DS	0.8	0.8	0.8	0.8	0.8	0.8	0.8	0.8	0.8	
	ASA vs SF	-0.5	-0.5	-0.5	-0.5	-0.5	-0.5	-0.5	-0.5	-0.5	
	ASD vs SF	-0.5	-0.5	-0.5	-0.5	-0.5	-0.5	-0.5	-0.5	-0.5	
	DS vs SF	-0.4	-0.4	-0.4	-0.4	-0.4	-0.4	-0.4	-0.4	-0.4	
	ASD vs ASA	0	0	0	0	0	0	0	0	0	
	ASD vs K	0	0	0	0	0	0	0	0	0	
	ASA vs K	-0.2	-0.2	-0.2	-0.2	-0.2	-0.2	-0.2	-0.2	-0.2	
	DS vs K	-0.4	-0.4	-0.4	-0.4	-0.4	-0.4	-0.4	-0.4	-0.4	
	SF vs K	0	0	0	0	0	0	0	0	0	
Cross-Correlations	ZSD vs SF	0	0	0	0	0	0	0	0	0	
	ZSA vs SF	-0.8	-0.8	-0.8	-0.8	-0.8	-0.8	-0.8	-0.8	-0.8	
	ZSD vs K	0	0	0	0	0	0	0	0	0	
	ZSA vs K	0	0	0	0	0	0	0	0	0	
	ZSD vs DS	-0.2	-0.2	-0.2	-0.2	-0.2	-0.2	-0.2	-0.2	-0.2	
	ZSA vs DS	0	0	0	0	0	0	0	0	0	
	ZSD vs ASD	0.5	0.5	0.5	0.5	0.5	0.5	0.5	0.5	0.5	
	ZSA vs ASD	0	0	0	0	0	0	0	0	0	
	ZSD vs ASA	-0.3	-0.3	-0.3	-0.3	-0.3	-0.3	-0.3	-0.3	-0.3	
	ZSA vs ASA	0.4	0.4	0.4	0.4	0.4	0.4	0.4	0.4	0.4	
Delay scaling parameter r_e	2.5	2.5	2.5	2.5	2.5	2.5	2.5	2.5	2.5	2.5	
	XPR [dB]	23.2	23.6	23.5	23.4	23.2	23.3	23.4	23.2	23.1	
		5.0	4.5	4.7	5.2	5.7	5.9	6.2	7.0	7.6	
Number of clusters N		3	3	3	3	3	3	2	2	2	
Number of rays per cluster M		20	20	20	20	20	20	20	20	20	
Cluster DS (C_{DS}) in [ns]		1.6	1.6	1.6	1.6	1.6	1.6	1.6	1.6	1.6	
Cluster ASD (C_{ASD}) in [deg]		0	0	0	0	0	0	0	0	0	
Cluster ASA (C_{ASA}) in [deg]		11	11	11	11	11	11	11	11	11	
Cluster ZSA (C_{ZSA}) in [deg]		7	7	7	7	7	7	7	7	7	
Per cluster shadowing std ζ [dB]		3	3	3	3	3	3	3	3	3	
Correlation distance in the horizontal plane [m]	DS	30	30	30	30	30	30	30	30	30	
	ASD	18	18	18	18	18	18	18	18	18	
	ASA	15	15	15	15	15	15	15	15	15	
	SF	37	37	37	37	37	37	37	37	37	
	K	12	12	12	12	12	12	12	12	12	
	ZSA	15	15	15	15	15	15	15	15	15	
	ZSD	15	15	15	15	15	15	15	15	15	

f_c is carrier frequency in GHz; d_{20} is BS-UT distance in km.
NOTE 1: DS = rms delay spread, ASD = rms azimuth spread of departure angles, ASA = rms azimuth spread of arrival angles, ZSD = rms zenith spread of departure angles, ZSA = rms zenith spread of arrival angles, SF = shadow fading, and K = Ricean K-factor.
NOTE 2: The sign of the shadow fading is defined so that positive SF means more received power at UT than predicted by the path loss model.
NOTE 3: All large scale parameters are assumed to have no correlation between different floors.
NOTE 4: The following notation for mean ($\mu_{lgX}=\text{mean}\{\log_{10}(X)\}$) and standard deviation ($\sigma_{lgX}=\text{std}\{\log_{10}(X)\}$) is used for logarithmized parameters X.
NOTE 5: For all considered scenarios the AOD/AOA distributions are modelled by a wrapped Gaussian distribution, the ZOD/ZOA distributions are modelled by a Laplacian distribution and the delay distribution is modelled by an exponential distribution.
NOTE 6: For UMA and frequencies below 6 GHz, use $f_c=6$ when determining the values of the frequency-dependent LSP values
NOTE 7: For UMi and frequencies below 2 GHz, use $f_c=2$ when determining the values of the frequency-dependent LSP values
NOTE 8: For satellite (e.g.GEO/LEO), the departure angle spreads are zeros, i.e. μ_{lgASD} and μ_{lgZSD} are $-\infty$, and corresponding standard deviations are zeros.

Table 6.7.2-6a: Channel model parameters for Suburban Scenario (NLOS) in S band

Scenarios		Suburban NLOS								
		10°	20°	30°	40°	50°	60°	70°	80°	90°
Delay spread (DS) $lgDS=\log_{10}(DS/1s)$	μ_{lgDS}	-7.91	-8.39	-8.69	-8.59	-8.64	-8.74	-8.98	-9.28	-9.28
	σ_{lgDS}	1.42	1.46	1.46	1.21	1.18	1.13	1.37	1.50	1.50
AOD spread (ASD) $lgASD=\log_{10}(ASD/1^\circ)$	μ_{lgASD}	-3.54	-3.63	-3.66	-3.66	-3.66	-3.57	-3.18	-2.71	-2.71
	σ_{lgASD}	1.80	1.43	1.68	1.48	1.55	1.38	1.62	1.63	1.63
AOA spread (ASA) $lgASA=\log_{10}(ASA/1^\circ)$	μ_{lgASA}	0.91	0.70	0.38	0.30	0.28	0.23	0.10	0.04	0.04
	σ_{lgASA}	1.70	1.33	1.52	1.46	1.44	1.44	1.24	1.04	1.04
ZOA spread (ZSA) $lgZSA=\log_{10}(ZSA/1^\circ)$	μ_{lgZSA}	-1.90	-1.70	-1.75	-1.80	-1.80	-1.85	-1.45	-1.19	-1.19
	σ_{lgZSA}	1.63	1.24	1.54	1.25	1.21	1.20	1.38	1.58	1.58
ZOD spread (ZSD) $lgZSD=\log_{10}(ZSD/1^\circ)$	μ_{lgZSD}	-2.01	-1.67	-1.75	-1.49	-1.53	-1.57	-1.48	-1.62	-1.62
	σ_{lgZSD}	1.79	1.31	1.42	1.28	1.40	1.24	0.98	0.88	0.88
Shadow fading (SF) [dB]	σ_{SF}	Table 6.6.2-3								
Cross-Correlations	ASD vs DS	0.4	0.4	0.4	0.4	0.4	0.4	0.4	0.4	0.4
	ASA vs DS	0.6	0.6	0.6	0.6	0.6	0.6	0.6	0.6	0.6
	ASA vs SF	0	0	0	0	0	0	0	0	0
	ASD vs SF	-0.6	-0.6	-0.6	-0.6	-0.6	-0.6	-0.6	-0.6	-0.6
	DS vs SF	-0.4	-0.4	-0.4	-0.4	-0.4	-0.4	-0.4	-0.4	-0.4
	ASD vs ASA	0.4	0.4	0.4	0.4	0.4	0.4	0.4	0.4	0.4
	ASD vs K	N/A	N/A	N/A	N/A	N/A	N/A	N/A	N/A	N/A
	ASA vs K	N/A	N/A	N/A	N/A	N/A	N/A	N/A	N/A	N/A
	DS vs K	N/A	N/A	N/A	N/A	N/A	N/A	N/A	N/A	N/A
	SF vs K	N/A	N/A	N/A	N/A	N/A	N/A	N/A	N/A	N/A
Cross-Correlations	ZSD vs SF	0	0	0	0	0	0	0	0	0
	ZSA vs SF	-0.4	-0.4	-0.4	-0.4	-0.4	-0.4	-0.4	-0.4	-0.4
	ZSD vs K	N/A	N/A	N/A	N/A	N/A	N/A	N/A	N/A	N/A
	ZSA vs K	N/A	N/A	N/A	N/A	N/A	N/A	N/A	N/A	N/A
	ZSD vs DS	-0.5	-0.5	-0.5	-0.5	-0.5	-0.5	-0.5	-0.5	-0.5
	ZSA vs DS	0	0	0	0	0	0	0	0	0
	ZSD vs ASD	0.5	0.5	0.5	0.5	0.5	0.5	0.5	0.5	0.5
	ZSA vs ASD	-0.1	-0.1	-0.1	-0.1	-0.1	-0.1	-0.1	-0.1	-0.1
	ZSD vs ASA	0	0	0	0	0	0	0	0	0
	ZSA vs ASA	0	0	0	0	0	0	0	0	0
Delay scaling parameter r_τ		2.28	2.33	2.43	2.26	2.71	2.10	2.19	2.06	2.06
XPR [dB]	μ_{XPR}	20.6	16.7	13.2	11.3	9.6	7.5	9.1	11.7	11.7
	σ_{XPR}	8.5	12.0	12.8	13.8	12.5	11.2	10.1	13.1	13.1

Number of clusters N	4	4	4	4	4	3	3	3	3
Number of rays per cluster M	20	20	20	20	20	20	20	20	20
Cluster DS (c_{DS}) in [ns]	1.6	1.6	1.6	1.6	1.6	1.6	1.6	1.6	1.6
Cluster ASD (c_{ASD}) in [deg]	0	0	0	0	0	0	0	0	0
Cluster ASA (c_{ASA}) in [deg]	15	15	15	15	15	15	15	15	15
Cluster ZSA (c_{ZSA}) in [deg]	7	7	7	7	7	7	7	7	7
Per cluster shadowing std ζ [dB]	3	3	3	3	3	3	3	3	3
Correlation distance in the horizontal plane [m]	DS	40	40	40	40	40	40	40	40
	ASD	50	50	50	50	50	50	50	50
	ASA	50	50	50	50	50	50	50	50
	SF	50	50	50	50	50	50	50	50
	K	N/A							
	ZSA	50	50	50	50	50	50	50	50
	ZSD	50	50	50	50	50	50	50	50

f_c is carrier frequency in GHz; d_{20} is BS-UT distance in km.

NOTE 1: DS = rms delay spread, ASD = rms azimuth spread of departure angles, ASA = rms azimuth spread of arrival angles, ZSD = rms zenith spread of departure angles, ZSA = rms zenith spread of arrival angles, SF = shadow fading, and K = Ricean K-factor.

NOTE 2: The sign of the shadow fading is defined so that positive SF means more received power at UT than predicted by the path loss model.

NOTE 3: All large scale parameters are assumed to have no correlation between different floors.

NOTE 4: The following notation for mean ($\mu_{lgX}=\text{mean}\{\log_{10}(X)\}$) and standard deviation ($\sigma_{lgX}=\text{std}\{\log_{10}(X)\}$) is used for logarithmized parameters X.

NOTE 5: For all considered scenarios the AOD/AOA distributions are modelled by a wrapped Gaussian distribution, the ZOD/ZOA distributions are modelled by a Laplacian distribution and the delay distribution is modelled by an exponential distribution.

NOTE 6: For UMa and frequencies below 6 GHz, use $f_c = 6$ when determining the values of the frequency-dependent LSP values

NOTE 7: For UMi and frequencies below 2 GHz, use $f_c = 2$ when determining the values of the frequency-dependent LSP values

NOTE 8: For satellite (e.g.GEO/LEO), the departure angle spreads are zeros, i.e. μ_{lgASD} and μ_{lgZSD} are $-\infty$, and corresponding standard deviations are zeros.

Table 6.7.2-6b: Channel model parameters for Suburban Scenario (NLOS) in Ka band

Scenarios	Suburban NLOS									
	10°	20°	30°	40°	50°	60°	70°	80°	90°	
Delay spread (DS) $lgDS=\log_{10}(DS/1s)$	μ_{lgDS}	-7.43	-7.63	-7.86	-7.96	-7.98	-8.45	-8.21	-8.69	-8.69
	σ_{lgDS}	0.50	0.61	0.56	0.58	0.59	0.47	0.36	0.29	0.29
AOD spread (ASD) $lgASD=\log_{10}(ASD/1^\circ)$	μ_{lgASD}	-2.89	-2.76	-2.64	-2.41	-2.42	-2.53	-2.35	-2.31	-2.31
	σ_{lgASD}	0.41	0.41	0.41	0.52	0.70	0.50	0.58	0.73	0.73
AOA spread (ASA) $lgASA=\log_{10}(ASA/1^\circ)$	μ_{lgASA}	1.49	1.24	1.06	0.91	0.98	0.49	0.73	-0.04	-0.04
	σ_{lgASA}	0.40	0.82	0.71	0.55	0.58	1.37	0.49	1.48	1.48
ZOA spread (ZSA) $lgZSA=\log_{10}(ZSA/1^\circ)$	μ_{lgZSA}	0.81	1.06	1.12	1.14	1.29	1.38	1.36	1.38	1.38
	σ_{lgZSA}	0.36	0.41	0.40	0.39	0.35	0.36	0.29	0.20	0.20
ZOD spread (ZSD) $lgZSD=\log_{10}(ZSD/1^\circ)$	μ_{lgZSD}	-3.09	-2.93	-2.91	-2.78	-2.70	-3.03	-2.90	-3.20	-3.20
	σ_{lgZSD}	0.32	0.47	0.46	0.54	0.45	0.36	0.42	0.30	0.30
Shadow fading (SF) [dB]	σ_{SF}	Table 6.6.2-3								
Cross-Correlations	ASD vs DS	0.4	0.4	0.4	0.4	0.4	0.4	0.4	0.4	0.4
	ASA vs DS	0.6	0.6	0.6	0.6	0.6	0.6	0.6	0.6	0.6
	ASA vs SF	0	0	0	0	0	0	0	0	0
	ASD vs SF	-0.6	-0.6	-0.6	-0.6	-0.6	-0.6	-0.6	-0.6	-0.6
	DS vs SF	-0.4	-0.4	-0.4	-0.4	-0.4	-0.4	-0.4	-0.4	-0.4
	ASD vs ASA	0.4	0.4	0.4	0.4	0.4	0.4	0.4	0.4	0.4
	ASD vs K	N/A	N/A	N/A	N/A	N/A	N/A	N/A	N/A	N/A
	ASA vs K	N/A	N/A	N/A	N/A	N/A	N/A	N/A	N/A	N/A
	DS vs K	N/A	N/A	N/A	N/A	N/A	N/A	N/A	N/A	N/A
	SF vs K	N/A	N/A	N/A	N/A	N/A	N/A	N/A	N/A	N/A
Cross-Correlations	ZSD vs SF	0	0	0	0	0	0	0	0	0
	ZSA vs SF	-0.4	-0.4	-0.4	-0.4	-0.4	-0.4	-0.4	-0.4	-0.4
	ZSD vs K	N/A	N/A	N/A	N/A	N/A	N/A	N/A	N/A	N/A
	ZSA vs K	N/A	N/A	N/A	N/A	N/A	N/A	N/A	N/A	N/A
	ZSD vs DS	-0.5	-0.5	-0.5	-0.5	-0.5	-0.5	-0.5	-0.5	-0.5
	ZSA vs DS	0	0	0	0	0	0	0	0	0
	ZSD vs ASD	0.5	0.5	0.5	0.5	0.5	0.5	0.5	0.5	0.5

	ZSA vs ASD	-0.1	-0.1	-0.1	-0.1	-0.1	-0.1	-0.1	-0.1	-0.1
	ZSD vs ASA	0	0	0	0	0	0	0	0	0
	ZSA vs ASA	0	0	0	0	0	0	0	0	0
	ZSD vs ZSA	0	0	0	0	0	0	0	0	0
Delay scaling parameter r_t		2.3	2.3	2.3	2.3	2.3	2.3	2.3	2.3	2.3
XPR [dB]	μ_{XPR}	22.5	19.4	15.5	13.9	11.7	9.8	10.3	15.6	15.6
	σ_{XPR}	5.0	8.5	10.0	10.6	10.0	9.1	9.1	9.1	9.1
Number of clusters N		4	4	4	4	4	3	3	3	3
Number of rays per cluster M		20	20	20	20	20	20	20	20	20
Cluster DS (C_{DS}) in [ns]		1.6	1.6	1.6	1.6	1.6	1.6	1.6	1.6	1.6
Cluster ASD (C_{ASD}) in [deg]		0	0	0	0	0	0	0	0	0
Cluster ASA (C_{ASA}) in [deg]		15	15	15	15	15	15	15	15	15
Cluster ZSA (C_{ZSA}) in [deg]		7	7	7	7	7	7	7	7	7
Per cluster shadowing std ζ [dB]		3	3	3	3	3	3	3	3	3
Correlation distance in the horizontal plane [m]	DS	40	40	40	40	40	40	40	40	40
	ASD	50	50	50	50	50	50	50	50	50
	ASA	50	50	50	50	50	50	50	50	50
	SF	50	50	50	50	50	50	50	50	50
	K	N/A								
	ZSA	50	50	50	50	50	50	50	50	50
	ZSD	50	50	50	50	50	50	50	50	50

f_c is carrier frequency in GHz; d_{20} is BS-UT distance in km.

NOTE 1: DS = rms delay spread, ASD = rms azimuth spread of departure angles, ASA = rms azimuth spread of arrival angles, ZSD = rms zenith spread of departure angles, ZSA = rms zenith spread of arrival angles, SF = shadow fading, and K = Ricean K-factor.

NOTE 2: The sign of the shadow fading is defined so that positive SF means more received power at UT than predicted by the path loss model.

NOTE 3: All large scale parameters are assumed to have no correlation between different floors.

NOTE 4: The following notation for mean ($\mu_{lgX}=\text{mean}\{\log_{10}(X)\}$) and standard deviation ($\sigma_{lgX}=\text{std}\{\log_{10}(X)\}$) is used for logarithmized parameters X.

NOTE 5: For all considered scenarios the AOD/AOA distributions are modelled by a wrapped Gaussian distribution, the ZOD/ZOA distributions are modelled by a Laplacian distribution and the delay distribution is modelled by an exponential distribution.

NOTE 6: For UMa and frequencies below 6 GHz, use $f_c = 6$ when determining the values of the frequency-dependent LSP values

NOTE 7: For UMi and frequencies below 2 GHz, use $f_c = 2$ when determining the values of the frequency-dependent LSP values

NOTE 8: For satellite (e.g.GEO/LEO), the departure angle spreads are zeros, i.e. μ_{lgASD} and μ_{lgZSD} are $-\infty$, and corresponding standard deviations are zeros.

Table 6.7.2-7a: Channel model parameters for Rural Scenario (LOS) at S band

Scenarios		Rural LOS								
		10°	20°	30°	40°	50°	60°	70°	80°	90°
Delay spread (DS) $\lg DS = \log_{10}(DS/1s)$	μ_{lgDS}	-9.55	-8.68	-8.46	-8.36	-8.29	-8.26	-8.22	-8.2	-8.19
	σ_{lgDS}	0.66	0.44	0.28	0.19	0.14	0.1	0.1	0.05	0.06
AOD spread (ASD) $\lg ASD = \log_{10}(ASD/1^\circ)$	μ_{lgASD}	-3.42	-3	-2.86	-2.78	-2.7	-2.66	-2.53	-2.21	-1.78
	σ_{lgASD}	0.89	0.63	0.52	0.45	0.42	0.41	0.42	0.5	0.91
AOA spread (ASA) $\lg ASA = \log_{10}(ASA/1^\circ)$	μ_{lgASA}	-9.45	-4.45	-2.39	-1.28	-0.99	-1.05	-0.9	-0.89	-0.81
	σ_{lgASA}	7.83	6.86	5.14	3.44	2.59	2.42	1.78	1.65	1.26
ZOA spread (ZSA) $\lg ZSA = \log_{10}(ZSA/1^\circ)$	μ_{lgZSA}	-4.2	-2.31	-0.28	-0.38	-0.38	-0.46	-0.49	-0.53	-0.46
	σ_{lgZSA}	6.3	5.04	0.81	1.16	0.82	0.67	1	1.18	0.91
ZOD spread (ZSD) $\lg ZSD = \log_{10}(ZSD/1^\circ)$	μ_{lgZSD}	-6.03	-4.31	-2.57	-2.59	-2.59	-2.65	-2.69	-2.65	-2.65
	σ_{lgZSD}	5.19	4.18	0.61	0.79	0.65	0.52	0.78	1.01	0.71
Shadow fading (SF) [dB]	σ_{SF}	Table 6.6.2-3								
K-factor (K) [dB]	μ_K	24.72	12.31	8.05	6.21	5.04	4.42	3.92	3.65	3.59
	σ_K	5.07	5.75	5.46	5.23	3.95	3.75	2.56	1.77	1.77
Cross-Correlations	ASD vs DS	0	0	0	0	0	0	0	0	0
	ASA vs DS	0	0	0	0	0	0	0	0	0
	ASA vs SF	0	0	0	0	0	0	0	0	0

	ASD vs SF	0	0	0	0	0	0	0	0
	DS vs SF	-0.5	-0.5	-0.5	-0.5	-0.5	-0.5	-0.5	-0.5
	ASD vs ASA	0	0	0	0	0	0	0	0
	ASD vs K	0	0	0	0	0	0	0	0
	ASA vs K	0	0	0	0	0	0	0	0
	DS vs K	0	0	0	0	0	0	0	0
	SF vs K	0	0	0	0	0	0	0	0
Cross-Correlations	ZSD vs SF	0.01	0.01	0.01	0.01	0.01	0.01	0.01	0.01
	ZSA vs SF	-0.17	-0.17	-0.17	-0.17	-0.17	-0.17	-0.17	-0.17
	ZSD vs K	0	0	0	0	0	0	0	0
	ZSA vs K	-0.02	-0.02	-0.02	-0.02	-0.02	-0.02	-0.02	-0.02
	ZSD vs DS	-0.05	-0.05	-0.05	-0.05	-0.05	-0.05	-0.05	-0.05
	ZSA vs DS	0.27	0.27	0.27	0.27	0.27	0.27	0.27	0.27
	ZSD vs ASD	0.73	0.73	0.73	0.73	0.73	0.73	0.73	0.73
	ZSA vs ASD	-0.14	-0.14	-0.14	-0.14	-0.14	-0.14	-0.14	-0.14
	ZSD vs ASA	-0.20	-0.20	-0.20	-0.20	-0.20	-0.20	-0.20	-0.20
	ZSA vs ASA	0.24	0.24	0.24	0.24	0.24	0.24	0.24	0.24
	ZSD vs ZSA	-0.07	-0.07	-0.07	-0.07	-0.07	-0.07	-0.07	-0.07
Delay scaling parameter r_t		3.8	3.8	3.8	3.8	3.8	3.8	3.8	3.8
XPR [dB]	μ_{XPR}	12	12	12	12	12	12	12	12
	σ_{XPR}	4	4	4	4	4	4	4	4
Number of clusters N		2	2	2	2	2	2	2	2
Number of rays per cluster M		20	20	20	20	20	20	20	20
Cluster DS (C_{DS}) in [ns]		N/A							
Cluster ASD (C_{ASD}) in [deg]		0.39	0.31	0.29	0.37	0.61	0.9	1.43	2.87
Cluster ASA (C_{ASA}) in [deg]		10.81	8.09	13.7	20.05	24.51	26.35	31.84	36.62
Cluster ZSA (C_{ZSA}) in [deg]		1.94	1.83	2.28	2.93	2.84	3.17	3.88	4.17
Per cluster shadowing std ζ [dB]		3	3	3	3	3	3	3	3
Correlation distance in the horizontal plane [m]	DS	50	50	50	50	50	50	50	50
	ASD	25	25	25	25	25	25	25	25
	ASA	35	35	35	35	35	35	35	35
	SF	37	37	37	37	37	37	37	37
	K	40	40	40	40	40	40	40	40
	ZSA	15	15	15	15	15	15	15	15
	ZSD	15	15	15	15	15	15	15	15

f_c is carrier frequency in GHz; d_{20} is BS-UT distance in km.

NOTE 1: DS = rms delay spread, ASD = rms azimuth spread of departure angles, ASA = rms azimuth spread of arrival angles, ZSD = rms zenith spread of departure angles, ZSA = rms zenith spread of arrival angles, SF = shadow fading, and K = Ricean K-factor.

NOTE 2: The sign of the shadow fading is defined so that positive SF means more received power at UT than predicted by the path loss model.

NOTE 3: All large scale parameters are assumed to have no correlation between different floors.

NOTE 4: The following notation for mean ($\mu_{lgX}=\text{mean}\{\log_{10}(X)\}$) and standard deviation ($\sigma_{lgX}=\text{std}\{\log_{10}(X)\}$) is used for logarithmized parameters X.

NOTE 5: For all considered scenarios the AOD/AOA distributions are modelled by a wrapped Gaussian distribution, the ZOD/ZOA distributions are modelled by a Laplacian distribution and the delay distribution is modelled by an exponential distribution.

NOTE 6: For UMA and frequencies below 6 GHz, use $f_c=6$ when determining the values of the frequency-dependent LSP values

NOTE 7: For UMi and frequencies below 2 GHz, use $f_c=2$ when determining the values of the frequency-dependent LSP values

NOTE 8: For satellite (e.g.GEO/LEO), the departure angle spreads are zeros, i.e. μ_{lgASD} and μ_{lgZSD} are $-\infty$, and corresponding standard deviations are zeros.

Table 6.7.2-7b: Channel model parameters for Rural Scenario (LOS) at Ka band.

Scenarios		Rural LOS								
		10°	20°	30°	40°	50°	60°	70°	80°	90°
Delay spread (DS) $\lg DS = \log_{10}(DS/1s)$	μ_{lgDS}	-9.68	-8.86	-8.59	-8.46	-8.36	-8.3	-8.26	-8.22	-8.21
	σ_{lgDS}	0.46	0.29	0.18	0.19	0.14	0.15	0.13	0.03	0.07
AOD spread (ASD) $\lg ASD = \log_{10}(ASD/1^\circ)$	μ_{lgASD}	-4.03	-3.55	-3.45	-3.38	-3.33	-3.29	-3.24	-2.9	-2.5
	σ_{lgASD}	0.91	0.7	0.55	0.52	0.46	0.43	0.46	0.44	0.82
AOA spread (ASA) $\lg ASA = \log_{10}(ASA/1^\circ)$	μ_{lgASA}	-9.74	-4.88	-2.6	-1.92	-1.56	-1.66	-1.59	-1.58	-1.51
	σ_{lgASA}	7.52	6.67	4.63	3.45	2.44	2.38	1.67	1.44	1.13
ZOA spread (ZSA) $\lg ZSA = \log_{10}(ZSA/1^\circ)$	μ_{lgZSA}	-5.85	-3.27	-0.88	-0.93	-0.99	-1.04	-1.17	-1.19	-1.13
	σ_{lgZSA}	6.51	5.36	0.93	0.96	0.97	0.83	1.01	1.01	0.85
ZOD spread (ZSD) $\lg ZSD = \log_{10}(ZSD/1^\circ)$	μ_{lgZSD}	-7.45	-5.25	-3.16	-3.15	-3.2	-3.27	-3.42	-3.36	-3.35
	σ_{lgZSD}	5.3	4.42	0.68	0.73	0.77	0.61	0.74	0.79	0.65
Shadow fading (SF) [dB]	σ_{SF}	Table 6.6.2-3								
K-factor (K) [dB]	μ_K	25.43	12.72	8.40	6.52	5.24	4.57	4.02	3.70	3.62
	σ_K	7.04	7.47	7.18	6.88	5.28	4.92	3.40	2.22	2.28
Cross-Correlations	ASD vs DS	0	0	0	0	0	0	0	0	0
	ASA vs DS	0	0	0	0	0	0	0	0	0
	ASA vs SF	0	0	0	0	0	0	0	0	0
	ASD vs SF	0	0	0	0	0	0	0	0	0
	DS vs SF	-0.5	-0.5	-0.5	-0.5	-0.5	-0.5	-0.5	-0.5	-0.5
	ASD vs ASA	0	0	0	0	0	0	0	0	0
	ASD vs K	0	0	0	0	0	0	0	0	0
	ASA vs K	0	0	0	0	0	0	0	0	0
	DS vs K	0	0	0	0	0	0	0	0	0
	SF vs K	0	0	0	0	0	0	0	0	0
Cross-Correlations	ZSD vs SF	0.01	0.01	0.01	0.01	0.01	0.01	0.01	0.01	0.01
	ZSA vs SF	-0.17	-0.17	-0.17	-0.17	-0.17	-0.17	-0.17	-0.17	-0.17
	ZSD vs K	0	0	0	0	0	0	0	0	0
	ZSA vs K	-0.02	-0.02	-0.02	-0.02	-0.02	-0.02	-0.02	-0.02	-0.02

ZSD vs DS	-0.05	-0.05	-0.05	-0.05	-0.05	-0.05	-0.05	-0.05	-0.05	-0.05
ZSA vs DS	0.27	0.27	0.27	0.27	0.27	0.27	0.27	0.27	0.27	0.27
ZSD vs ASD	0.73	0.73	0.73	0.73	0.73	0.73	0.73	0.73	0.73	0.73
ZSA vs ASD	-0.14	-0.14	-0.14	-0.14	-0.14	-0.14	-0.14	-0.14	-0.14	-0.14
ZSD vs ASA	-0.20	-0.20	-0.20	-0.20	-0.20	-0.20	-0.20	-0.20	-0.20	-0.20
ZSA vs ASA	0.24	0.24	0.24	0.24	0.24	0.24	0.24	0.24	0.24	0.24
ZSD vs ZSA	-0.07	-0.07	-0.07	-0.07	-0.07	-0.07	-0.07	-0.07	-0.07	-0.07
Delay scaling parameter r_r	3.8	3.8	3.8	3.8	3.8	3.8	3.8	3.8	3.8	3.8
XPR [dB]	μ_{XPR}	12	12	12	12	12	12	12	12	12
	σ_{XPR}	4	4	4	4	4	4	4	4	4
Number of clusters N	2	2	2	2	2	2	2	2	2	2
Number of rays per cluster M	20	20	20	20	20	20	20	20	20	20
Cluster DS (C_{DS}) in [ns]	N/A	N/A	N/A	N/A	N/A	N/A	N/A	N/A	N/A	N/A
Cluster ASD (C_{ASD}) in [deg]	0.36	0.3	0.25	0.35	0.53	0.88	1.39	2.7	4.97	
Cluster ASA (C_{ASA}) in [deg]	4.63	6.83	12.91	18.9	22.44	25.69	27.95	31.45	28.01	
Cluster ZSA (C_{ZSA}) in [deg]	0.75	1.25	1.93	2.37	2.66	3.23	3.71	4.17	4.14	
Per cluster shadowing std ζ [dB]	3	3	3	3	3	3	3	3	3	3
Correlation distance in the horizontal plane [m]	DS	50	50	50	50	50	50	50	50	50
	ASD	25	25	25	25	25	25	25	25	25
	ASA	35	35	35	35	35	35	35	35	35
	SF	37	37	37	37	37	37	37	37	37
	K	40	40	40	40	40	40	40	40	40
	ZSA	15	15	15	15	15	15	15	15	15
	ZSD	15	15	15	15	15	15	15	15	15

f_c is carrier frequency in GHz; d_{20} is BS-UT distance in km.

NOTE 1: DS = rms delay spread, ASD = rms azimuth spread of departure angles, ASA = rms azimuth spread of arrival angles, ZSD = rms zenith spread of departure angles, ZSA = rms zenith spread of arrival angles, SF = shadow fading, and K = Ricean K-factor.

NOTE 2: The sign of the shadow fading is defined so that positive SF means more received power at UT than predicted by the path loss model.

NOTE 3: All large scale parameters are assumed to have no correlation between different floors.

NOTE 4: The following notation for mean ($\mu_{\lg X} = \text{mean}\{\log_{10}(X)\}$) and standard deviation ($\sigma_{\lg X} = \text{std}\{\log_{10}(X)\}$) is used for logarithmized parameters X.

NOTE 5: For all considered scenarios the AOD/AOA distributions are modelled by a wrapped Gaussian distribution, the ZOD/ZOA distributions are modelled by a Laplacian distribution and the delay distribution is modelled by an exponential distribution.

NOTE 6: For UMa and frequencies below 6 GHz, use $f_c = 6$ when determining the values of the frequency-dependent LSP values

NOTE 7: For UMi and frequencies below 2 GHz, use $f_c = 2$ when determining the values of the frequency-dependent LSP values

NOTE 8: For satellite (e.g.GEO/LEO), the departure angle spreads are zeros, i.e. $\mu_{\lg \text{ASD}}$ and $\mu_{\lg \text{ZSD}}$ are $-\infty$, and corresponding standard deviations are zeros.

Table 6.7.2-8a: Channel model parameters for Rural Scenario (NLOS) at S band

Scenarios		Rural NLOS								
		10°	20°	30°	40°	50°	60°	70°	80°	90°
Delay spread (DS)	$\mu_{\lg \text{DS}}$	-9.01	-8.37	-8.05	-7.92	-7.92	-7.96	-7.91	-7.79	-7.74
IgDS= $\log_{10}(\text{DS}/1\text{s})$	$\sigma_{\lg \text{DS}}$	1.59	0.95	0.92	0.92	0.87	0.87	0.82	0.86	0.81
AOD spread (ASD)	$\mu_{\lg \text{ASD}}$	-2.9	-2.5	-2.12	-1.99	-1.9	-1.85	-1.69	-1.46	-1.32
IgASD= $\log_{10}(\text{ASD}/1^\circ)$	$\sigma_{\lg \text{ASD}}$	1.34	1.18	1.08	1.06	1.05	1.06	1.14	1.16	1.3
AOA spread (ASA)	$\mu_{\lg \text{ASA}}$	-3.33	-0.74	0.08	0.32	0.53	0.33	0.55	0.45	0.4
IgASA= $\log_{10}(\text{ASA}/1^\circ)$	$\sigma_{\lg \text{ASA}}$	6.22	4.22	3.02	2.45	1.63	2.08	1.58	2.01	2.19

ZOA spread (ZSA) lgZSA= $\log_{10}(ZSA/1^\circ)$	μ_{lgZSA}	-0.88	-0.07	0.75	0.72	0.95	0.97	1.1	0.97	1.35
	σ_{lgZSA}	3.26	3.29	1.92	1.92	1.45	1.62	1.43	1.88	0.62
ZOD spread (ZSD) lgZSA= $\log_{10}(ZSD/1^\circ)$	μ_{lgZSD}	-4.92	-4.06	-2.33	-2.24	-2.24	-2.22	-2.19	-2.41	-2.45
	σ_{lgZSD}	3.96	4.07	1.7	2.01	2	1.82	1.66	2.58	2.52
Shadow fading (SF) [dB]	σ_{SF}	Table 6.6.2-3								
K-factor (K) [dB]	μ_K	N/A	N/A	N/A	N/A	N/A	N/A	N/A	N/A	
	σ_K	N/A	N/A	N/A	N/A	N/A	N/A	N/A	N/A	
Cross-Correlations	ASD vs DS	0.32	0.19	0.23	0.25	0.15	0.08	0.13	0.15	0.64
	ASA vs DS	0.3	0.32	0.32	0.4	0.45	0.39	0.51	0.27	0.05
	ASA vs SF	0.02	0	0	0.01	0.02	0.02	0.04	0.01	0.06
	ASD vs SF	0.45	0.52	0.54	0.53	0.55	0.56	0.56	0.58	0.47
	DS vs SF	-0.36	-0.39	-0.41	-0.37	-0.4	-0.41	-0.4	-0.46	-0.3
	ASD vs ASA	0.45	0.12	0.07	0.22	0.16	0.14	0.2	-0.04	-0.11
	ASD vs K	N/A	N/A	N/A	N/A	N/A	N/A	N/A	N/A	N/A
	ASA vs K	N/A	N/A	N/A	N/A	N/A	N/A	N/A	N/A	N/A
	DS vs K	N/A	N/A	N/A	N/A	N/A	N/A	N/A	N/A	N/A
	SF vs K	N/A	N/A	N/A	N/A	N/A	N/A	N/A	N/A	N/A
Cross-Correlations	ZSD vs SF	-0.06	-0.04	-0.04	-0.05	-0.06	-0.07	-0.11	-0.05	-0.1
	ZSA vs SF	-0.07	-0.17	-0.19	-0.17	-0.19	-0.2	-0.19	-0.23	-0.13
	ZSD vs K	N/A	N/A	N/A	N/A	N/A	N/A	N/A	N/A	N/A
	ZSA vs K	N/A	N/A	N/A	N/A	N/A	N/A	N/A	N/A	N/A
	ZSD vs DS	0.58	0.67	0.65	0.73	0.79	0.81	0.79	0.7	0.42
	ZSA vs DS	0.06	0.03	0	-0.09	-0.2	-0.22	-0.32	-0.41	-0.35
	ZSD vs ASD	0.6	0.41	0.37	0.32	0.19	0.16	0.2	0.15	0.28
	ZSA vs ASD	0.21	-0.02	-0.09	-0.1	-0.12	-0.11	-0.1	-0.14	-0.25
	ZSD vs ASA	0.33	0.35	0.31	0.37	0.46	0.44	0.49	0.27	0.07
	ZSA vs ASA	0.1	0.21	0.22	0.07	-0.04	-0.12	-0.29	-0.26	-0.36
Delay scaling parameter r_f	1.7	1.7	1.7	1.7	1.7	1.7	1.7	1.7	1.7	1.7
	μ_{XPR}	7	7	7	7	7	7	7	7	7
	σ_{XPR}	3	3	3	3	3	3	3	3	3

Number of clusters N	3	3	2	2	2	2	2	2	2
Number of rays per cluster M	20	20	20	20	20	20	20	20	20
Cluster DS (C_{DS}) in [ns]	N/A	N/A	N/A	N/A	N/A	N/A	N/A	N/A	N/A
Cluster ASD (C_{ASD}) in [deg]	0.03	0.05	0.07	0.1	0.15	0.22	0.5	1.04	2.11
Cluster ASA (C_{ASA}) in [deg]	18.16	26.82	21.99	22.86	25.93	27.79	28.5	37.53	29.23
Cluster ZSA (C_{ZSA}) in [deg]	2.32	7.34	8.28	8.76	9.68	9.94	8.9	13.74	12.16
Per cluster shadowing std ζ [dB]	3	3	3	3	3	3	3	3	3
Correlation distance in the horizontal plane [m]	DS	36	36	36	36	36	36	36	36
	ASD	30	30	30	30	30	30	30	30
	ASA	40	40	40	40	40	40	40	40
	SF	120	120	120	120	120	120	120	120
	K	N/A	N/A	N/A	N/A	N/A	N/A	N/A	N/A
	ZSA	50	50	50	50	50	50	50	50
	ZSD	50	50	50	50	50	50	50	50

f_c is carrier frequency in GHz; d_{20} is BS-UT distance in km.

NOTE 1: DS = rms delay spread, ASD = rms azimuth spread of departure angles, ASA = rms azimuth spread of arrival angles, ZSD = rms zenith spread of departure angles, ZSA = rms zenith spread of arrival angles, SF = shadow fading, and K = Ricean K-factor.

NOTE 2: The sign of the shadow fading is defined so that positive SF means more received power at UT than predicted by the path loss model.

NOTE 3: All large scale parameters are assumed to have no correlation between different floors.

NOTE 4: The following notation for mean ($\mu_{lgX}=\text{mean}\{\log_{10}(X)\}$) and standard deviation ($\sigma_{lgX}=\text{std}\{\log_{10}(X)\}$) is used for logarithmized parameters X.

NOTE 5: For all considered scenarios the AOD/AOA distributions are modelled by a wrapped Gaussian distribution, the ZOD/ZOA distributions are modelled by a Laplacian distribution and the delay distribution is modelled by an exponential distribution.

NOTE 6: For UMa and frequencies below 6 GHz, use $f_c=6$ when determining the values of the frequency-dependent LSP values.

NOTE 7: For UMi and frequencies below 2 GHz, use $f_c=2$ when determining the values of the frequency-dependent LSP values

NOTE 8: For satellite (e.g.GEO/LEO), the departure angle spreads are zeros, i.e. μ_{lgASD} and μ_{lgZSD} are $-\infty$, and corresponding standard deviations are zeros.

Table 6.7.2-8b: Channel model parameters for Rural Scenario (NLOS) at Ka band

Scenarios		Rural NLOS								
		10°	20°	30°	40°	50°	60°	70°	80°	90°
Delay spread (DS) $\lg DS = \log_{10}(DS/1s)$	μ_{lgDS}	-9.13	-8.39	-8.1	-7.96	-7.99	-8.05	-8.01	-8.05	-7.91
	σ_{lgDS}	1.91	0.94	0.92	0.94	0.89	0.87	0.82	1.65	0.76
AOD spread (ASD) $\lg ASD = \log_{10}(ASD/1^\circ)$	μ_{lgASD}	-2.9	-2.53	-2.16	-2.04	-1.99	-1.95	-1.81	-1.56	-1.53
	σ_{lgASD}	1.32	1.18	1.08	1.09	1.08	1.06	1.17	1.2	1.27
AOA spread (ASA) $\lg ASA = \log_{10}(ASA/1^\circ)$	μ_{lgASA}	-3.4	-0.51	0.06	0.2	0.4	0.32	0.46	0.33	0.24
	σ_{lgASA}	6.28	3.75	2.95	2.65	1.85	1.83	1.57	1.99	2.18
ZOA spread (ZSA) $\lg ZSA = \log_{10}(ZSA/1^\circ)$	μ_{lgZSA}	-1.19	-0.11	0.72	0.69	0.84	0.99	0.95	0.92	1.29
	σ_{lgZSA}	3.81	3.33	1.93	1.91	1.7	1.27	1.86	1.84	0.59
ZOD spread (ZSD) $\lg ZSD = \log_{10}(ZSD/1^\circ)$	μ_{lgZSD}	-5.47	-4.06	-2.32	-2.19	-2.16	-2.24	-2.29	-2.65	-2.23
	σ_{lgZSD}	4.39	4.04	1.54	1.73	1.5	1.64	1.66	2.86	1.12
Shadow fading (SF) [dB]	σ_{SF}	Table 6.6.2-3								
K-factor (K) [dB]	μ_K	N/A	N/A	N/A	N/A	N/A	N/A	N/A	N/A	N/A
	σ_K	N/A	N/A	N/A	N/A	N/A	N/A	N/A	N/A	N/A
Cross-Correlations	ASD vs DS	0.33	0.24	0.21	0.26	0.16	0.12	0.29	0.14	0.59
	ASA vs DS	0.32	0.34	0.33	0.43	0.46	0.38	0.37	0.28	0.06
	ASA vs SF	0.02	0	0	0.01	0.01	0.02	0.04	0.01	0.04
	ASD vs SF	0.45	0.52	0.54	0.53	0.55	0.56	0.54	0.57	0.46
	DS vs SF	-0.36	-0.38	-0.42	-0.36	-0.39	-0.42	-0.36	-0.44	-0.27

	ASD vs ASA	0.45	0.13	0.08	0.21	0.12	0.15	0.22	-0.03	-0.11
	ASD vs K	N/A								
	ASA vs K	N/A								
	DS vs K	N/A								
	SF vs K	N/A								
Cross-Correlations	ZSD vs SF	-0.07	-0.04	-0.04	-0.05	-0.06	-0.06	-0.09	-0.06	-0.08
	ZSA vs SF	-0.06	-0.16	-0.19	-0.16	-0.19	-0.2	-0.17	-0.22	-0.11
	ZSD vs K	N/A								
	ZSA vs K	N/A								
	ZSD vs DS	0.55	0.65	0.64	0.73	0.78	0.77	0.74	0.75	0.52
	ZSA vs DS	0.06	0.02	0.04	-0.06	-0.16	-0.17	-0.3	-0.35	-0.28
	ZSD vs ASD	0.61	0.41	0.39	0.44	0.15	0.2	0.3	0.11	0.41
	ZSA vs ASD	0.19	-0.02	-0.06	-0.08	-0.13	-0.09	-0.09	-0.14	-0.25
	ZSD vs ASA	0.38	0.35	0.33	0.4	0.46	0.45	0.33	0.29	0.06
	ZSA vs ASA	0.12	0.21	0.22	0.11	0.02	-0.08	-0.2	-0.16	-0.18
	ZSD vs ZSA	0.05	-0.03	-0.08	-0.2	-0.25	-0.24	-0.37	-0.31	-0.32
Delay scaling parameter r_t		1.7	1.7	1.7	1.7	1.7	1.7	1.7	1.7	1.7
XPR [dB]	μ_{XPR}	7	7	7	7	7	7	7	7	7
	σ_{XPR}	3	3	3	3	3	3	3	3	3
Number of clusters N		3	3	2	2	2	2	2	2	2
Number of rays per cluster M		20	20	20	20	20	20	20	20	20
Cluster DS (C_{DS}) in [ns]		N/A								
Cluster ASD (C_{ASD}) in [deg]		0.03	0.05	0.07	0.09	0.16	0.22	0.51	0.89	1.68
Cluster ASA (C_{ASA}) in [deg]		18.21	24.08	22.06	21.4	24.26	24.15	25.99	36.07	24.51
Cluster ZSA (C_{ZSA}) in [deg]		2.13	6.52	7.72	8.45	8.92	8.76	9	13.6	10.56
Per cluster shadowing std ζ [dB]		3	3	3	3	3	3	3	3	3
Correlation distance in the horizontal plane [m]	DS	36	36	36	36	36	36	36	36	36
	ASD	30	30	30	30	30	30	30	30	30
	ASA	40	40	40	40	40	40	40	40	40
	SF	120	120	120	120	120	120	120	120	120
	K	N/A								
	ZSA	50	50	50	50	50	50	50	50	50
	ZSD	50	50	50	50	50	50	50	50	50

f_c is carrier frequency in GHz; d_{20} is BS-UT distance in km.

- NOTE 1: DS = rms delay spread, ASD = rms azimuth spread of departure angles, ASA = rms azimuth spread of arrival angles, ZSD = rms zenith spread of departure angles, ZSA = rms zenith spread of arrival angles, SF = shadow fading, and K = Ricean K-factor.
- NOTE 2: The sign of the shadow fading is defined so that positive SF means more received power at UT than predicted by the path loss model.
- NOTE 3: All large scale parameters are assumed to have no correlation between different floors.
- NOTE 4: The following notation for mean ($\mu_{\log X} = \text{mean}\{\log_{10}(X)\}$) and standard deviation ($\sigma_{\log X} = \text{std}\{\log_{10}(X)\}$) is used for logarithmized parameters X.
- NOTE 5: For all considered scenarios the AOD/AOA distributions are modelled by a wrapped Gaussian distribution, the ZOD/ZOA distributions are modelled by a Laplacian distribution and the delay distribution is modelled by an exponential distribution.
- NOTE 6: For UMa and frequencies below 6 GHz, use $f_c = 6$ when determining the values of the frequency-dependent LSP values.
- NOTE 7: For UMi and frequencies below 2 GHz, use $f_c = 2$ when determining the values of the frequency-dependent LSP values.
- NOTE 8: For satellite (e.g. GEO/LEO), the departure angle spreads are zeros, i.e. $\mu_{\log \text{ASD}}$ and $\mu_{\log \text{ZSD}}$ are $-\infty$, and corresponding standard deviations are zeros.

6.8. Additional modelling components

6.8.1 Time-varying Doppler shift

The Doppler shift generally depends on the time evolution of the channel as the joint results due to the movement of Tx and Rx, or scatterer movement. As mentioned above, the movement of BS and UE are time-varying, especially in the spaceborne case. Then, the more general form to describe the phase rotation due to the Doppler shift can be calculated as:

$$\exp\left(j2\pi\int_{t_0}^t \frac{\hat{r}_{rx,n,m}^T(\theta) \cdot \vec{v}(\theta)}{\lambda_0} d\theta\right) \cdot \exp\left(j2\pi\int_{t_0}^t \frac{\hat{r}_{tx,n,m}^T(\theta) \cdot \vec{v}_{sat}(\theta)}{\lambda_0} d\theta\right).$$

Here, $\hat{r}_{rx,n,m}(t)$ is the normalized vector that points into the direction of the incoming wave as seen from the Rx at time t . $\vec{v}(t)$ denotes the velocity vector of the Rx at time t . $\hat{r}_{tx,n,m}(t)$ is the normalized vector that points into the direction of the outgoing wave as seen from the Tx at time t . $\vec{v}_{sat}(t)$ denotes the velocity vector of the Tx at time t . While t_0 denotes a reference point in time that defines the initial phase, e.g. $t_0 = 0$.

6.8.2 Faraday rotation

The Faraday rotation is introduced to describe the rotation of the polarization due to the interaction of the electromagnetic wave with the ionized medium in the earth's magnetic field along the path. In case of propagation for spaceborne BS above the ionosphere, the Faraday rotation should be calculated as:

$$F_r = \begin{bmatrix} \cos(\psi_{n,m}) & -\sin(\psi_{n,m}) \\ \sin(\psi_{n,m}) & \cos(\psi_{n,m}) \end{bmatrix} \quad (6.8-1)$$

The equations 7.5-28 and 7.5-29 in [12] should be updated by post-multiplied with F_r for the channel coefficient generation of the m^{th} path in the n^{th} cluster, as equations 6.8-1a and 6.8-1b, respectively:

$$H_{u,s,n,m}^{\text{NLOS}}(t) = \sqrt{\frac{P_n}{M}} \begin{bmatrix} F_{rx,u,\theta}(\theta_{n,m,ZOA}, \phi_{n,m,AOA}) \\ F_{rx,u,\phi}(\theta_{n,m,ZOA}, \phi_{n,m,AOA}) \end{bmatrix}^T \begin{bmatrix} \exp(j\Phi_{n,m}^{\theta\theta}) & \sqrt{\kappa_{n,m}^{-1}} \exp(j\Phi_{n,m}^{\theta\phi}) \\ \sqrt{\kappa_{n,m}^{-1}} \exp(j\Phi_{n,m}^{\phi\theta}) & \exp(j\Phi_{n,m}^{\phi\phi}) \end{bmatrix} \begin{bmatrix} \cos(\psi_{n,m}) & -\sin(\psi_{n,m}) \\ \sin(\psi_{n,m}) & \cos(\psi_{n,m}) \end{bmatrix} \begin{bmatrix} F_{tx,s,\theta}(\theta_{n,m,ZOD}, \phi_{n,m,AOD}) \\ F_{tx,s,\phi}(\theta_{n,m,ZOD}, \phi_{n,m,AOD}) \end{bmatrix} \exp\left(j2\pi \frac{\hat{r}_{rx,n,m}^T \bar{d}_{rx,u}}{\lambda_0}\right) \exp\left(j2\pi \frac{\hat{r}_{tx,n,m}^T \bar{d}_{tx,s}}{\lambda_0}\right) \exp\left(j2\pi \frac{\hat{r}_{rx,n,m}^T \bar{v}}{\lambda_0} t\right) \quad (6.8-1a)$$

$$H_{u,s,1}^{\text{LOS}}(t) = \begin{bmatrix} F_{rx,u,\theta}(\theta_{\text{LOS,ZOA}}, \phi_{\text{LOS,AOA}}) \\ F_{rx,u,\phi}(\theta_{\text{LOS,ZOA}}, \phi_{\text{LOS,AOA}}) \end{bmatrix}^T \begin{bmatrix} 1 & 0 \\ 0 & -1 \end{bmatrix} \begin{bmatrix} \cos(\psi_{n,m}) & -\sin(\psi_{n,m}) \\ \sin(\psi_{n,m}) & \cos(\psi_{n,m}) \end{bmatrix} \begin{bmatrix} F_{tx,s,\theta}(\theta_{\text{LOS,ZOD}}, \phi_{\text{LOS,AOD}}) \\ F_{tx,s,\phi}(\theta_{\text{LOS,ZOD}}, \phi_{\text{LOS,AOD}}) \end{bmatrix} \cdot \exp\left(-j2\pi \frac{d_{3D}}{\lambda_0}\right) \exp\left(j2\pi \frac{\hat{r}_{rx,LOS}^T \bar{d}_{rx,u}}{\lambda_0}\right) \exp\left(j2\pi \frac{\hat{r}_{tx,LOS}^T \bar{d}_{tx,s}}{\lambda_0}\right) \exp\left(j2\pi \frac{\hat{r}_{rx,LOS}^T \bar{v}}{\lambda_0} t\right) \quad (6.8-1b)$$

where $\psi_{n,m}$ is calculated as [11]:

$$\psi = \frac{108}{f^2} \quad (6.8-2)$$

where ψ is the faraday rotation in degree and f is the central carrier frequency in GHz.

6.9 Channel models for link level simulations

The link level models follow the same principles as the link level models specified in TR38.901 section 7.7.

6.9.1 CDL models

The CDL models are defined for the S and Ka bands and are applicable to different environments and elevation angles. NTN-CDL-A and NTN-CDL-B are constructed to represent two different channel profiles for NLOS, while NTN-CDL-C and NTN-CDL-D are constructed for LOS. The parameters of these models can be found in Tables 6.9.1-1 to 6.9.1-4.

Table 6.9.1-1a: Void

Table 6.9.1-1b: Void

Due to the long propagation distance between the NTN gNB and ground UE, the azimuth and elevation angular spreads of departure, ASD and ZSD, can be considered zero, and all cluster AOD and ZOD angles the same. The coordinate system can be chosen in such a way that all AODs are zero. With the NTN gNB at an elevation angle α with respect to the UE, ZOD of all clusters is $90^\circ + \alpha$, as shown in Figure 6.9.1-1. The CDL models in Tables 6.9.1-1 to 6.9.1-4 use 50° elevation angle between the NTN gNB and UE, resulting in ZODs equal to 190° . For a desired elevation angle α_{desired} , the cluster ZOD needs to be set to

$$\theta_{n,\text{ZOD},\text{desired}} = 90 + \alpha_{\text{desired}} \quad (6.9-1)$$

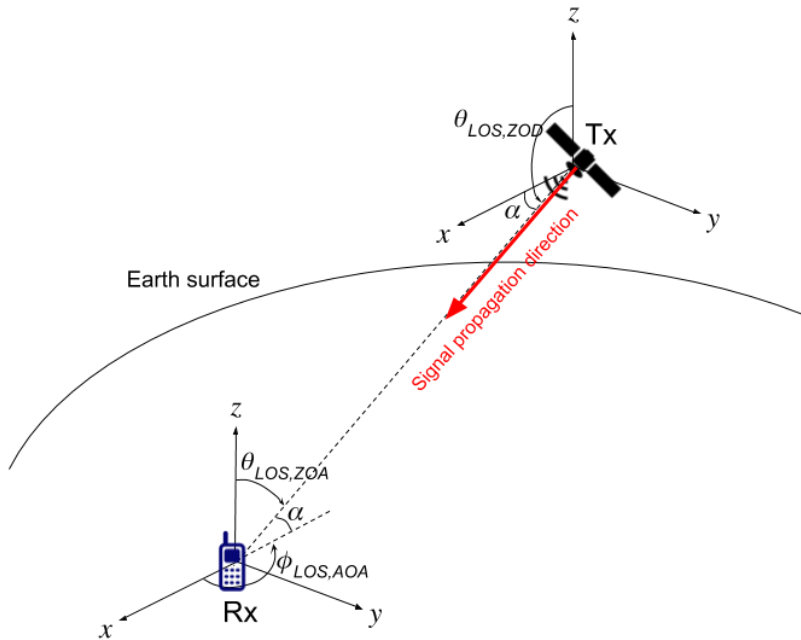


Figure 6.9.1-1 Elevation angle α at UE with NTN gNB

Depending on the frequency band, environment scenario, and elevation angle of the intended link level simulations, suitable DS, ASA, ZSA, and Rician K-factor in case of LOS, can be determined from the channel model parameters in Section 6.7.2.

Each CDL model can be scaled in delay and AOA to achieve desired RMS delay spread and ASA according to the procedures specified respectively in subclauses 7.7.3 and 7.7.5.1 of TR 38.901 [12]. With the same angle scaling principle, each CDL model can also be scaled in ZOA to achieve desired ZSA, taking into account the difference between the desired elevation angle and reference elevation angle, by

$$\theta_{n,\text{ZOA},\text{scaled}} = \frac{\text{ZSA}_{\text{desired}}}{\text{ZSA}_{\text{model}}} (\theta_{n,\text{ZOA},\text{model}} - \mu_{\text{ZOA},\text{model}}) + \mu_{\text{ZOA},\text{desired}} - \Delta\alpha \quad (6.9-2)$$

where

- $\theta_{n,\text{ZOA,scaled}}$ is the scaled ZOA,
- ZSA_{desired} is the desired ZSA,
- ZSA_{model} is the RMS zenith angular spread of the reference model,
- $\theta_{n,\text{ZOA,model}}$ is the cluster ZOA of the reference model,
- $\mu_{\text{ZOA,model}}$ is the mean angle of ZOA of the reference model,
- $\mu_{\text{ZOA,desired}}$ is the desired mean ZOA,
- $\Delta\alpha = \alpha_{\text{desired}} - \alpha_{\text{model}}$ is the difference between the desired and reference elevation angles between the NTN gNB and UE.

The resultant ZOA angles after scaling may need to be wrapped to the domain [0,180] by the same rule in TR 38.901: if $\theta_{n,\text{ZOA}} \in [180^{\circ}, 360^{\circ}]$, it should be set to $(360^{\circ} - \theta_{n,\text{ZOA}})$.

For LOS channel models, the K-factor of NTN-CDL-C and NTN-CDL-D can be set to a desired value following the procedure described in subclause 7.7.6 of TR 38.901.

Doppler shift due to UE and satellite motion should be calculated based on section 6.8.1. For simulations over a few TTIs, constant speed for the UE and the satellite and constant satellite elevation angle may be considered

$$\alpha_{\text{model}} = 50^{\circ}$$

Table 6.9.1-1 NTN-CDL-A at elevation

Cluster #	Normalized delay	Power in [dB]	AOD in [°]	AOA in [°]	ZOD in [°]	ZOA in [°]
1	0	0	0	178.8	140	35.6
2	1.0811	-4.675	0	-115.7	140	22.9
3	2.8416	-6.482	0	111.5	140	127.4
Per-Cluster Parameters						
Parameter	c_{ASD} in [°]	c_{ASA} in [°]	c_{ZSD} in [°]	c_{ZSA} in [°]	XPR in [dB]	
Value	0	15	0	7	10	

$$\alpha_{\text{model}} = 50^{\circ}$$

Table 6.9.1-2 NTN-CDL-B at elevation

Cluster #	Normalized delay	Power in [dB]	AOD in [°]	AOA in [°]	ZOD in [°]	ZOA in [°]
1	0	0	0	-174.6	140	42.2
2	0.7249	-1.973	0	144.9	140	63.4
3	0.7410	-4.332	0	-119.8	140	89.7
4	5.7392	-11.914	0	-88.8	140	174.1
Per-Cluster Parameters						
Parameter	c_{ASD} in [°]	c_{ASA} in [°]	c_{ZSD} in [°]	c_{ZSA} in [°]	XPR in [dB]	
Value	0	15	0	7	10	

$$\alpha_{\text{model}} = 50^\circ$$

Table 6.9.1-3 NTN-CDL-C at elevation

Cluster #	Cluster PAS	Normalized Delay	Power in [dB]	AOD in [°]	AOA in [°]	ZOD in [°]	ZOA in [°]
1	Specular(LOS path)	0	-0.394	0	-180	140	40
	Laplacian	0	-10.618	0	-180	140	40
2	Laplacian	14.8124	-23.373	0	-75.9	140	87.1
Per-Cluster Parameters							
Parameter		c_{ASD} in [°]	c_{ASA} in [°]	c_{ZSD} in [°]	c_{ZSA} in [°]	XPR in [dB]	
Value		0	11	0	7	16	

$$\alpha_{\text{model}} = 50^\circ$$

Table 6.9.1-4 NTN-CDL-D at elevation

Cluster #	Cluster PAS	Normalized Delay	Power in [dB]	AOD in [°]	AOA in [°]	ZOD in [°]	ZOA in [°]
1	Specular(LOS path)	0	-0.284	0	-180	140	40
	Laplacian	0	-11.991	0	-180	140	40
2	Laplacian	0.5596	-9.887	0	-135.4	140	146.2
3	Laplacian	7.3340	-16.771	0	-121.5	140	136.0
Per-Cluster Parameters							
Parameter		c_{ASD} in [°]	c_{ASA} in [°]	c_{ZSD} in [°]	c_{ZSA} in [°]	XPR in [dB]	
Value		0	11	0	7	16	

6.9.2 TDL models

The Tapped Delay Line (TDL) models are filtered from the CDL models according to the section 7.7.4 of TR 38.901 [12] by assuming isotropic UE antenna. Two TDL models, namely NTN-TDL-A and NTN-TDL-B are constructed to represent two different channel profiles for NLOS, while NTN-TDL-C and NTN-TDL-D are constructed for LOS. The parameter of these models can be found in Tables 6.9.2-1 to 6.9.2-4.

Table 6.9.2-1a: Void

Table 6.9.2-1b: Void

The Doppler spectrum for each tap is defined as described in subclause 7.7.2 of TR 38.901. Each TDL model can be scaled in delay to achieve desired RMS delay spread according to the procedure specified in subclause 7.7.3 of TR 38.901. For LOS channel models, the K-factor of NTN-TDL-C and NTN-TDL-D can be set to a desired value following the procedure described in subclause 7.7.6 of TR 38.901.

Additional Doppler shift due to satellite motion should be taken into account according to the following formula:

$$f_{d,shift} = (v_{sat} / c) \times \left(\frac{R}{R+h} \cos \alpha_{model} \right) \times f_c,$$

Where v_{sat} denotes the satellite speed, c denotes the speed of light, R denotes the earth radius, h denotes the satellite altitude, α_{model} denotes the satellite elevation angle, and f_c denotes the carrier frequency.

This additional Doppler shift should be applied to all taps of the TDL model.

The satellite speed, satellite elevation angle and UE speed should be considered to be constant during the simulation duration, if limited to few TTIs.

An illustration of the effect of additional Doppler shift due to satellite motion on the Doppler power spectrum is displayed on the next figure.

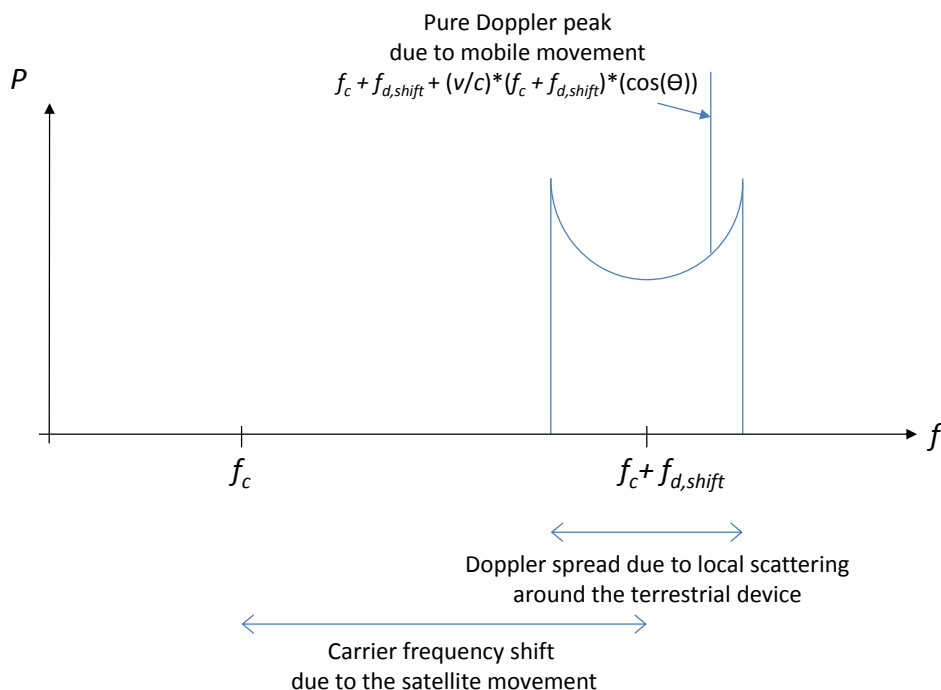


Figure 6.9.2-1: Illustration of Doppler power spectrum in NTN in LOS conditions

Table 6.9.2-1. NTN-TDL-A at elevation $\alpha_{\text{model}} = 50^\circ$

Tap #	Normalized delay	Power in [dB]	Fading distribution
1	0	0	Rayleigh
2	1.0811	-4.675	Rayleigh
3	2.8416	-6.482	Rayleigh

Table 6.9.2-2. NTN-TDL-B at elevation $\alpha_{\text{model}} = 50^\circ$

Tap #	Normalized delay	Power in [dB]	Fading distribution
1	0	0	Rayleigh
2	0.7249	-1.973	Rayleigh
3	0.7410	-4.332	Rayleigh
4	5.7392	-11.914	Rayleigh

Table 6.9.2-3. NTN-TDL-C at elevation $\alpha_{\text{model}} = 50^\circ$

Tap #	Normalized delay	Power in [dB]	Fading distribution
1	0	-0.394	LOS path
	0	-10.618	Rayleigh
2	14.8124	-23.373	Rayleigh

NOTE: The first tap follows a Ricean distribution with a K-factor of $K_1 = 10.224$ dB and a mean power of 0 dB.

Table 6.9.2-4. NTN-TDL-D at elevation $\alpha_{\text{model}} = 50^\circ$

Tap #	Normalized delay	Power in [dB]	Fading distribution
1	0	-0.284	LOS path
	0	-11.991	Rayleigh
2	0.5596	-9.887	Rayleigh
3	7.3340	-16.771	Rayleigh

NOTE: The first tap follows a Ricean distribution with a K-factor of $K_1 = 11.707$ dB and a mean power of 0 dB.

6.10 Channel model calibration

6.10.1 NTN channel model features per deployment scenarios

Table 6.10.1-1: NTN channel model features per deployment scenarios

	Deployment-D1	Deployment-D2	Deployment-D3	Deployment-D4	Deployment-D5
Platform orbit and altitude	GEO at 35 786 km	GEO at 35 786 km	Non-GEO down to 600 km	Non-GEO down to 600 km	HAPS between 8 km and 50 km
Carrier Frequency on the link between Air / space-borne platform and UE	Around 20 GHz for DL Around 30 GHz for UL (Ka band)	Around 2 GHz for both DL and UL (S band)	Around 2 GHz for both DL and UL (S band)	Around 20 GHz for DL Around 30 GHz for UL (Ka band)	Below 6 GHz
Maximum Channel Bandwidth (DL + UL)	Up to 2 * 800 MHz	Up to 2 * 20 MHz	Up to 2 * 20 MHz	Up to 2 * 800 MHz	Up to 2 * 80 MHz
UE antenna pattern + polarisation	VSAT type - circular polarisation Co-phased array - Dual Linear polarisation (Note 1)	Quasi Isotropic - Linear polarisation (Note 4) Co-phased array - Dual Linear polarisation (Note 2)	Quasi Isotropic - Linear polarisation (Note 4) Co-phased array - Dual Linear polarisation (Note 2)	VSAT type - circular polarisation Co-phased array - Dual Linear polarisation (Note 1)	Quasi Isotropic - Linear polarisation (Note 4) Co-phased array - Dual Linear polarisation (Note 2)
UE type	Handheld, nomadic, fixed, moving platform mounted	Handheld, moving platform mounted	Handheld, moving platform mounted	Handheld, nomadic, fixed, moving platform mounted	Handheld, moving platform mounted
Airborne & space borne antenna pattern modelling + polarisation	Bessel function and circular polarisation	Bessel function and circular polarisation	Bessel function and circular polarisation	Bessel function and circular polarisation	- Bessel function and circular polarisation - 3GPP antenna pattern of Base Station (Dual Linear polarisation)
Doppler cause	Mainly UE mobility	Mainly UE mobility	UE + satellite mobility	UE + satellite mobility	UE + HAPS mobility
O2I penetration loss	No	No	No	No	Possible
Atmospheric absorption	Mandatory	Negligible	Negligible	Mandatory	Negligible
Rain attenuation	(Note 3)	Negligible	Negligible	(Note 3)	Negligible
Cloud attenuation	(Note 3)	Negligible	Negligible	(Note 3)	Negligible
Scintillation	Tropospheric	Ionospheric	Ionospheric	Tropospheric	Negligible
Fast fading models (system level)	Flat fading (Note 6)	Flat fading (Note 6) or frequency selective fading (note 5) according to elevation and environments	Flat fading (Note 6) or frequency selective fading (note 5) according to elevation and environments	Flat fading (Note 6)	Frequency selective fading (note 5) according to elevation and environments
Link level model	Flat fading (Note 6)	CDL or TDL	CDL or TDL	Flat fading (Note 6)	CDL or TDL
Shadowing model	LMS (Land Mobile Satellite)	LMS	LMS	LMS	3GPP TR38.901 based

Note 1: As described in [48] as [M,N,P] = [2,4,2].

Note 2: As described in [48] as [M,N,P] = [1,2,2].

Note 3: Rain and cloud attenuation are not needed for system or link level simulations related to channel model, if they are already considered in the system dimensioning (e.g. link budget). If they need to be taken into account, ITU-R P618 models (Rain) and ITU-R P840 models (Cloud) shall be used.

Note 4: Quasi isotropic refers to dipole antenna which is omni-directional in one plane.

Note 5: The frequency selective fading refers to Geometry based Stochastic Channel Model or GSCM which is defined in (SCM/FP7 WINNER, 3GPP TR 38.901 etc.)

Note 6: Flat fading model refers to the 2 state model from ITU-R P681 (section 6). Since this model is based on time series, R1-1802975 proposes a method to adapt it to drop based simulations for system level evaluation.

7 Potential key impact areas on NR to support NTN

7.1 Specific constraints associated to NTN

This clause describes selected specific Non Terrestrial Network design constraints that need to be addressed when considering the Non-Terrestrial Network deployment scenarios.

Table 7.1-1: Specific design constraints of Non Terrestrial Network

Non Terrestrial Network Design Constraints	Differences between NTN and cellular systems
Propagation channel	<p>As detailed in clause 6, the main differences lies in different multi path delay and Doppler spectrum model .</p> <p>For narrowband signals and frequency bands below 6 GHz, the time dispersion may be ignored.</p> <p>We shall assume outdoor conditions and line-of-sight operations for the UE for communication via satellite. In HAPS system, indoor conditions are also addressed, which implies the need to consider non-line-of-sight conditions as well.</p>
Frequency Plan and channel Bandwidth	<p>The allocated spectrum to a satellite system is respectively 2 x 15 MHz (UL & DL) at S band and about 2 x 2500 MHz (UL & DL) at Ka band. In addition, satellite systems at S and Ka bands use mostly circular polarizations.</p> <p>Frequency re-use and flexibility of spectrum allocation in the different cells may be supported and therefore the maximum channel bandwidth per cell is assumed to be respectively 2 x 15 MHz (UL & DL) at S band and 2 x 800 MHz (UL & DL) at Ka band.</p> <p>For efficient spectrum usage, the system should always minimise the risk of inter cell interference.</p>
Power limited link budget	<p>The main design drivers of satellite and HAPS based communication systems are;</p> <ul style="list-style-type: none"> - To maximise the throughput for a given transmit power from the UE on the UL and from the satellite/HAPS on the DL. - To maximise the availability of the service under deep fading situations (typically between 20 and 30 dB in Ka band for 99.95% availability)
Cell pattern generation	<p>Space and HAPS systems typically feature larger cells compared to cellular networks. In addition, the cells may be moving (without a fixed earth reference point) in case of NGSO (Non Geostationary Satellite Orbit) satellite or HAPS system.</p> <p>These large cells especially at low operational elevation angles will create a significant differential propagation delay between a UE at cell centre and UE at cell edge and the ratio of the differential increases as the altitude of the satellite and HAPS decreases. In other words, the ratio between propagation delays at cell centre and cell edge is likely to be higher in the context of HAPS as compared to geostationary satellite systems.</p> <p>This will impact contention based access channels when the position of UEs is not known by the network.</p>
Propagation Delay characteristics	<p>Satellite systems feature much larger propagation delays than terrestrial systems. The one-way delay between the UE and the RAN (whether on-board the satellite/HAPS or on the ground) may reach up to 272.4 ms for GSO (Geostationary Synchronous Orbit) systems, and is greater than 14.2 ms for NGSO (Non-Geosynchronous Orbit) systems. In the case of HAPS, the one way delay is less than 1.6 ms and hence comparable with cellular networks. This larger delay will likely impact all signalling loops especially at access and transport (data transfer) levels.</p> <p>The analysis of the propagation delay is detailed in clause 5.3.</p>
Mobility of the infrastructure's transmission equipment	<p>In cellular networks, transmission equipment refers to base stations (gNB) or Remote Radio Heads (RRH). They are usually fixed, except when on board a moving platform such as a train.</p> <p>In Non-Terrestrial Networks, the transmission equipment is on board the space/HAPS. For GSO systems, the transmission equipment is quasi static with respect to the UE with only small Doppler effects. For HAPS, the transmission equipment is moving around or across a theoretical central point and hence creates Doppler. For NGSO systems, the satellites move relative to the earth and creates higher Doppler effects than for GSO systems.</p> <p>The Doppler depends on the relative satellite/HAPS velocity with respect to the UE, and on the frequency band. Doppler can be characterized by a maximum Doppler Shift and a Doppler variation rate.</p> <p>This effect will continuously modify the carrier frequency, phase and spacing and may create Inter Carrier Interference (ICI).</p> <p>As detailed in clause 5.3, assuming a worst case UE velocity of 1000 km/h:</p>

Non Terrestrial Network Design Constraints	Differences between NTN and cellular systems
	<ul style="list-style-type: none"> - For LEO in S band (2 GHz): +/- 48kHz Doppler Shift and - 544 Hz/s Doppler variation rate - For LEO in Ka band (20 GHz): +/- 480kHz Doppler Shift and – 5.44 kHz/s Doppler variation rate - For LEO in Ka band (30 GHz): +/- 720kHz Doppler Shift and – 8.16 kHz/s Doppler variation rate <p>Note, although these values are high, most of the Doppler shift and Doppler variation rate can be pre/post compensated, exploiting the knowledge of the satellite/HAPS motion that can be anticipated through modelling (e.g. ephemeris of satellites) as well as UE location if known.</p>
Service continuity between land-based 5G access and non-terrestrial based access networks	<p>Whenever a UE leaves or enters cellular coverage, a hand-over to or from the satellite/HAPS system can take place to ensure service continuity. The handover triggering mechanisms might be different for each direction e.g. leave satellite as soon as there is enough cellular signal, but only leave cellular when there is a very low cellular signal.</p> <p>The hand-over procedure should take into account the service enablers, the characteristics and the measurement reports of both access technologies. The following aspects should be considered:</p> <ul style="list-style-type: none"> - Support both non-transparent air/spaceborne (on-board processing) and bent-pipe architectures - Handover preparation and HO failure/RLF handling - Time synchronization - Measurement object coordination – incl. gap allocation & alignment - Lossless handover support - Specifics related to intra-Non Terrestrial network mobility, as well as between Non-Terrestrial and Cellular networks
Radio resource management adapted to network topology	<p>In order to support varying traffic demand while also taking UE mobility requirements into account, requires minimal response time of the access control functionality.</p> <p>In cellular systems, access control is typically located in the gNB close to the UE. Moreover coordination between gNBs is possible through the Xn interface (between gNBs interface) or via a central entity.</p> <p>In satellite systems, access control is mostly located at satellite base station, gateway or hub level which may prevent optimal response time for access control. Hence, pre-grants, Semi Persistent Scheduling (SPS) and/or grant free access scheme would be beneficial.</p>
Terminal mobility	The challenge is to support very high speed UEs such as aircraft systems featuring maximum speeds of 1000 km/h (see 3GPP TS 22.261 [6]).

7.2 NR features/protocols potentially affected

This clause identifies the NR Features/protocols **in bold** that may require some adaptations to support operation via Satellite or HAPS. Other solutions may be identified but don't require adaptations of the standard.

Table 7.2-1: NR Features/protocols that may require some adaptations to support operations via Satellite or HAPS

Non-Terrestrial Network design constraints	Impacted NR areas	NR Features that may require adaptations to support NR operation via Satellite or HAPS
Propagation channel	Physical Layer	<p>For satellite-based systems the signal is mostly direct LOS and follows a Ricean distribution with strong direct signal component; slow fading is possible, due to temporary signal masking e.g. under trees and bridges. For HAPS based systems, the signal contains significant multipath components and follows a Ricean model. Similarly to cellular systems, a frequent and fast fading of max 100 ms coherence time is expected, mainly due to signal components recombination.</p> <p>To improve performance, the receivers' synchronisation configuration at both UE and gNB level, could be adapted especially:</p> <ul style="list-style-type: none"> - The Reference signals in the physical signals (e.g. DL: PSS, SSS, Reference Signals; UL: DMRS, SRS), the Preamble sequence and aggregation (related to random access channel), to take into account the Doppler and possibly some specific multi path channel model. - The Cyclic Prefix to compensate for the delay spread and the jitter/phase. The sub-carrier spacing (SCS) of the OFDM signal may be extended with greater SCS values to accommodate larger Doppler (To Be Confirmed).
Frequency plan and channel Bandwidth	Physical Layer	<p>The carrier numbering could be reviewed to support the targeted spectrum (S band, Ka band) and the pairing between UL/DL bands with specific band separation.</p> <p>Specifically, for Ka band NTN deployment scenarios, the 5G radio interface mode foreseen for above 6 GHz bands shall be configured to support FDD access scheme (e.g. with two mono directional carriers operated in opposite direction on both UL and DL bands). This will require the system to configure and possibly adapt the MAC and network layer signalling in a specific manner.</p> <p>The carrier bandwidth could be extended up to a maximum of 800 MHz. Alternatively carrier aggregation method can be used to provide equivalent throughput while enabling a greater flexibility of carrier allocation between the cells while respecting frequency reuse constraints.</p>
Power limited link budget	Physical Layer	<p>To maximise the throughput / power ratio, the operation point in the power amplifier at satellite or at the UE shall be set as close as possible to the saturation point, when needed. To support this, several techniques can be considered and possibly combined together:</p> <ul style="list-style-type: none"> - Extended multicarrier modulation and coding schemes especially for the UL that features low Peak to Average Power Ratio (PAPR) that are more robust against distortions - PAPR reduction and nonlinear distortion mitigation through signal processing techniques (e.g. pre-distortion mechanisms). - Operating the high power amplifier (UE and satellite/HAPS level) with the minimum output back-off if necessary. <p>To maximise the signal availability with slow and deep fading, especially for UE at cell edge, it is recommended to provide modulation and coding schemes featuring very low SNR operating points or other alternatives especially for mMTC service enablers. This may lead to extend the Modulation Coding Scheme of NR towards very low Es/No to meet the reliability requirements of critical communications or low energy consumption scenarios.</p>
Power limited link budget	MAC layer (Resource Allocation)	<p>To maximise the spectral efficiency and accommodate limited power terminals, the MAC layer should be able to allocate Physical Resource Blocks in the most flexible way. Reduced size of Physical Resource Blocks should be considered (e.g. single tone transmission or transmission over one OFDM sub carrier of same or larger bandwidth than a single OFDM carrier).</p>

Non-Terrestrial Network design constraints	Impacted NR areas	NR Features that may require adaptations to support NR operation via Satellite or HAPS
Cell pattern generation	Physical layer	<p>The differential delay due to large cell size may create near far effect between UEs during the initial access procedure when the UEs positions are not known. This may require an extended acquisition window to improve performance.</p> <p>Note however that if the UE position becomes known during a session, the differential delay can be compensated by the network.</p> <p>For broadcast service, specific signalling may be needed to accommodate the larger and moving cells.</p>
Propagation Delay characteristics	Physical layer	<p>User traffic, such as voice or video conference services, is latency and jitter sensitive.</p> <p>In cellular networks, HARQ retransmission may lead to jitter (e.g. typically up to 8ms in the case of LTE FDD mode). A mitigation scheme called TTI Bundling on UL is defined. It allows to re-transmit the same symbols over up to 4 consecutive sub frames, without waiting for HI acknowledgment. It is optimised for short jitter.</p> <p>In Satellite/HAPS systems, as the propagation delays are significantly longer, HARQ scheme would create unacceptable jitter. The UL slot aggregation may need to be adapted to compensate for higher jitter. Possible solutions could be to increase the periodicity, the number of re-transmissions of symbols and/or decrease the slot duration.</p> <p>Further enhancements of HARQ process should not be precluded to compensate for the propagation delay characteristics.</p>
Propagation Delay characteristics	Access layer (MAC, RLC)	<p>In satellite/HAPS systems, the longer propagation delay impacts various protocol layers, retransmission mechanisms and response times in resource scheduling.</p> <p>The following mechanisms should be adapted to accommodate longer delays and provide latency compensation/reduction especially on delay sensitive applications. We recommend to minimise the number of exchanges between the UE and the network via the following features</p> <ul style="list-style-type: none"> - an Initial Access procedure (based on a random access scheme) by implementing novel methods, where data and access signalling are sent together, would help to meet this requirement (e.g. grant free access, 2 step RACH) - a Data Transfer procedure, by implementing flexible/extended receive window size, flexible acknowledgement policy in terms of frequency, event, flexible and ARQ/HARQ cross coordination, radio resource allocation, ACK free scheme or a latency adaptive HARQ-ACK feedback, to accommodate long delay channel
Propagation Delay characteristics	Physical Layer	<p>In terrestrial cellular systems, the gNB selects the most appropriate MCS (Modulation and Coding Scheme) based on the CQI (Channel Quality Indicator) reported by the UE as part of the AMC (Adaptive Modulation and Coding) procedure.</p> <p>In satellite systems, the propagation delay creates a larger response time for the AMC loop and hence requires a margin to compensate for the possible outdated CQI. This leads to a suboptimal use of the useful transmission capacity (lower spectral efficiency).</p> <p>In order to improve its efficiency, the AMC procedure could be modified with potential signalling extension.</p>
Node B or RRH mobility	Physical Layer	<p>In cellular networks based on an OFDM radio interface, the SCS (Sub Carrier Spacing) may be scaled in order to mitigate both the Doppler shift and Doppler variation rate.</p> <p>In satellite / HAPS systems, the SCS range of values may need to be extended especially for Ka band and large channel bandwidth (e.g. 800 MHz).</p>
Service Continuity between land based 5G access and satellite based access networks	Physical Layer, MAC layer (Resource Allocation) and above (Mobility Management)	<p>To support service continuity between the cellular and non-terrestrial networks or within non-terrestrial network, it is recommended to adopt a hard hand-over scheme or dual/multi-connectivity between terrestrial and non-terrestrial networks, when possible.</p> <p>The differences in propagation delay between cellular and non-terrestrial access network will create a significant jitter or possible data starvation.</p> <ul style="list-style-type: none"> - For delay sensitive applications, a temporary QoS degradation may be accommodated provided that it doesn't occur too often. - For data services with high reliability requirements, buffering or retransmission techniques (e.g. PDCP inherent capability) may be needed to compensate for such impairment.

Non-Terrestrial Network design constraints	Impacted NR areas	NR Features that may require adaptations to support NR operation via Satellite or HAPS
		<ul style="list-style-type: none"> - Delays may be compensated before starting the hand-over <p>The support of hand-over between cellular and non-terrestrial network will require:</p> <ul style="list-style-type: none"> - Extension of PDCP retransmission scheme in terms of repetition rate of data and duplication handling in PDCP layer - Extension of hand-over signalling at RRC, RLC, MAC layer
Radio resource management adapted to network topology	NAS, RRC, RLC, MAC, Physical Layer	<p>The mobility management should accommodate the specific cell patterns (size and position) of NTN networks. Moreover, cells in the non-terrestrial network may cross borders between countries.</p> <p>In particular, this will affect the identification method of cells, the design of tracking and location areas, the roaming and billing procedures as well as location based services.</p> <p>Furthermore, NGSO and HAPS systems generate cells which move around. This causes hand-over to occur not only for mobile units but also for fixed UEs. However, the hand-over caused by such NTN may be anticipated, by exploiting trajectory models such as satellite ephemeris.</p>
Radio resource management adapted to network topology	RAN Architecture	<p>In cellular networks, the access controller, which control radio resources allocation, is implemented in the gNB. The access controller may control the interface between the nominal gNB and the UE or the interface between a neighbouring gNB and the attached UE (in the latter case, the neighbouring gNB acts as a relay node).</p> <p>In Non-Terrestrial Networks, the access controller function is typically implemented</p> <ul style="list-style-type: none"> - on board the HAPS - at the satellite gateway/gateway level or on board the satellite for GSO and NGSO systems <p>In case of Ka band deployment scenarios, the NTN terminal may accommodate gNB functions as part of a Relay Node.</p> <p>The NTN specific topology may require some adaptations to the inter gNB protocols to cope with the propagation delay, the cell pattern and the cell mobility (NGSO and HAPS systems)</p>
Terminal mobility	Physical layer	<p>For NTN terminals moving at 1000 Km/h the response time of the power control loop should be decreased.</p> <ul style="list-style-type: none"> - Physical Frame & Sub-Frame structures: <ul style="list-style-type: none"> - The reduction of transmission slot duration could be considered (e.g. mini slot approach) to decrease the Power Control Loop response time - The extension of SCS values could be considered to support very high speed mobility UEs - Physical signals: <ul style="list-style-type: none"> - The mapping and scheduling of the power control command on physical radio resources may be revisited to enable a faster response time.

7.3 NR modifications to support the Non-Terrestrial Network deployment scenarios

For each deployment scenarios, the actual impacts on NR are identified.

7.3.1 Methodology

For each of the NR Features that may require adaptations to support NR operation via Satellite or HAPS, identified in chapter 7.2, the problem statement in terms of issue are assessed, potential areas of impact on NR protocol are identified.

Table 7.3.1-1: Areas of impacts on NR to support Non-Terrestrial networks

Non-Terrestrial network specifics	Effects	Impacted NR features
Motion of the space/aerial vehicles (especially for Non GEO based access network)	Moving cell pattern	Hand-over/paging
	Delay variation	TA adjustment
	Doppler	Init syncro downlink DMRS time density
		HARQ
Altitude	Long latency	MAC/RLC Procedures
		Physical layer Procedures (ACM, power control)
		TA in Random access response message RACH
Cell size	Differential delay	DMRS frequency density
		Cyclic prefix
Propagation channel	Impairments	
Duplex mode	Regulatory constraints	Access scheme (TDD/FDD)
Satellite or aerial Payload performance	Phase noise impairment	PT-RS
	Back-off	PAPR
Network architecture	RAN Mapping	Protocols

7.3.2 Motion of the space/aerial vehicles

7.3.2.1 Hand-Over and paging

7.3.2.1.1 Problem statement

NGSO satellites move rapidly with respect to any given UE location. As an example, on a 2-hour orbit, a LEO satellite is in view of a stationary UE from horizon to horizon for about 20 minutes. Since each LEO satellite may have many beams, the time such a UE stays within a beam is typically for only a few minutes. The fast pace of change creates problems for paging as well as handoffs for a stationary UE as well as a moving UE.

Since handover happens in general when the UE or relay is in CM-ACTIVE and RRC-CONNECTED state, the procedure is time critical to avoid loss data. In NTN systems based on NGSO satellites, the cells or spot beams are moving at high speeds and so the handover procedure from one spot beam to the next or from one satellite to the next has to be executed quickly otherwise the UE may not make use of the target beam and/or satellite resources efficiently and in the worst case may suffer loss of data.

NR beam management for mobility between spot-beams on the same base station cannot be ported to satellite to minimize the handoff overhead. The NR beam management might assume same frequency on the adjacent beams, but for, the adjacent beams on the same satellite may use different frequencies or different polarization. Thus, the beam management procedures may have to be modified.

The problem for paging needs more detailed explanation. In NR based cellular networks, a UE camps on a cell. The cell is uniquely identified by the RAN from which the UE is receiving the radio signals from. A collection of cells is called a Tracking Area. A collection of Tracking Areas is called as a Registration Area. A cell belongs to a Tracking area and

a Registration Area. As long as the UE stays within a Registration Area, no location update is needed. The UE in the CM-IDLE state will perform a Registration Area update when it moves out of a Tracking Area.

The AMF only needs to be aware of the UE location to the granularity of Registration Area when a UE is in the CM-IDLE state. If a packet arrives from internet for this UE in CM-IDLE state, the AMF attempts to page the UE on all cells belonging to the Registration Area in order to notify the arrival of packets to it. All RANs that receive the page transmits a page in the corresponding cells to reach UE that may be anywhere in the Registration Area.

In Non-GEO satellite access network, a UE camps on a beam of a satellite, but as beams move, it ends up camping on different beams and different satellites over time even though UE may not have moved. Unlike terrestrial framework where a cell on the ground is tied to radio communication with a RAN, in Non-GEO satellite access network, the satellite beams are moving. There is no correspondence between cells on the ground and satellite beams. The same cell on the ground is covered by different satellites and different beams over time. Therefore, for the initial Registration, the Satellite based radio access network will not be able to provide the Tracking Area information to AMF based on which beam and which satellite the Registration Request was received. Given that tracking areas are defined on the ground and Non-GEO beams are moving, there is no one-to-one correspondence between moving beams and fixed tracking areas or registration areas on the ground. However, this information is necessary for UE to determine if it needs to perform a registration area update with AMF in NR.

7.3.2.1.2 Assessment of conditions for NR operation in Non-Terrestrial networks

For handover and paging to operate successfully and efficiently in the NGSO satellite networks, the NR UEs may need to be capable of geo-location. One possibility is that the NR UE may be aware of their locations and may report this to the satellite RAN if needed. (For fixed installations, their location can be reported once at time of installation.)

The ephemeris information of the NGSO satellites can be used to determine their footprints of each of the beams, and its velocity all the time. Therefore, for a given UE location at any given time, the network has information as to which beam of which satellite covers that location best. It also knows the duration that UE location would remain to be covered by the beam and which beam on the same satellite, or a different satellite will be the best candidate to switch over next, and at what time. If positioning information of the UEs is available at the network, the possibility to simplify handover procedure and reduce measurement reporting overhead require further study.

7.3.2.1.3 NR impact considerations

No impact for HAPS or GEO satellite based NTN. For Non-GEO satellite based NTN, adaptation of the NR handover and paging protocols needs further study possibly taking advantage of the knowledge of the UE location and satellite ephemeris information.

7.3.2.2 TA adjustment

7.3.2.2.1 Problem statement

MEO, LEO and HAPS systems feature a strong varying delay because satellite/HAPS and UE are fast-moving and are not relatively static. In this case, the individual timing advances of the UEs may need to be dynamically updated and appropriate TA index values may be needed to solve the long strong delay in the overall distance of the propagation on NTN link.

The issues or technical problems to solve, related to TA alignment in Satellite communications, are as follows:

1. A strong delay variation is caused by moving satellites generating a fast change in the overall distance of the propagation from UE over Satellite to BS.
2. The delay is much longer over a satellite link than one TTI.

A strong delay variation is caused by moving satellites generating a fast change in the overall distance of the radio link between UE and BS via satellite. The delay is much higher and variable over a satellite radio link than over a terrestrial radio link. This delay largely exceeds the TTI (Equivalent to one frame) of NR which is equal to or less than 1 ms. However, the delay variation is quite predictable knowing the satellite orbits and UE position.

Hence, TA alignment is an important feature of NR that will be impacted by introduction of NTN in 5G to ensure that all uplink transmissions are synchronized at gNB reception point.

7.3.2.2.2 Assessment of conditions for NR operation in Non-Terrestrial networks

A timing advance command [20], T_A , for a TAG indicates adjustment of the current N_{TA} value, N_{TA_old} , to the new N_{TA} value, N_{TA_new} , by index values of $T_A = 0, 1, 2, \dots, 63$, where for a subcarrier spacing of $2^\mu \cdot 15$ kHz, $N_{TA_new} = N_{TA_old} + (T_A - 31) \cdot 16 \cdot 64 / 2^\mu$.

As shown in Figure 7.3.2.2.2-1, transmission of uplink frame number i from the UE shall start at $T_{TA} = (N_{TA} + N_{TA_offset}) \times T_C$ before the start of the corresponding downlink frame i at the UE, where N_{TA} can be derived by the UE based on the index value T_A from gNB, N_{TA_offset} depends on the duplex mode and frequency range in uplink transmission, and T_C is the basic timing unit [21][22][23].

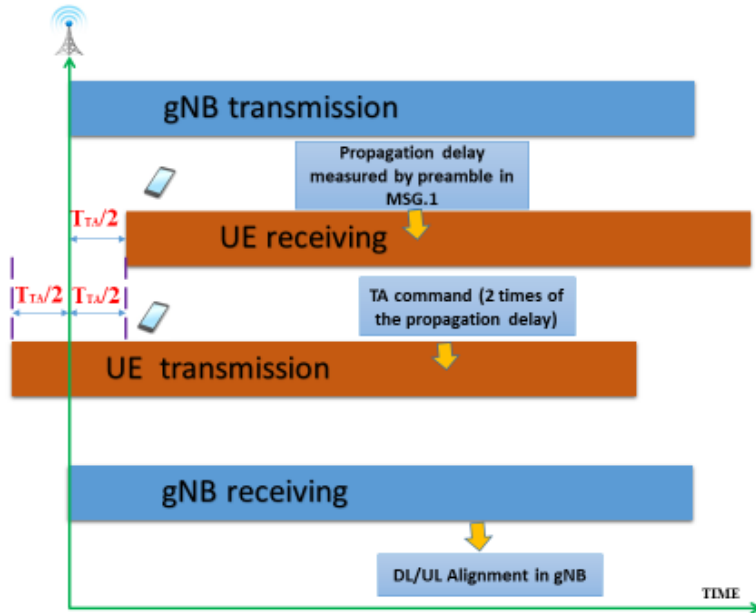


Figure 7.3.2.2.2-1: Time alignment at gNB with TA

In case of satellite, the high delay drift of individual non-GEO satellites is quite predictable because the motion of the satellites follows known paths. The very fast update of the TA is neither required in terrestrial links, nor in GEO satellite links. In both scenarios, the terminal mobility is dominating the TA requirements.

Another technical issue that arises is that the delay variation over the satellite link is much more than a TTI. E.g. if the SCS is increasing from 15 kHz to 60 kHz, the TTI goes down from 1 ms to 250 µs. The required TA adjustment range for satellite links will become larger than the TTI with any SCS selection and the transmission timing of the UE has to be adjusted over the borders of individual TTIs.

Table 7.3.2.2.2-1: TA granularity, and step size with SCS

Subcarrier spacing (SCS) configuration parameter, μ	SCS [kHz]	RB band- width [kHz]	TA gran- ularity [Ts]	T_{step} [ns]	Max Ta step size [µs]
0	15	180	1024	520.83	16,6
1	30	360	512	260.42	8,3
2	60	720	256	130.21	4,15
3	120	1440	128	65.10	2,1
4	240	2880	64	32.55	1

This max Ta step should be valid only for extended cyclic prefix. With normal cyclic prefix, we expect this maximum step not to exceed the normal CP length (e.g. CP length is 4.7 µs in 15kHz SCS case). It means that the number of Ta commands to be sent per second to track the maximum drift of 35 µs/s is about 10 per second for 15 kHz SCS case, 40 per second for 60 kHz SCS, and 80 per second for 120 kHz SCS case. The number of Ta commands to be sent per second is important but can be implemented.

7.3.2.2.3 NR impact considerations

Solutions need to be studied to ensure alignment of uplink signals over the NTN links to overcome the predictable delay of NTN.

7.3.2.3 Initial synchronization in downlink

7.3.2.3.1 Problem statement

In order to access the 5G network, the UE has to detect the PSS and the SSS. Those synchronization signals allow time and frequency correction, and Cell Id detection. UE in cellular network has to get good one-shot detection probability at -6 dB received baseband SNR condition with less than 1% false alarm rate as defined in chapter 7.1.5 of [24], with robustness against initial frequency offset up to 5 ppm.

We expect that requirements (SNR level of -6 dB, frequency error robustness of 5 ppm and 1% false alarm) defined for terrestrial UE will be kept the same for NTN UE. Even if the SNR level of NTN systems is typically in the range of -3 to 13 dB SNR.

In cellular networks, transmission equipment (gNB or RRH) are usually fixed, except when on board a moving platform such as a train.

In Non-Terrestrial Networks, the transmission equipment is on board the satellite/HAPS.

- For geostationary systems, the transmission equipment is quasi static with respect to the UE with only small Doppler shift.
- For HAPS, the transmission equipment is moving around or across a theoretical central point but creates small Doppler shift.
- For non-geostationary systems, the satellites move relative to the earth and creates higher Doppler shift than for geostationary systems.

The Doppler shift depends on the relative satellite/HAPS velocity with respect to the UE, and on the frequency band.

In term of Doppler shift, the worst case for NTN systems corresponds to non-geostationary systems, at lowest altitude (i.e. 600 km), where the speed of the satellite embedding transmission equipment is 7.5 km/s.

As detailed in clause 5.3, assuming a worst case NTN terminal velocity of 1000 km/h:

- For LEO in S band (2 GHz): Up to +/- 48kHz Doppler Shift in downlink for the whole satellite coverage (spot)
- For LEO in Ka band (20 GHz): Up to +/- 480kHz Doppler Shift in downlink for the whole satellite coverage (spot)

If frequency error robustness requirement is 5 ppm (i.e. 10kHz for S band, 100 kHz for Ka band), it means that this worst case described above is not covered by current 5G specifications. To be inferior or equal to 5ppm error, the satellite altitude has to be above 13000 km.

Actually, the Doppler shift amplitude to be compensated is less than 48 kHz for S band and 480 kHz for Ka band, because in satellite communication systems, all satellites whether GSO or NGSO generate multi beams and each beam foot print corresponds to a cell. The Max Doppler shift amplitude observed at the satellite coverage foot print edges will be reduced within each beam footprint. The lower the beam width, the less the Doppler shift amplitude.

7.3.2.3.2 Assessment of conditions for NR operation in Non-Terrestrial networks

In case the altitude of the satellite is above a certain altitude (about 13 000 km) or if center beam pre-compensation is sufficient to reach the 5 ppm requirements, no impact is foreseen.

7.3.2.3.3 NR impact considerations

In case the above conditions are not met, further studies are required to accommodate the high Doppler shift during the cell synchronization procedure in non-Terrestrial networks.

Note that this high Doppler shift can be known based on UE location and satellite ephemeris and hence could be for example pre compensated. This could prevent impact on the NR but may need to be confirmed with further study.

7.3.2.4 DMRS time density

7.3.2.4.1 Problem statement

As analyzed in Section 5.3, the maximum Doppler variation rates during the field tests appeared in the scenarios of LEO at the altitude of 600 km, and are -544 Hz/s with carrier frequency of 2 GHz, -5.44 kHz/s with carrier frequency of 20GHz and -8.16 kHz/s with carrier frequency of 30 GHz, where the maximum Doppler variation rate is the maximum slope (maximum derivative) of the Doppler shift curves. In NR network, there are up to 4 DMRS symbols per slot and the duration of one slot can be configured to 1 ms, 0.5 ms, 0.25 ms, 0.125 ms or 0.0625 ms, which correspond to the subcarrier spacing of 15 kHz, 30 kHz, 60 kHz, 120 kHz and 240 kHz respectively, as shown in Figure 7.3.2.4.1-1. Table 7.3.2.4.1-1 summarizes the potential maximum Doppler shift in one slot in NTN based on the observed maximum Doppler variation rate during the field tests. As shown in Table 7.3.2.4.1-1, it is observed that the potential maximum Doppler shifts are up to 0.544 Hz with carrier frequency of 2 GHz in DL/UL, up to 5.44 Hz with carrier frequency of 20 GHz in DL and up to 8.16 Hz with carrier frequency of 30 GHz in UL.

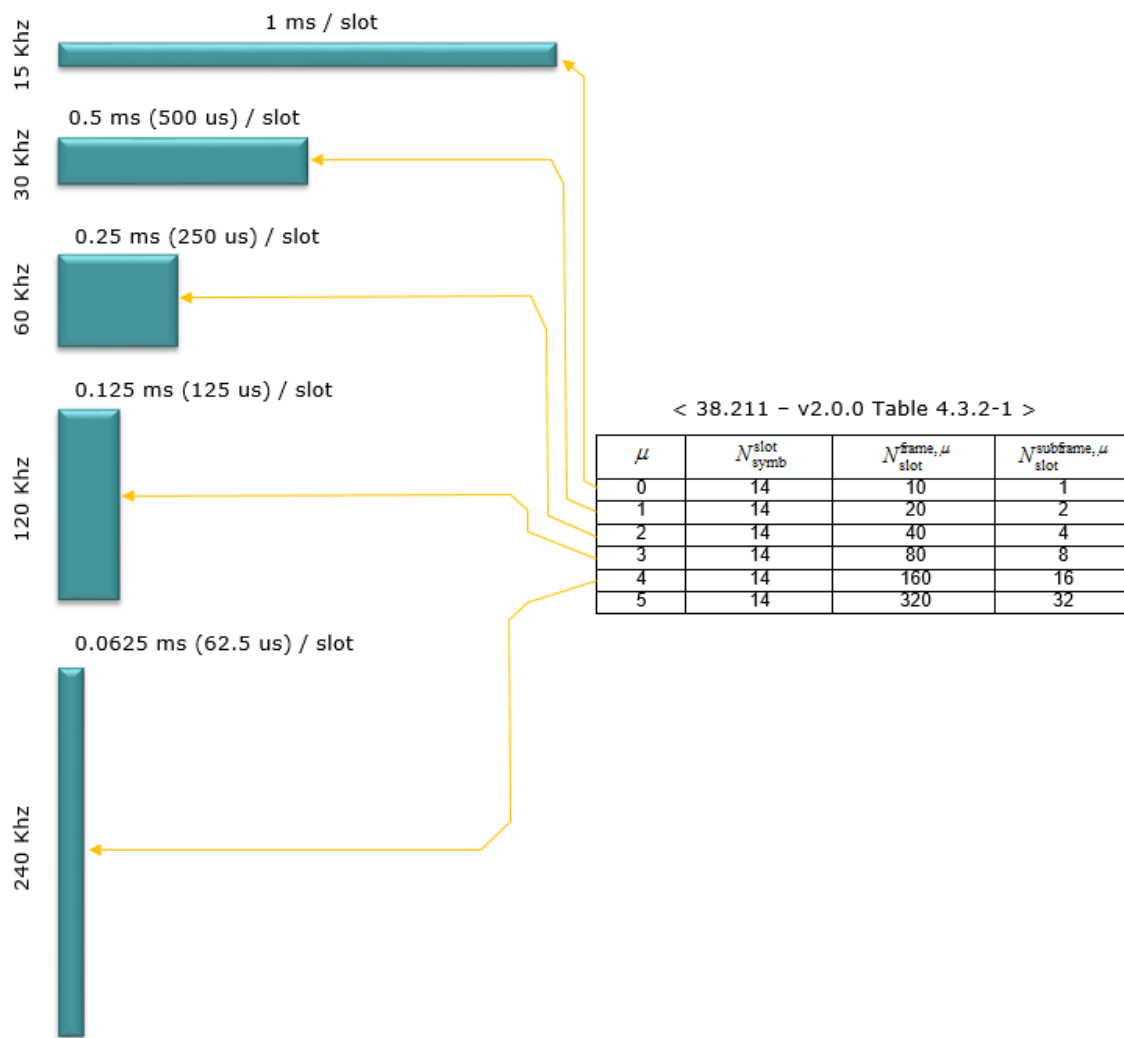


Figure 7.3.2.4.1-1: Slot duration depending on μ configuration

Table 7.3.2.4.1-1 Potential maximum Doppler Shift in one slot in NTN

Carrier frequency when the altitude of LEO satellite is 600km	Maximum Doppler variation (Hz/s)	Duration of one slot (ms)	Potential maximum Doppler shift in one slot (Hz)
2 GHz (DL/UL)	- 544	1	0.544
		0.5	0.272
		0.25	0.136
		0.125	0.068
		0.0625	0.034
20 GHz (DL)	-5440	1	5.44
		0.5	2.72
		0.25	1.36
		0.125	0.68
		0.0625	0.34
30 GHz (UL)	-8160	1	8.16
		0.5	4.08
		0.25	2.04
		0.125	1.02
		0.0625	0.51

In the existing LTE network, the frequency error at the UE side shall be within ± 0.1 PPM observed over a period of 0.5 ms [25]. In NR network, the frequency error at the UE side shall be within ± 0.1 PPM observed over a period of 1 ms[26].

7.3.2.4.2 Assessment of conditions for NR operation in Non-Terrestrial networks

The frequency error corresponding to ± 0.1 PPM is ± 200 Hz with carrier frequency of 2 GHz, ± 2 kHz with carrier frequency of 20 GHz and ± 3 kHz with carrier frequency of 30 GHz. Compared to the requirement of frequency error at the UE side, the maximum Doppler shift in one slot in LEO scenarios during field test is negligible, see Table 7.3.2.4.1-1. This result is also valid for other configurations with higher DMRS time density per time slot as configurable in 5G NR. Similar conclusion could be observed at the eNB side too [27][40].

7.3.2.4.3 NR impact considerations

As a conclusion, no impact on NR specifications is needed for DMRS positioning in time in NTN deployment scenarios because the maximum Doppler Variation in NTN is negligible compared to the minimum requirement of frequency error at both gNB and UE sides in NR.

7.3.3 Altitude of the space/aerial vehicles

7.3.3.1 HARQ

The HARQ process is a very time-critical mechanism. HARQ operation becomes even more critical at extremely long RTT, i.e., as in case of NTN and extreme coverage scenarios.

In satellite communication, the RTT normally exceeds the maximum conventional HARQ timers (after which an ACK is received) or the maximum possible number of HARQ processes (i.e., a flexible pool of parallel HARQ processes similar to LTE). This is also true even for LEO constellations, where the RTT varies between 15 to 63 times longer than that of the terrestrial RTT [28]. Thereby, simply extending the number of HARQ processes linearly to RTT induced by the satellite channel might not be feasible for some UEs due to memory restrictions and the maximum possible parallel processing channels [41][42][43][44][45]. Furthermore, gNBs also have to consider this latency impact on the number of their active HARQ processes. Therefore, it is important to study the impact on NR HARQ operation for the introduced NTN delays. Figure 7.3.3.1-1 depicts the HARQ feedback RTT, i.e., from data retransmission time up to acknowledge reception at a bent-pipe satellite. The figure also shows the backhauling delay T_{p1} as well as the forward/reverse satellite link delay T_{p2} , i.e., where the RTT = $2(T_{p1} + T_{p2}) = 2 * T_p$.

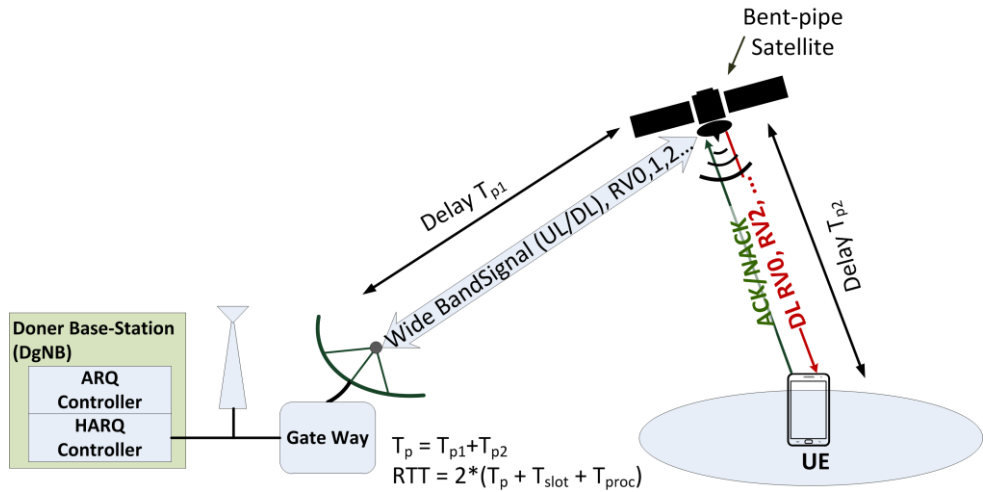


Figure 7.3.3.1-1: Bent-pipe Satellite HARQ feedback operation with a maximum RTT (from sending a NACK until receiving a retransmission redundancy version (RV))

7.3.3.1.1 Problem statement

NR has extended the number of HARQ processes in Rel. 15 to 16 processes [29]. For NR NTN satellite transmission, the number of HARQ processes may need to be further extended flexibly according to the induced RTT delay. Here, the minimum required number of HARQ processes can be computed directly from the RTT delay of each satellite constellation, e.g., LEO, MEO and GEO, using the following formula [28]:

$$N_{HARQ,min} \geq \frac{T_{HARQ}}{T_{slot}}, \quad (7.3.3.1-1)$$

where $N_{HARQ,min}$ is the minimum required number of HARQ processes, T_{slot} is 1ms assuming a reference numerology 15 kHz subcarrier spacing, and T_{HARQ} is the time duration between the initial transmission of one transport block (TB) and the corresponding ACK/NACK complete decoding.

The T_{HARQ} is depicted in Figure 7.3.3.1.1-1 considering the RTT ($2 * T_p$), transmission time ($2 * T_{slot}$), and processing time, T_{proc1} and T_{proc2} , for decoding the TB and the ACK/NACK frame, respectively. T_{HARQ} is illustrated in details in Figure 7.3.3.1.1-1.

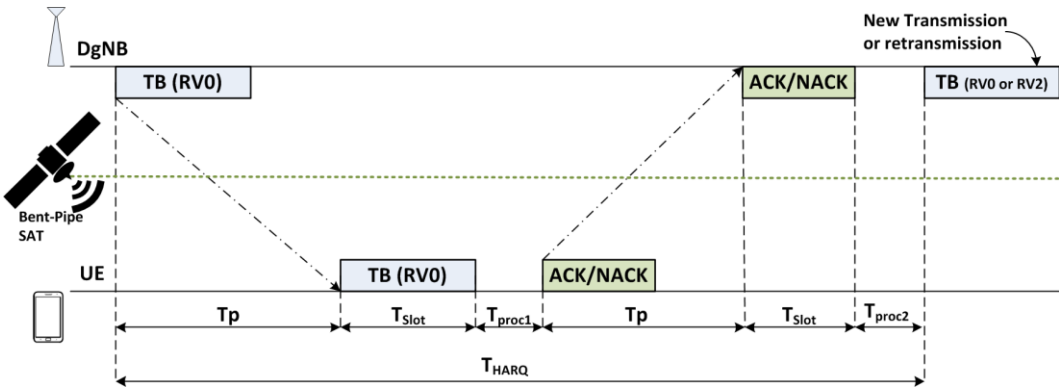


Figure 7.3.3.1-1: Timing diagram of a single HARQ process for a NTN with a single bent-pipe satellite in the link

Table 7.3.3.1-1 gives an overview of the number of HARQ processes, $N_{HARQ,min}$, based on different T_{HARQ} values (including the RTT) for different satellite constellations, LEO, MEO, and GEO [5].

Table 7.3.3.1.1-1: The minimum required number of the HARQ processes, $N_{\text{HARQ,min}}$, assuming a 1ms slot duration for 15 kHz reference subcarrier-spacing

constellation	Max. T_{HARQ}	$N_{\text{HARQ,min}}$ processes for 1 ms slot operation	UE side feasibility
Terrestrial	16ms	16	Feasible (Rel. 15)
LEO	50ms	50	Feasible (with HARQ extension)
MEO	180ms	180	FFS (impact on TBS/MCS)
GEO/HEO	600ms	600	FFS (impact on TBS/MCS)

NOTE*: For larger subcarrier spacing (SCS), i.e., $2^k * 15 \text{ kHz}$, the min. required number of the HARQ processes might be scaled by 2^k .

7.3.3.1.2 Assessment of conditions for NR operation in non-terrestrial networks

Handling a higher number of parallel HARQ processes and its feasibility for NTN have been addressed in [46] [41] [32]. The impacts of NTN delays on the existing HARQ-supporting mechanisms need to be addressed in a subsequent study.

At least the following principles can be considered in further study:

- **Enhancing existing HARQ operation** to extend the HARQ processing accommodating low to moderate NTN RTT delays.
- **Limiting HARQ capabilities and/or disabling HARQ** for long RTT delays.

7.3.3.1.3 NR impact considerations

It is required to study the impact on NR HARQ operation due to the long RTT delay of a non-terrestrial network. The impacts should be considered as well for the NTN UEs and serving gNBs, when the number of HARQ processes is either extended to satisfy high reliability scenarios or limited/disabled for longer NTN delays.

7.3.3.2 MAC/RLC procedures

7.3.3.2.1 Problem statement

UE operating in GEO satellite access networks can experience a one-way propagation time of 240 ms at the minimum, 270 ms at the maximum between UE and satellite base station. The base station can observe the acknowledgement of packets sent to the UE only after the round trip plus some processing time, which is more than $\frac{1}{2}$ second later. Similarly the UE can observe acknowledgement for its packet sent to the base station in about the same time interval. For the LEO satellite systems with typical 600 km orbit, the one way propagation delay changes continuously between 2 ms when the satellite is directly above, and 7 ms when the satellite is seen with 10° elevation.

ARQ requires that the transmitted packets be buffered in anticipation of potential packet loss and released only after the successful receipt of an acknowledgement, or until a time-out mechanism reinitiating a retransmission. The long round trip delay requires larger transmission buffer, and potentially limits the number of retransmission allowed for each transmitted packet in both the forward and return links. Note that in LEO satellite systems, the ARQ transmit buffer size, and retransmission mechanism must be designed for the longest possible delay, i.e. at the lowest elevation.

Scheduling mechanisms must be able to cope with the long RTT. UL scheduling delay parameters are expected to be redefined to accommodate the RTT of the associated deployment scenario.

7.3.3.2.2 Assessment of conditions for NR operation in Non-Terrestrial networks

For efficient ARQ operation in GEO or NGSO satellite networks, NR UE and base stations must size their transmission buffer and the retransmission time-out mechanism according to the longest round-trip delay to be anticipated. The number of retransmissions allowed before a packet is dropped from the retransmission buffer may also be adjusted.

UL scheduling delay parameters are expected to be redefined to accommodate the RTT of the associated deployment scenario.

7.3.3.2.3 NR impact considerations

No impacts on the ARQ protocol itself, except parameter sizing needs to account for the longer delay of the NTN network.

7.3.3.3 Physical layer procedures (ACM, power control)

7.3.3.3.1 Problem statement

As mentioned in section 7.3.3.2.1, UE operating in GEO satellite access networks can experience a one-way propagation time up to 270 msec. Using LEO satellite access network with 600 km orbit, the one way propagation delay changes continuously between 2 ms, and 7 ms. The slow reaction time is expected to have performance impact on some of the physical layer procedures particularly those with close loops such as power control and ACM.

7.3.3.3.2 Assessment of conditions for NR operation in Non-Terrestrial networks

While slower reaction on the control loops affects the performance of all the control loops between UE and base station, most of them require some adjustments in implementation, but not fundamentally different design.

While the link margin may be different for specific links and systems depending on applications, satellite power is typically at a premium. Due to the large free space loss and limited EIRP and battery power available at UE, power margin is also limited for mobile terminals. Thus, a very limited amount of power control, if at all, is available for the GEO satellite links. Due to the long delay in the loop, the power control is not expected to track fast fading, but may be used to track slower power variations.

For Ka-band satellites, ACM is an essential tool that maintains connection through rain fades, which typically changes somewhat slower than the $\frac{1}{2}$ second round trip delay. It generally works well with some hysteresis to avoid excessive oscillations between two ACM modulation coding modes. But, this reaction time is too slow for ACM to adapt for changes of signal strength for mobile terminals when line of sight is interrupted by shadowing.

For GEO systems in S-band, the main issue is multipath fading, which can be much faster than $\frac{1}{2}$ second round trip delay. As such, ACM will not be able to follow it. ACM algorithm typically attempts to settle on a modulation coding mode that closes the link if possible, by giving up some power to maintain a margin.

For LEO satellites, ACM may also be used to adapt for the large variation of free space loss. The variation is sufficiently slow compared to the 20 ms worst case round trip delay. It should also be able to react to shadowing fades to a large extent, but still unable to follow fast fading.

7.3.3.3.3 NR impact considerations

Further studies need to be performed to define the required margin for power and ACM control loops to accommodate to the long RTT.

7.3.4 Cell size (Beam foot print)

7.3.4.1 PRACH and Random access

7.3.4.1.1 Problem statement

The RTT in NTN can be much larger than the RTT in terrestrial network as analyzed in Section 5.3. Therefore, it is necessary to consider its impact on PRACH and random access procedure. As shown in Figure 7.3.4.1.1-1, for one given beam covering a cell, there is one common propagation delay for all served UEs and one relative propagation delay for each served UE. If the common propagation delay can be compensated, then the NTN PRACH signal design will depend on the relative propagation delay, which is limited up to 200km in current specifications regarding TA range. However even if only the difference value left, a NTN PRACH signal design and PRACH procedure design are still needed since the common propagation delay could be thousands of kilometers which cannot be ignored.

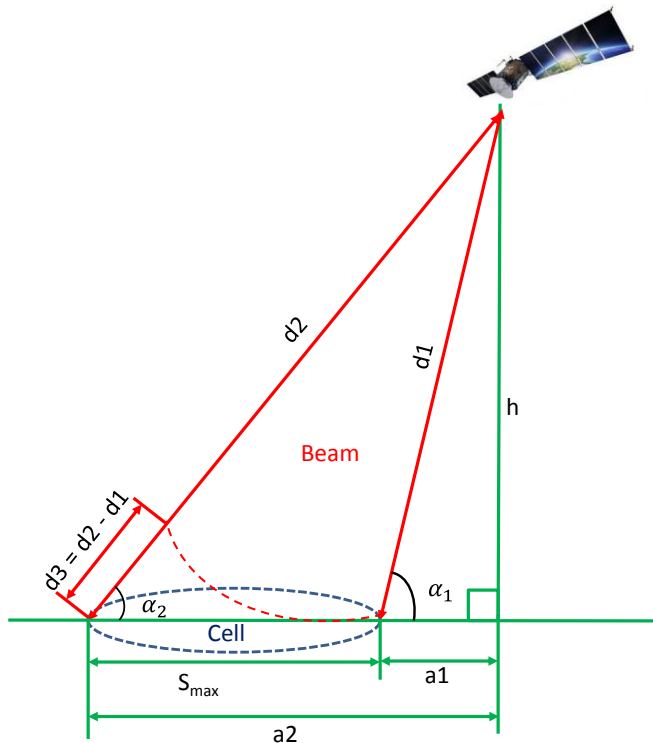


Figure 7.3.4.1.1-1: NTN systems, new geometry and the cell size

7.3.4.1.2 Assessment of conditions for NR operation in Non-Terrestrial networks

Random Access Response

For non-terrestrial networks, the round-trip time can be much larger than the round-trip time in terrestrial networks (up to 600 ms for the case of GEO satellites, with bent pipe architecture). However the current window for the PRACH response in NR, which starts at $\lceil (\Delta \cdot N_{\text{slot}}^{\text{subframe},\mu} \cdot N_{\text{symb}}^{\text{slot}}) / T_{\text{sf}} \rceil \cdot T_{\text{sf}} / (N_{\text{slot}}^{\text{subframe},\mu} \cdot N_{\text{symb}}^{\text{slot}})$ symbols after transmitting the last symbol of the preamble and has the size of "rar-WindowLength", cannot cover this round-trip time [30]. Therefore, the random access response window length in NR should be revisited to accommodate the round-trip time of NTN. However, extending the RA response window size in the existing procedure introduces unnecessary UE monitoring intervals thus more power saving due to large propagation delay in NTNs. Therefore, the solution to handle long propagation delay with the consideration of power saving at the UE side needs to be further studied.

PRACH Sequence and Format

Considering that the cell size of NTN HAPS is not extremely large, the current NR preamble format design should be enough to support HAPS. The current NR preamble format design should be enough to support HAPS but for Satellite it needs to be revisited [30][31][23][39][32]. As shown in Figure 7.3.4.1.1-1, the difference $d_3 = d_2 - d_1$ depends on the elevation angle, as listed in Table 7.3.4.1.2-1.

Table 7.3.4.1.2-1 Differential delay $d_3 = d_2 - d_1$ vs. satellite elevation angle

α_2 [degree]	cell radius ($S_{\text{max}} / 2$) [km]	d_3 [km]
10	200	390
20	200	372
30	200	343
40	200	303
50	200	254
60	200	197
70	200	134
80	200	67

Clearly, the difference d_3 exceeds the maximum cell coverage supported by the NR preamble format of 2x 100 km for satellite elevation angles below 60 degrees. In such a case, NR preamble format needs to be extended for NTN system considering different footprint of NTN cells. So it should be further studied if new random access preamble format is needed for spaceborne vehicles.

The effect of the residual differential delay may be mitigated as follows:

- Case 1: NTN differential delay \leq Max currently specified NR PRACH CP duration.
In this case no change is required to the specified NR RACH procedure.
- Case 2: NTN differential delay $>$ Max currently specified NR PRACH CP duration.
In this case different solutions are possible which are for further study.

RACH Procedure

For PRACH procedure, huge propagation delay [66.7 μ s, 120ms] [3] corresponding to BS heights [8km, 35786km] will lead to long RA response procedure [33][32]. As a result, it is necessary to shorten the RA transmission/retransmission delay and design an NTN-specific RAR window based on the given BS information to make the UE efficient and power saving.

7.3.4.1.3 NR impact considerations

Regarding NR PRACH waveform/format, no NR spec impacts are identified if the GNSS based techniques are applicable at the UE side, otherwise, potential enhancements w.r.t PRACH waveform/format may be needed which are for further study. For RACH procedures, potential enhancements can be studied regardless of whether the GNSS based techniques are applicable or not.

7.3.4.2 TA in Random access response message

7.3.4.2.1 Problem statement

The Timing advance mechanisms ensure that transmissions from all UEs operating in the same cell are synchronized when received by the same gNB. A TA command is provided to the UE in a RAR message during initial access, as well as later, to adjust the uplink transmission timing for PUCCH/PUSCH/SRS. TA adjustment is analyzed in Section 7.3.2.2.

The timing advance (N_{TA}) is given by:

$$N_{TA} = TA * 16 * \frac{64}{2^\mu}$$

where $\mu = 0, 1, 2, 3, 4, 5$ and TA is an integer between 0 and 3846.

The maximum value of the TA command sent in RAR message constraints the maximum distance between an UE and the serving base station, which also defines the maximum allowed cell size, as illustrated in Table 7.3.4.2.1-1.

Table 7.3.4.2.1-1: Terrestrial link distance for 5G NR

Subcarrier spacing	15 kHz $\mu=0$	30 kHz $\mu=1$	60 kHz $\mu=2$	120 kHz $\mu=3$	240 kHz $\mu=4$	480 kHz $\mu=5$
Maximum timing advance (ms)	0.67	0.335	0.1675	0.0838	0.0419	0.0209
Maximum link distance (TA = 3846) (km)	300	150	75	37.5	18.75	9.38

Even at 15kHz, the maximum cell size is below the satellite altitude, for both LEO and GEO scenarios. Therefore, it is not expected that the timing advance mechanism can be reused as is for satellite networks.

For HAPS scenarios, the HAPS altitude is quite negligible compared to the maximum link distance for low numerology. In these cases, the maximum allowed cell size for terrestrial operations needs to be slightly reduced to ensure the maximum link distance is never exceeded. For high numerology however, the maximum link distance may be smaller than the HAPS altitude, leading to the same conclusion as for satellite operations.

7.3.4.2.2 Assessment of conditions for NR operation in Non-Terrestrial networks

Compensation of entire propagation delay by TA

For satellite operations, it is expected that TA mechanism cannot be reused as is to compensate for the propagation delay. For HAPS operations, the mechanism can be reused as is in some cases (low numerology and/or low HAPS altitude). The maximum cell size shall then be redefined to ensure that the maximum allowed link distance is never exceeded.

Common delay known and handled by the network

In this case, TA compensates only for differential delay/distance, so that the maximum TA value defines the maximum allowed differential delay/distance. Considering Figure 7.3.4.1.1-1, it can be easily shown that the maximum differential distance is achieved when α_2 is minimum. As shown in Table 7.3.4.2.2-1, the maximum differential distance is almost equal to the maximum cell diameter for $\alpha_2 = 10^\circ$.

Table 7.3.4.2.2-1: Maximum cell size for $\alpha_2 = 10^\circ$, SCS=15kHz, GEO/MEO/LEO cases

NTN vehicle altitude orbit	Min Elevation angle α_2 (deg)	Max Differential distance $d_3 = d_2 - d_1$ (km)	Maximum cell diameter S_{\max} (km)
GEO (at 35 786 km)	10°	300 km	304.66
MEO at 10 000 km	10°	300 km	304.73
LEO at 1500 km	10°	300 km	305.05
LEO at 600 km	10°	300 km	305.50

In first approximation, it can be stated that the existing TA mechanism can compensate the differential delay if the cell diameter does not exceed the maximum link distance given in Table 7.3.4.2.1-1.

7.3.4.2.3 NR impact considerations

In HAPS operations, extension of the maximum TA value could be considered to extend the maximum allowed cell size, especially for high numerology.

In satellite operations, it is expected that the network can take into account the common propagation delay. To extend the maximum cell size, different approaches can be studied further.

7.3.5 Propagation channel

7.3.5.1 DMRS frequency density

7.3.5.1.1 Problem statement

For PDSCH, the mapping to physical resources of the Demodulation reference signals is described in chapter 7.4.1.1.2 of [21] recalled below. There is either one DM-RS symbol per slot or 2 in consecutive OFDM symbols within a slot. The resource elements of this DM-RS symbol are scattered over different subcarriers according to two configuration types.

In configuration type 1, DM-RS symbols are inserted every 2 subcarriers in PDSCH. In configuration type 2, DM-RS symbols are inserted every 5 subcarriers in PDSCH.

Table 7.3.5.1.1-1: Minimum coherence bandwidth of PDSCH supported for a given SCS value

SCS (kHz)	Minimum supported coherence bandwidth (assumed no orthogonally required) (kHz)	
	Configuration type 1	Configuration type 2
15	30	75
30	60	150
60	120	300
120	240	600

For PBCH, the mapping to physical resources of the Demodulation reference signals is specified in Table 7.4.3.1-1 of [21]. DM-RS are inserted every four subcarriers in PBCH on all OFDM symbols.

For PDCCH, the DM-RS symbols are inserted every 4 subcarriers as for PBCH (chapter 7.4.1.3.2 in [21]).

Table 7.3.5.1.1-2: Minimum coherence bandwidth of PBCH/PDCCH supported for a given SCS value

SCS (kHz)	Minimum supported coherence bandwidth (kHz)
15	60
30	120
60	240
120	480

The minimum coherence bandwidth for each NTN deployment scenario can be computed with the following formula:

$$\text{Minimum coherence bandwidth} = 1/(\alpha * \text{delay spread})$$

with alpha being a constant between 1 and 50. As a worst case, it is set to 50 for the DM-RS mapping selection. The maximum delay spread depends on the UE antenna directivity.

Table 7.3.5.1.1-3: Maximum delay spread and minimum coherence bandwidth for each deployment scenario

	D1, GEO, Ka band	D2, GEO, S band	D3, LEO, S band	D4, LEO, Ka band	D5, HAPS, S band
Maximum Delay spread (ns)	10	100	100	10	150
Min coherence bandwidth (NOTE 1, NOTE 2)	>> MHz	200 kHz	200 kHz	>> MHz	133 kHz

NOTE 1: In Ka band, typical antenna directivity is taken into account in the delay spread estimate

NOTE 2: In S band, delay spread in satellite scenarios is lower than in HAPS scenario, because the min operating SNR is lower which leads to discard largest delay spread.

7.3.5.1.2 Assessment of conditions for NR operation in Non-Terrestrial networks

For S band, the minimal coherence bandwidth has been computed with the formula in the previous clause and an alpha value corresponding to a theoretical worst case (Alpha set to 50). This may put some constraints on the SCS value selection which needs to be further studied.

7.3.5.1.3 NR impact considerations

Enhancement to NR specifications with respect to DMRS frequency diversity may not be needed depending on possible SCS choice constraints that needs to be further studied.

7.3.5.2 Cyclic prefix

7.3.5.2.1 Problem statement

Originally, the NR CP has been dimensioned for terrestrial transmissions characterized by high delay spread due to multi path propagation. This clause describes selection criteria of the CP that need to be addressed when considering using NR in Non-Terrestrial Network deployment scenarios.

7.3.5.2.2 Assessment of conditions for NR operation in Non-Terrestrial networks

Delay spread in satellite propagation channels

Signal echoes are associated to the presence of indirect rays that reach the receiver antenna and carry a significant energy with respect to the energy of the direct ray.

ITU-R recommendation [34] defines for the 2 GHz band three parameter sets of wideband models, including LOS and NLOS cases, applicable for an elevation range from 15 to 55° and for urban, suburban and rural environments. The delay spread of these three parameter sets ranges between 180 ns to 250 ns, whereas the 250 ns are stated to cover 90% of the cases.

For higher elevations than 55°, we assume that the delay spread of the satellite channel will be in the same range or even lower due to the traveling distances of the echoes arriving at a receiver.

Few papers are available on delay spread measurements in Ka-Band. Reference [35] is stating the coherence bandwidth to be 30 MHz at 40 GHz with omnidirectional antennas. According to [36], the coherence bandwidth (Δf_c) of a channel with maximum delay spread T_m is

$$(\Delta f_c) \approx 1 / (5T_m)$$

For the stated coherence bandwidth in [35], this results in a maximum delay spread of $T_m = 25$ ns for omni-directional antennas. For directional antennas, echoes with significant delay are normally filtered out by the antenna radiation pattern, so flat fading can be assumed for Ka-band signals.

CP length defined in NR

The possible CP lengths currently defined for New Radio [21] are summarized in the following table:

Table 7.3.5.2.2-1: CP lengths and minimum/maximum RF bandwidth of NR as currently defined in [21]

Subcarrier spacing (SCS) configuration parameter μ	SCS [kHz]	normal CP length [μ s]	extended CP length [μ s]
0	15	4,688	Not defined
1	30	2,344	Not defined
2	60	1,172	16,67
3	120	0,586	Not defined
4	240	0,293	Not defined

7.3.5.2.3 NR impact considerations

It is observed that lower numerologies ($\mu = 0, 1$) are associated with CP lengths exceeding the requirement of NTN, resulting in a slightly reduced spectral efficiency due to the over-dimensioned CP (e.g. overhead is for $\mu = 0$: $(4.688\mu s - 0.25\mu s) / 66.67 \mu s = 6.7\%$).

High numerologies ($\mu = 3, 4$) result in CP lengths which are well matching to propagation characteristics in Ka-Band.

The extended CP for a SCS of 60 kHz is not required, because it is significantly larger than required for satellite applications.

Enhancement to NR specification is not expected for NTN applications due to the NTN channel model delay spread compatible with the existing specified CP values.

7.3.6 Duplex mode

7.3.6.1 FDD/TDD Duplexing mode

7.3.6.1.1 Problem statement

Most of the existing satellite systems operate in the frequency bands designated for FDD mode, with defined transmit direction. For some frequency bands, TDD mode is possible.

When considering TDD mode, a guard time is necessary to prevent UE to simultaneously Transmit and reception. This guard time directly depends on the propagation delay between UE and gNB. This guard time will directly impact the useful throughput and hence the spectral efficiency.

When considering Non-Terrestrial networks, this guard time should commensurate the round trip delay.

Guard time would range between 2×7 ms for LEO at 600 km and 2×270 ms for GEO satellite access networks since NTN terminals can experience a one-way propagation time of

- 240 ms at minimum and 270 ms at maximum between UE and satellite base station for GEO
- 2 ms at minimum and 7 ms at maximum between UE and satellite base station for LEO at 600 km altitude

Such excessive guard time would lead to a very inefficient radio interface especially in GEO or even MEO based access.

It may be acceptable in the case of LEO access system with the need to deal with the variable delay.

7.3.6.1.2 Assessment of conditions for NR operation in Non-Terrestrial networks

The applicability of the duplexing mode TDD or FDD depends on the regulations (ITU-R and/or national) associated to the targeted spectrum.

7.3.6.1.3 NR impact considerations

FDD is preferred duplexing mode for most NR based NTN access network.

In case the regulations allow it, TDD mode can be considered for both HAPS and LEO satellite based access network with potential NR impacts if required.

7.3.7 Satellite or aerial Payload performance

7.3.7.1 PT-RS

7.3.7.1.1 Problem statement

Phase variations in time domain can be caused by different phenomena: presence of phase noise, frequency drifts due to Doppler shift, or due to insufficient frequency synchronization (e.g. residual CFO), etc. Phase noise, caused by imperfect oscillator implementation technology destroys the orthogonality of subcarriers in OFDM-based systems especially in FR2. Phase noise causes CPE, resulting in a constant rotation angle of the modulation constellation, and ICI, resulting in scattering of the constellation points in OFDM based systems. Doppler effects and/or residual CFO cause frequency shifts translated into time domain phase ramps at OFDM symbol level.

The phase variations translating all the above effects may significantly degrade the performance and need compensation. When mild, these variations can be absorbed by the DM-RS in the channel estimation process. But when strong phase variations are present, which is particularly the case at carrier frequencies above 6GHz, more frequent support than the one provided by DM-RS is necessary in order to track the remaining variations.

In NR, PT-RS has been introduced in [21], [23] to compensate for phase errors. PT-RS configuration in NR is very flexible and allows user-specific configuration depending on scheduled MCS/bandwidth, UE RF characteristics, DM-RS configuration, waveform, etc.

7.3.7.1.2 Assessment of conditions for NR operation in Non-Terrestrial networks

It has been proposed that eMBB should be supported for NTN and the modulation order might not always be low. PT-RS is needed in NTN at high carrier frequencies, where the maximum received SNR is limited by the phase noise.

Considering the high speed of airborne/spaceborne vehicles, CFO and Doppler shift/spread might be worse in NTN and therefore CFO and Doppler estimation need to be considered.

A number of phase noise masks such as DTH or VSAT use cases considered in [37], or other state of the art bent pipe of satellite or HAPS payloads as described in Annex B are considered as pertinent for non-terrestrial communications. Phase noise masks pertinent for terrestrial equipment operating in mmWave have been defined in NR in [38].

The performance of phase tracking algorithms is highly dependent on a large set of variables such as carrier frequency, subcarrier spacing, UE specific RF characteristics, configured MCS/bandwidth, frame length, DMRS configuration, Doppler, receiver implementation options, etc.

7.3.7.1.3 NR impact considerations

PTRS is needed in NR supporting NTN for phase error compensation. PTRS configuration in NR is very flexible. Typical phase noise masks of state of the art bent pipe of satellite or HAPS payloads in Non-Terrestrial networks can be efficiently compensated by the current NR design in the absence of important Doppler shifts and/or residual CFO at a carrier frequency of up to 30 GHz. Some further investigation is needed in the case of important Doppler shifts and/or residual CFO, or in the presence of the specific phase noise masks of on board payloads significantly different from the ones considered in cellular network so far, or with very large channel bandwidths.

7.3.7.2 PAPR

7.3.7.2.1 Problem statement

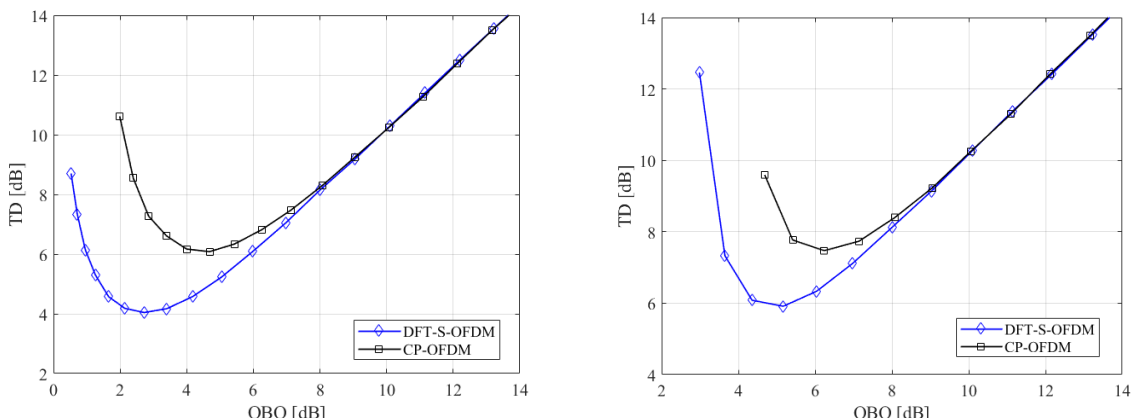
A key component in the satellite payload architecture is a PA. It exhibits nonlinear behavior when driven near saturation in an effort to increase power efficiency. Nonlinear distortion causing constellation warping and clustering, thus complicating signal reception. One measurement that determines the vulnerability of the transmitted signal to nonlinear distortion is the PAPR, with higher values associated with worse impact.

In the NR downlink, CP-OFDM is used. CP-OFDM is composed of superposition of narrowband orthogonal subcarriers, resulting in higher PAPR values compared with the underlying modulation in a single carrier. The PAPR is a function of the number of subcarriers in the signal, as well as the underlining modulation.

The amount of distortion caused by nonlinear amplifier characteristics is a function of the PAPR of the signal. The greater the PAPR, the greater the distortion can be. The distortion can be reduced by increasing the backoff of the amplifier operating point. But this reduces the amplifier efficiency accordingly. Tradeoffs are often made between the amplifier OBO and the nonlinear signal distortion, such that the total degradation of output power and signal distortion is minimized.

As an example, the figures (NOTE 1) below show the total degradation of CP-OFDM with over a typical satellite transponder is about 6 dB for QPSK modulation and 7.6 dB for 16-QAM, whereas that for DFT-spread-OFDM is about 4 dB for QPSK and 6 dB for 16-QAM. The difference between CP-OFDM and DFT-spread-OFDM is 1.6-2 dB.

NOTE 1: See ETSI TR 103 297 "Satellite Earth Stations and Systems (SES), SC-FDMA based radio waveform technology for Ku/Ka band satellite service", , V.1.1.1., (2017-07). Pages 29-30.



QPSK Modulation

Figure 7.3.7.2.1-1: DFT-S-OFDM vs CP-OFDM total degradation

(b) 16-QAM modulation

The additional 2 dB output backoff may represent 20 to 40 percent reduction of link capacity compared to State of the art satellite radio interface, depending on whether the satellite is bandwidth limited or power limited.

As for HAPS, the payload architecture may be very similar to satellite, and power amplifier remains to be a key component, although SSPA is likely to be used instead of traveling wave tube. Regardless, the PAPR difference between CP-OFDM and DFT-spread-OFDM also requires different OBO which translates to different total distortion. The higher total distortion of CP-OFDM ultimately means lower capacity. In this case, however, the problem may be less acute, since the payload power efficiency may not be as critical.

7.3.7.2.2 Assessment of conditions for NR operation in Non-Terrestrial networks

The use of CP-OFDM in the downlink does not restrict NR operation in non-terrestrial networks, but it may affect the system performance:

- In one case, a satellite transponder is sufficiently wide and sufficiently powerful to accommodate more than one FDM carriers, each of which is a different NR CP-OFDM signal. The satellite amplifier is backed off to minimize the intermodulation between these FDM carriers within the same transponder. For such cases, the distortion introduced by the amplifier nonlinearity is small, with little impact.
- In second and much more common case for communicating to small UEs, the satellite amplifier is used to send only one NR CP-OFDM downlink. It is highly desirable to operate the amplifier with as small OBO as possible. But, due to the higher PAPR of CP-OFDM signal, sufficient OBO is necessary. To close the link, it may be necessary to reduce the size of CP-OFDM carrier or operate the CP-OFDM carrier with a lower modulation and coding mode. Either way, the forward link capacity is reduced significantly.

On the uplink, DFT-spread-OFDM might be beneficial.

7.3.7.2.3 NR impact considerations

PAPR reduction techniques of CP-OFDM signal on the downlink would be beneficial to optimize the capacity of non-terrestrial networks and therefore could be considered in future studies.

7.3.8 Network architecture

7.3.8.1 Protocols

7.3.8.1.1 Problem statement

Non-Terrestrial networks differ from typical cellular networks in terms of network architecture, deployment scenarios as well as coverage which may span across several countries.

Potential impacts on the NR specifications could be minimized through suitable mapping options of the Logical NG RAN architecture onto the NTN network architecture.

The respective NG-RAN logical architecture and the NTN network architecture are depicted below. The area of impacts associated to the NG-RAN mapping options need to be identified.

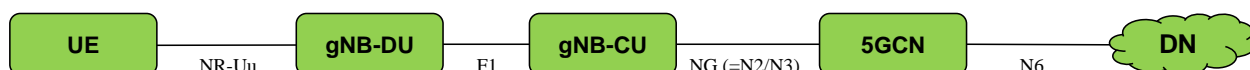


Figure 7.3.8.1.1-1: 3GPP NG-RAN (or NR radio access) architecture defined in TS 38.401

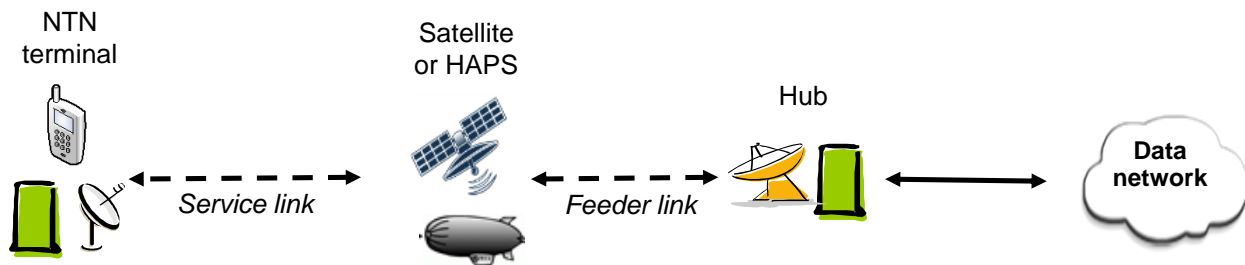


Figure 7.3.8.1.1-2: Typical Non-Terrestrial network physical architecture

Furthermore, when dealing with mobility of UEs, one should distinguish:

- The mobility induced by the motion of the NTN platform, in particular when considering Non-Geostationary Satellites;
- The mobility of the terrestrial equipment:
 - when moving from one beam to another beam generated by a satellite or a HAPS
- The mobility of UE between beams generated by different satellites or HAPS
- The mobility of UE between NTN (Satellite or HAPS) and cellular access

Location update, paging and hand-over RAN related protocols may need to be adapted to accommodate

- The extended delay of NTN for intra NTN access mobility
- The differential delay when mobility between satellite access and cellular access
- The mobility of the cell pattern generated by non geo-stationary satellites

7.3.8.1.2 Assessment of conditions for NR operation in Non-Terrestrial Networks

RAN architecture mapping

There are several options to instantiate the RAN architecture in Non-Terrestrial networks. It depends on whether the satellite or HAPS implement a bent pipe payload or a processed payload. This leads to the following example mapping options that prevent the need to create new interfaces or reference points. Note that there may exist other mapping options not listed here.

Table 7.3.8.1.2-1: RAN architecture example mapping options in Non-Terrestrial networks

Satellite/HAPS payload	NG RAN architecture
Bent pipe	Mapping option 1
Processed – low	Mapping option 2
Processed - high	Mapping option 3

A bent pipe satellite/HAPS payload implements Radio frequency conversion, analogue filtering and amplification. A processed payload implements some RAN functions. The type of gNB functions that can be embarked will be constrained by the available power and mass on board satellite/HAPS.

Here under are depicted different mapping options of the logical NG RAN architecture onto the physical architecture of Non-Terrestrial networks which prevents to modify the NG RAN architecture.

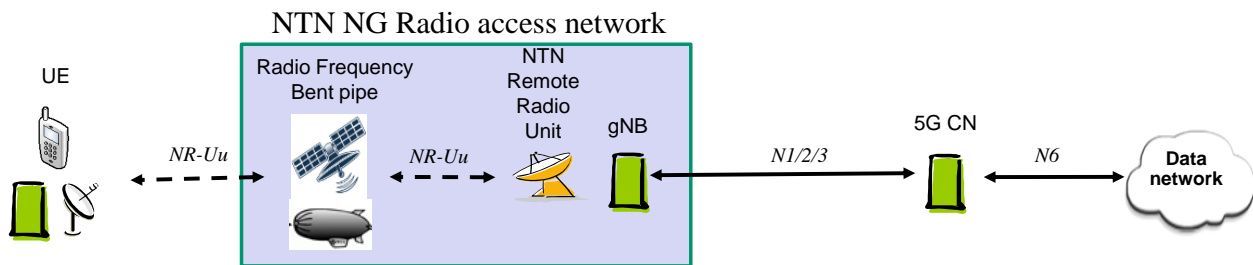


Figure 7.3.8.1.2-1: Mapping option 1 - NG RAN architecture in Non Terrestrial network with bent pipe payload

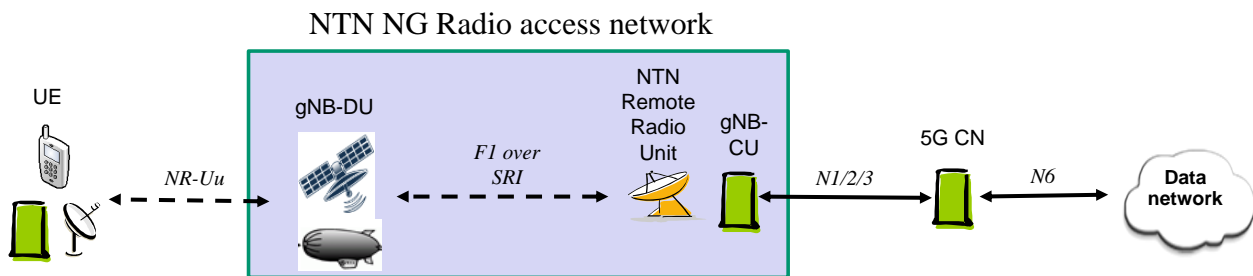


Figure 7.3.8.1.2-2: Mapping option 2 - NG RAN architecture in Non Terrestrial network with gNB-DU processed payload

NOTE: SRI refers to Satellite Radio Interface

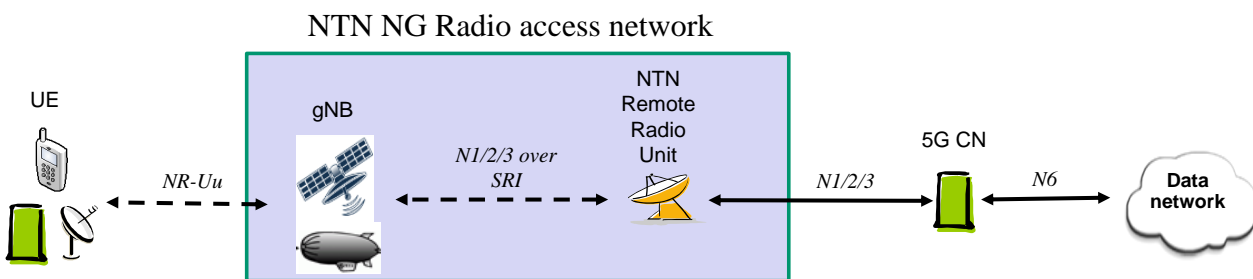


Figure 7.3.8.1.2-3: Mapping option 3 - NG RAN architecture in Non Terrestrial network with gNB processed payload

Table 7.3.8.1.2-2 highlights the difference in terms of interfaces transported by the satellite links and NG RAN functions implemented in the NTN physical entities.

Table 7.3.8.1.2-2: Mapping options of the logical architecture of NR RAN onto the physical architecture of Non-Terrestrial networks

Mapping options	Satellite/HAPS Service link	Satellite/HAPS feeder link	Terminal side	Network side
1 –Bentpipe payload	NR-Uu radio interface	NR-Uu radio interface	UE	NTN Remote Radio Unit + gNB
2 –Processed payload (gNB-DU)	NR-Uu radio interface	F1 over Satellite radio interface (SRI)	UE	NTN Remote Radio Unit + SRI modems + gNB-CU
3 –Processed payload (gNB)	NR-Uu radio interface	N1, N2, N3 over Satellite radio interface (SRI)	UE	NTN Remote Radio Unit + SRI modems

Given that Non-terrestrial networks feature longer propagation delays, the timers associated to the protocols transported over the feeder and service links may require to be extended. This applies for example to F1 as well as N1, N2 and N3 reference points.

In mapping option 1, the Satellite or HAPS implements an RF repeater (with frequency conversion), whereas in mapping option 2, they implement some kind of "intermediate" node which could be based on the outcomes of 3GPP TR 38.874: "Study on Integrated Access and Backhaul".

It is recommended to consider the outcome of this TR 38.874 and see how it can be applicable to Non-Terrestrial networks (especially for NTN deployment scenarios 2 and 3) and what areas of impact it may create. Other mapping options may be considered depending on different CU-DU lower layer split for NR that may be defined (See TR 38.816).

Location update, paging and hand-over RAN related protocols

Table 7.3.8.1.2-3 identifies the possible areas of impact on NR associated to Location update, paging and hand-over RAN related protocols in different types of non-terrestrial networks.

Table 7.3.8.1.2-3: Potential areas of impact on NR specifications associated to Location update, paging and hand-over RAN related protocols for different types of non-terrestrial networks

NTN Deployment scenarios	GEO	Non GEO	HAPS
Cell pattern	Earth fixed: same as in cellular	Motion over earth or earth fixed	Motion over earth (e.g. rotating) & Possibly UE altitude dependent
Tracking area	Tracking area congruent with cell pattern: same as in cellular	For further study	Same as for GEO and cellular networks
Potential areas of impact on NR specifications	Mobility management procedures (Paging, hand-over, location update): Potential extension of some timers	Location update, paging and hand-over RAN related protocols to be adapted depending on tracking area design Handling of network identities to be adapted	Case 1: tracking area corresponds to HAPS coverage: no impact Case 2: Tracking area smaller than HAPS total coverage, same impact as for Non GEO are expected

7.3.8.1.3 NR impact considerations

Thanks to suitable mapping options of the logical architecture of NG RAN onto the physical architecture of non terrestrial network, modifications of the NG RAN architecture are not needed in terms of reference points, interfaces or functions.

However the N1/N2/3 and GTP based F1 interface protocols may need to be adapted to accommodate the non terrestrial networks feeder link characteristics (long delay, BER). Depending on the non-terrestrial network deployment scenarios,

other impacts on NR specification may have to be considered among which, location update, paging and hand-over RAN related protocols and handling of network identifies.

Last, it may be considered how the architecture being defined in 3GPP TR38.874 "Study on Integrated Access and Backhaul" can be used in the context of various Non-Terrestrial networks deployment scenarios.

8 Recommendations on the way forward

8.1 General outcomes

This report has

- provided detailed descriptions of some deployment scenarios for non-terrestrial networks and the related system parameters such as altitude, orbit, etc.
- defined a way to generate Non-Terrestrial network channel models leveraging on the models defined in TR 38.901 "Study on channel model for frequencies from 0.5 to 100 GHz (Release 14)"
- identified potential key impact areas on the NR to support Non-Terrestrial networks

In line with 3GPP TR 38.901, the study considered channel models in Non-Terrestrial networks operating in any frequency bands between 0.5 and 100 GHz.

8.2 Reference deployment scenarios

A number of scenarios is considered in clause 5.1 "Scenarios overview" including GEO, Non-GEO as well as HAPS based access networks. The intent is to assess relatively worst-case scenarios with respect to Doppler shift, Doppler variation rate, Delay and Delay variation rate. For non-GEO deployment scenarios, the altitude has been set to 600 km, which is pessimistic with respect to the Doppler, and Doppler rate, related effects.

Non-Terrestrial access networks can be used to serve directly User Equipment or indirectly via a relay node.

8.3 Non-Terrestrial network channel modelling

Leveraging on the models defined in TR 38.901 "Study on channel model for frequencies from 0.5 to 100 GHz (Release 14)", complementary features and specific parameters have been identified and proposed in chapter 6 of this report to generate Non-Terrestrial network channel models for all possible deployment scenarios characterised by altitude/orbit of space/aerial vehicles, user environments (rural, sub-urban, urban and dense urban), targeted user equipment type (omni or directive antennas, LOS/NLOS conditions) as well as frequency bands.

8.4 NR impacts to support Non-Terrestrial networks

8.4.1 Type of potential NR impacts

The potential NR impacts are characterised according to the classification in Table 8.4.1-1:

Table 8.4.1-1: Type of Potential area of NR impacts to support Non-Terrestrial networks

Type of Potential area of impact	Modifications of 3GPP NR specifications
Higher layers impact	Layer 2/3 protocols/architecture
Physical layer impact	Parameters settings, procedures or physical channels and signals

8.4.2 Assessment of potential NR impacts to support Non-Terrestrial networks

Table 8.4.2-1 identifies the potential area of impacts on the NR specification. This will depend on the deployment scenarios. The intent is to identify the main studies to be carried out taking into account the defined NTN channel model

to enable operation of NR in Non-Terrestrial networks. Other areas of impact are identified which could lead to performance improvement.

Table 8.4.2-1: Evaluation of NR impacts to support Non-Terrestrial networks

Non-Terrestrial network specifics	Effects	Impacted NR features	Potential areas of impact to be further studied	Comment
Motion of the space/aerial vehicles	Moving cell pattern	Hand-over/paging	Higher layers impact	Paging and Hand-over procedures should be adapted to take into account the relative motion of the cell pattern with respect to the tracking area. Further analysis on tracking area design may need to be carried out. Mobility management is also to be considered (NOTE 1)
	Delay variation	TA adjustment	Physical layer impact	Alignment of uplink signals may need to be considered
	Doppler	Initial downlink synchronization	No impact	The preferred SCS values for Non-Terrestrial Networks may be respectively 60 KHz for frequency bands lower than 6 GHz and 240 KHz for frequency bands above 6 GHz. However it can also operate with lower SCS value
		DMRS time density	No impact	The preferred DM-RS configuration may be type 1 to cope with Doppler variation rate
Altitude	Long latency	HARQ	Higher Layers & physical layer Impact	Need to adapt the HARQ specification. Deactivation and/or enhancements of NR HARQ can be considered
		Physical layer Procedures (ACM, power control)	Physical layer impact	The operation/configuration of Adaptive power and coding/modulation control loop protocols may have to be adapted.
		MAC/RLC Procedures	Higher layers impact	Timers limit of MAC/RLC and higher layers loop protocols may have to be extended
Cell size	Differential delay	TA in Random access response message	Physical layer impact	Doppler/Delay (NOTE 2) compensation technique (NOTE 3) can be implemented. Further analysis/simulations using the NTN channel model is needed. Adaptations of PRACH format and random access procedure may have to be considered.
		Random access	Physical layer impact	
Propagation channel	Impairments	DMRS frequency density	No impact	Non terrestrial network propagation channel may feature a frequency selective at most comparable with cellular channel
	Impairments	Cyclic prefix	No impact	Non terrestrial network propagation channel may feature a worse delay spread at most comparable to cellular channels.
Duplex scheme	Regulatory constraints	Duplexing mode (TDD/FDD)	Higher layers impact	FDD is preferred especially for most satellite systems. TDD can be considered for HAPS and for LEO
Satellite or aerial Payload performance	Phase noise impairment	PT-RS	Potential constraint on the operation to be further studied	Satellite Radio links are typically operated with relatively low order modulation scheme, in most of the cases up to 16QAM
	Back-off	PAPR	Physical layer impact	Uplink: It is recommended to use DFT-S OFDM Downlink: Low PAPR scheme may improve performance. However not mandatory to support non-terrestrial networks

NOTE 1: Some of the considered deployment scenarios assume indirect access based on fixed or even mobile relays. For NGSO-based deployment scenarios NTN and/or relays mounted on a moving platform such as a train, mobility management also needs further studies.

NOTE 2: The common delay, the Differential delay as well as their time variation may need to be compensated.

NOTE 3: Doppler/Delay compensation techniques can be implemented especially for Non GEO satellites:

- GNSS based techniques: The User Equipment equipped with a GNSS receiver determines its position and the universal time. Thanks to pre-loaded / updated ephemeris of the satellite constellation which can be theoretical or actual, the UE is able to compute the position and motion of the possible serving satellites enabling to determine the Doppler shift and variation rate as well as the absolute Delay and Delay variation.
- Non GNSS based techniques can also be envisaged and implemented.

Annex A: Example of reference scenario for calibration of large scale parameters

For large scale calibration, fast fading is not modelled. The calibration parameters can be found in Table A-1.

Table A-1: Simulation assumptions for large scale calibration

Parameter	Values
Scenarios	NGSO satellite at 1500km, suburban environment
Satellite position	(7871,0,0)
Number of beams	4
Beam layout (as seen from satellite)	
Beam centre	B ₁ : (6371,0,0), elevation = 90° B ₂ : (6347, 481,278), elevation = 65° B ₃ : (6347, 481,-278), elevation = 65° B ₄ : (5242,3622,0), elevation = 45°
Satellite antenna pattern parameter	ka = 10
Satellite EIRP	36dBW/MHz
Bandwidth	5MHz
UE antenna configurations	Co-phased array – Dual linear polarization (M, N, P) = (1, 2, 2), $d_H = 0.5\lambda$, Polarization: 0°, 90°
UE orientation	TBD
Handover margin (for calibration)	0dB
UE distribution	Uniform dropping, 25 users per beam
UE attachment	Geometric
UE noise figure	7 dB
Fast fading channel	Fast fading channel is not modelled
Carrier Frequency	2 GHz
Metrics	1) Coupling loss – serving cell (based on LOS pathloss) 2) Geometry (based on LOS pathloss) with and without white noise

Annex B: Non Terrestrial network characteristics

B.1 NTN Phase noise masks

DTH P1 and P2 and VSAT P1 and P2 phase noise masks were previously defined by DVB [37], in the context of satellite communications.

Annex C: Change History

Change history							
Date	Meeting	TDoc	CR	Rev	Cat	Subject/Comment	New version
2017-06	RP-76	RP-170983				Skeleton report provided as input to RAN #76	0.0.0
2017-06	RP-76	RP-171453				Agreed version as output of RAN #76 including pCRs of RP-170917, RP-170918, RP-171447, RP-171448.	0.1.0
2017-09	RP-77	RP-172074				Agreed version as output of RAN #77 including pCRs of RP-171578, RP-171579, RP-171580, RP-172075.	0.2.0
2017-11	RP-78	RP-172179				Cleanup of v0.2.0 to align with 3GPP drafting rules	0.2.1
2017-12	RP-78	RP-172794				Agreed version as output of RAN #78 including pCRs of RP-172274, RP-172768, RP-172769	0.3.0
2018-03	RP-79	RP-180545				Agreed version as output of RAN #79 including pCRs of RP-180036, RP-180135, RP-180180, RP-180543	0.4.0
2018-06	RP-80	RP-181393				Agreed version as output of RAN #80 including pCRs of RP-180661, RP-181381, RP-181382, RP-181383, RP-181392, RP-181394	1.0.0
2018-06	RP-80					Approved TR version (including editorial cleanup of v1.0.0)	15.0.0
2019-06	RP-84	RP-190842	0001	-	F	Corrections for TR 38.811 Chapter 6 Non-Terrestrial Networks channel models Note: Some renumbering of clauses/figures/equations, reuse of reference numbers could not be implemented.	15.1.0
2019-09	RP-85	RP-191750	0002		F	Correction to NTN channel models	15.2.0
2019-09	RP-85	RP-191825	0003		F	Corrections for TR38.811 Section 6.8.2 Non-Terrestrial Networks channel models	15.2.0
2019-09	RP-85	RP-191827	0004		F	Correction to NTN channel models (Ionospheric scintillations)	15.2.0
2019-09	RP-85	RP-191835	0005		F	CR TR 38.811 Section 6.9.2 and 5.3.4	15.2.0
2020-07	RP-88e	RP-200717	0006		F	Correction for inconsistent shadow fading parameters in NTN rural scenario	15.3.0
2020-09	RP-89e	RP-201919	0007		F	Corrected implementation for inconsistent shadow fading parameters in NTN rural scenario	15.4.0
2020-09	RP-89e	RP-201957	0008		F	Correction to NTN channel model	15.4.0